

TOWSON UNIVERSITY
OFFICE OF GRADUATE STUDIES

**A MODELLING FRAMEWORK TO EXPLORE BIOENERGETIC EFFECTS OF
ENVIRONMENTAL STRESS AND INTERSPECIFIC INTERACTIONS**

by

Andrew G. East

A thesis

Presented to the faculty of

Towson University

in partial fulfillment

of the requirements for the degree

Master of Science

Environmental Science Program

Towson University
Towson, Maryland 21252

(December, 2016)

© 2016 By Andrew G. East
All Rights Reserved

TOWSON UNIVERSITY
OFFICE OF GRADUATE STUDIES

THESIS APPROVAL PAGE

This is to certify that the thesis prepared by Andrew East

entitled A Modelling Framework to Explore Bioenergetic
Effects of Environmental Stress and Interspecific
Interactions

has been approved by the thesis committee as satisfactorily completing the thesis
requirements for the degree Master of Science in Environmental Science

Chris J. Salice Chris J. Salice 12/5/16
Chairperson, Thesis Committee Signature Type Name Date

JAY A. NELSON JAY A. NELSON 11/21/16
Committee Member Signature Type Name Date

SUSAN E. GREGORIC SUSAN E. GREGORIC 11/21/16
Committee Member Signature Type Name Date

Committee Member Signature Type Name Date

Janet V. DeLany Janet V. DeLany, DEd 12-6
Dean of Graduate Studies Type Name Date

Table of Contents:

Acknowledgements	v
Abstract	vii
List of Figures	ix
I. A Bioenergetic Model Accounting for the “Neighborhood Effect and Characteristics of Experimental Environments on <i>Daphnia magna</i>	1
a. Introduction	1
b. Methods	7
c. Results	21
d. Discussion	29
e. Literature Cited	37
f. Appendix / Supplementary Information	42
II. An Energetic Model Accounting for Morphology and Experimental Characteristics of <i>Lymnaea stagnalis</i>	48
a. Introduction	48
b. Methods	53
c. Results	60
d. Discussion	64
e. Literature Cited	68
III. Modelling Experimentally Observed Indirect Energetic Facilitation between Co-occurring <i>Lymnaea stagnalis</i> and <i>Daphnia magna</i>	71
a. Introduction	71
b. Methods	76
c. Results	84
d. Discussion	103
e. Literature Cited	110
Curriculum Vitae	114

Acknowledgements

Patience is a virtue but persistence might be more important.

First, thanks go out to my advisor Dr. Chris Salice—without his persistence about persistence, this venture would've never left the ground. Secondly, thanks go to my committee members Dr. Susan Gresens and Dr. Jay Nelson—their input was vital to several defining details that give this work its identity. Thirdly, a shout-out to all the Salice Lab crew—without their hands, time, and ears this would have been a much thinner and more stressful work. Lastly, but certainly not least, thanks to my family and friends for their patience with my occasionally misguided devotion to this pursuit.

The paragraph below from the Proceedings of the first National Bobwhite Quail Symposium (1972) sums up my thoughts about the nature of graduate school as a “labor of love” and my hopes for those I’ve worked with.

And then, there were the myriad services performed by graduate and undergraduate wildlife students of the Department of Zoology, who turned on the switches, drove the cars, collected the money, and generally sweated and strained as a labor of love. May they all achieve their lifetime ambition which is generally not a whole lot more than seeing that this old planet survives and that its wildlife gets a fair shake.

Howard R. Jarrell
Secretary
National Bobwhite Quail Symposium

But seeing the world in terms of decentralized interactions is a difficult shift for many people. It requires a fundamental shift in perspective, a new way of looking at the world. At some deep level, people have strong attachments to centralized ways of thinking. When people see patterns in the world (like a flock of birds), they often assume that there is some type of centralized control (a leader of the flock). [...] According to this way of thinking, a pattern can exist only if someone (or something) creates and orchestrates the pattern. Everything must have a single cause, an ultimate controlling factor. The continuing resistance to evolutionary theories is an example: Many people still insist that someone or something must have explicitly designed the complex, orderly structures that we call Life. [...] One of the basic tenets of Artificial Life is that the best way to learn about living systems is to try to construct living systems (or, at least, models and simulations of living systems). This idea holds true whether the learners are scientists or children. To help people move beyond the centralized mindset, it makes sense to provide them with opportunities to create, experiment, and play with decentralized systems.

Summarized from Resnick M. (1994). *Artificial Life*, vol. 1.

Abstract:

The overarching theme of this thesis research was to further develop methods to improve ecological risk assessment of anthropogenic stressors. The main objective was to develop a bioenergetic, individual-based multi-species model that could be used to predict population-level dynamics arising from indirect energetic interactions between species. Ultimately, the goal would be to apply such a model to predict effects of chemical stressors on ecological receptors. To facilitate model development and evaluation, several experiments were performed—one to calibrate single species sub-models, and another to demonstrate the effectiveness of the model in predicting population dynamics in single and multi-species scenarios.

The two focal organisms were *Daphnia magna* and *Lymnaea stagnalis* for their environmental and regulatory relevance. Individual bioenergetic models for each species were developed from Dynamic Energy Budget models. These bioenergetic models were then inserted into individual-based models specific to each organisms' behavioral characteristics. *D. magna* models were greatly influenced by localized density-dependent effects termed 'Neighborhood Effect' and *L. stagnalis* models were greatly influenced by their movement pattern and 'S'-shaped growth patterns. Connecting the individual models in a single, multi-species model required modelling indirect energetic facilitation from *L. stagnalis* to *D. magna* by using a model simplification whereby snail waste was functionally converted to daphnia resources as algae.

Experimental results from *D. magna* populations supported the individual daphnid model and the importance of the 'Neighborhood Effect.' Multi-species experimental observations confirmed the existence of indirect energetic facilitation between snails and daphnid populations and provided valuable insight into graded levels of facilitation.

In summary, the results of this thesis demonstrate that a combination of model and experimental methods exist that can provide useful linkages between single species energetic data and higher levels of biological organization. More importantly, the success of the multi-species model emerged from rather simple connections between individual species models. This provides a very useful framework for linking models for single species responses to chemical stressors that may prove valuable to ecotoxicological research and ecological risk assessment.

List of Tables and Figures:

Chapter I.

Figure 1. Nested levels of biological organization	3
Table 1. Moderately hard water recipe	8
Figure 2. Dynamic Energy Budget schematic	13
Figure 3. Neighborhood Effect on reproductive output	16
Figure 4. Cumulative reproduction as function of length	17
Figure 5a and 5b. Effect of pyraclostrobin on length and \dot{k}_M	18
Table 2. Model parameters for <i>Daphnia magna</i>	20
Figure 6. Count of experimental <i>D. magna</i> populations through time	22
Figure 7. Density of experimental <i>D. magna</i> populations through time	22
Figure 8. Histograms of experimental <i>D. magna</i> populations lengths on selected timepoints	23
Figure 9a, 9b, 9c, and 9d. experimental <i>D. magna</i> population counts through time against modelled <i>D. magna</i> population counts.	25
Figure 10. Experimental <i>D. magna</i> length histograms against modelled length distributions	26
Figure 11. Modelled effect of pyraclostrobin on <i>D. magna</i> populations	28
Figure A1. Age-based mortality model output	43
Figure A2. Age- and starvation-based mortality model output	44
Figure A3. Age- and starvation-based mortality model output at low food levels ..	45
Figure A4. Effect of size and food density on starvation mortality cut-off	46
Figure A5. Neighborhood Effect on movement	46
Figure A6. Additional cumulative reproduction functions	46
Figure A7. Adjustment of cumulative reproduction by length function by \dot{k}_M increase	47
Figure A8a and A8b. Simulated <i>D. magna</i> population count and length distributions at selected timepoints under varying stressor effects	47

Chapter II.

Figure 1. Hypothetical von Bertalanffy and juvenile assimilation lag growth curves	52
Table 1. Model parameters for <i>Lymnaea stagnalis</i>	59

Figure 2. Experimentally observed <i>L. stagnalis</i> growth against model output	60
Figure 3a and 3b. Model evaluation of food amount and timing of application	62
Figure 4a and 4b. Two examples of varying simulated environment shapes	63
Figure 5a and 5b. Model evaluation of environment shape	63

Chapter III.

Figure 1. Conceptual model of energy flows between <i>L. stagnalis</i> , <i>D. magna</i> , lettuce, and algae	78
Table 1. Experiment treatment codes	78
Figure 2. Image of modelled environment	81
Figure 3. Relationship between <i>L. stagnalis</i> length and algae-based carbon concentration	83
Figure 4. Relationship between total and algae-based carbon concentrations	83
Figure 5. Experimental population counts for all treatments and replicates	85
Figure 6. Experimental population mean counts for all treatments	86
Figure 7. Distributions of lengths for treatments across selected timepoints	87
Figure 8. Length distributions stacked by treatment for selected timepoints	87
Figure 9. Length distributions stacked by day for all treatments	88
Figure 10. Growth through 28 days of starting <i>D. magna</i> with fitted von Bertalanffy functions for all treatments.....	90
Figure 11. Relationship between length and dry mass of juvenile and adult <i>D. magna</i>	91
Figure 12. Relationship between length and dry mass of juvenile and adult <i>D. magna</i> labeled by treatment	91
Figure 13. Elemental proportions for adult and sub-adult <i>D. magna</i>	92
Figure 14. Relationships between size and elemental proportions for adult <i>D. magna</i> by treatment	93
Figure 15. Algae-based and total carbon concentrations by physical distribution, treatments, and time	95
Figure 16. Growth of <i>Lymnaea stagnalis</i> by treatment through time with fitted von Bertalanffy functions	96
Figure 17. Model output against experimental data from ASD scenario	99
Figure 18. Model output against experimental data from SLD scenario.....	99
Figure 19. Model output against experimental data from ASLD scenario	100

Figure 20a, 20b, and 20c. Model output against experimental data for all scenarios	100
Figure 21a, 21b, 21c, and 21d. Experimental data for all treatments against AD treatment	101

Chapter I.

A Bioenergetic Model Accounting for the “Neighborhood Effect” and Characteristics of Experimental Environments on *Daphnia magna*

Introduction:

In light of expanding human activities and their ecological impacts, robust approaches are needed by which these impacts can be explored and predicted to limit further loss of biodiversity and ecosystem services (Hoekstra and Wiedmann, 2015; Mace, 2014). Chemical stressors released to the environment as a result of increased anthropogenic activities can reduce biodiversity and alter ecosystem function (Beketov et al., 2013; McMahon et al., 2012). As such, Ecological Risk Assessment (ERA) is used to inform policy and ideally does so by providing robust estimates of the likelihood and magnitude of adverse ecological effects from exposure to environmental stressors including chemicals (EPA, 1998; 2004). In turn, a key goal of ecotoxicological research is to provide data and tools that inform ERAs and lead to improved understanding and prediction of effects of manufactured chemicals on natural systems. Most efforts to improve our ability to predict adverse effects of chemicals are based on integrating ecological methods and toxicological information (Truhaut, 1977; Chapman, 2002; and Leiss, 2002) in order to specifically address the source of adverse effects (Heugens et al., 2001).

All ERAs include three main components: problem formulation, risk analysis (analyzing the potential ecological effects), and then risk characterization--which is a discussion of the analysis results and inherent uncertainties (EPA, 1998; 2004). In essence, ERAs represent the

linkage between science, public policy, and conservation of natural environments. In practice, the ecotoxicological data used to estimate potential ecological effects and subsequently, *risk*, are typically obtained from highly controlled, single-species, laboratory toxicity tests (e.g., Heugens et al., 2001)). The disparity between data obtained from toxicity tests and the natural systems they are designed to protect (Forbes et al., 2011) has been a common criticism of ERA methods (Rohr et al., 2016). Rohr et al. (2016) suggested approaching this disconnect from both complex system level experiments/models and sub- or organismal level experiments/models. This ‘top-down’ and ‘bottom-up’ combined approach will allow linking ecological and stressor complexities (Laender et al., 2008a and 2008b; Beketov and Leiss, 2001; Faber and Wensem, 2012; Gabsi and Preuss, 2014; Gabsi et al., 2014; Smetanova et al. 2014; Orlinskiy et al., 2015) to mechanistic drivers (Laetz et al., 2009; Sibly et al., 2013; Forbes and Calow, 2013b). Not only are these methodological suggestions likely to increase confidence in ERA output, but they also avoid the costly, complicated, and unlikely shift away from single species toxicity tests (Rohr et al., 2016). One possible path forward for connecting levels or organization is to start at the individual-level and seek to predict effects under increasing ecological complexity.

Efforts to implement the abovementioned advances in ERA are perhaps most likely to occur through mathematical methods that link levels of biological organization. This approach would not necessarily require additional study designs beyond organism-level laboratory assessment, but may provide risk estimates relevant to higher levels of biological organization (Rohr et al., 2016; Suter et al., 2005). Linking levels of biological organization has been well-supported and modeled through energetic flow between trophic levels (e.g., Carpenter et al. (1987); Fath et al. (2004)) due to both observed manipulations (e.g, Carpenter et al. 1987) and theoretical reliance on laws of thermodynamics (Fath et al., 2004). In the context of stress

ecology, Sokolova (2013) provided a strong argument for the conceptual connection between organismal bioenergetics and the organism's ability to tolerate/mitigate stress. The organism, when exposed to a stressor, can be thought of as moving through a spectrum from a 'pejus' level (stressed but ecologically functional) to a 'pessimum' (lethal level) where basal metabolic demands cannot be met. A spectrum of bioenergetic demand due to stressor exposure follows a strong logical and observed base that mitigation or tolerance of stress can be explained by the ability or inability to generate ATP (Sokolova, 2012). As well, interactions between energy and stressors have similar characteristics at multiple levels of biological organization. Utilization of bioenergetic principles and processes in a formalized modelling framework could allow a robust

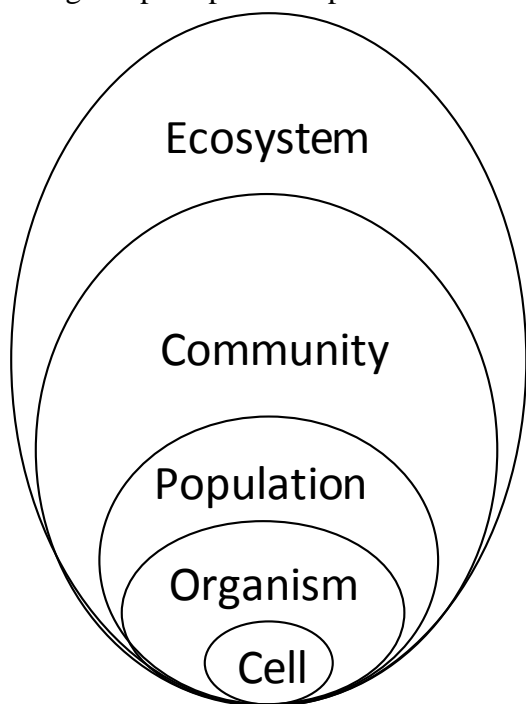


Figure 1. Conceptual schematic demonstrating *nested* framework of system level compartments.

quantitative linkage between toxicity tests and larger natural systems (e.g., Martin et al. 2013; Jager et al., 2014) Predicting adverse effects of anthropogenic stressors necessitates linking chemical effects on individual survival and reproduction to impacts on populations and the corresponding communities and ecosystems. Ideally, as suggested by the Adverse Outcome Pathway (AOP) framework (Ankley, et al., 2010)) models that include the individual level can ultimately be extended to lower levels of biological organization (cellular and molecular) but model

simplicity and reduced data requirements are important considerations (Jusup et al., 2016 and Rohr et al., 2016). This *nested* conceptual model (organisms within populations within

communities, etc. See Figure 1 below.), when informed by the bioenergetics within and among system compartments, can be used to quantitatively describe and ideally predict effects observed at different ecological scales. The Dynamic Energy Budget Theory for Metabolic Organization (DEB) is a specific framework with a strong mathematical foundation (Kooijman, 2010) that can provide the modeling core of this *nested* framework—describing the growth and reproduction of individual organisms in context of resource density and stressor exposure (Kooijman, 2010).

Bioenergetic models based on DEB principles are distinguished from more traditional static bioenergetic budget models (e.g., Wisconsin model, Kitchell et al, 1977) by their dynamic, systems-based approach and theoretical basis in cellular mechanisms. One of the core advantages of the DEB model for organism growth and reproduction (in relation to traditional methods) is the removal of age or life-stage as a critical parameter. For example, within DEB models, life-stage changes are determined by accumulation of energy into “buffers” that contribute to maturity and influence reproductive allocation and other potential fluxes that determine growth or maintenance. This is distinctly different than relying on observations of mean age at first reproduction, for example, and provides a mechanistic and “first principles” platform of support (see Jusup et al., 2016).

Although the DEB theory provides a powerful framework of modeling and theory development, there is a continuing discussion on the value/strength of DEB models (Jusup et al., 2016). One particular concern regarding DEB models is the number and abstractness of DEB parameters and state variables that present a barrier to use and cannot easily be directly tied to empirical observation. For example, the DEB model state variable ‘reserve’ does not correspond to a more intuitive and measureable energy storage as, for example, fat reserves. DEB ‘reserve’ is energy that has been assimilated but not yet allocated. While this allows the DEB model

dynamics to perform so well, the definition: “[...] reserve does *not* mean ‘set apart for later use’; reserve ‘molecules’ [...] [are] ‘waiting’ to be used” does not provide much room for empirical measurement (Kooijman, 2010, pg. 3). In an effort to avoid these difficulties, Jager et al. (2012) provided derivations of the functions in a standard DEB model that can effectively predict growth and reproduction but using a much simpler and shorter set of equations. Not only have these simplifications of DEB models been shown effective in common toxicity test organisms *Daphnia magna* (Jager et al., 2012) and *Lymnaea stagnalis* (Zimmer et al., 2012), but their derivation to von Bertalanffy growth functions (von Bertalanffy, 1938) allow a useful relation to commonly applied bioenergetic-based growth models (WI model, etc.).

Another valuable and key distinction between static bioenergetic models, like the WI model, and DEB models is the fairly strict focus on individual energetics. Common applications of the WI model rely on an “average” animal that represents the mean of a population (see review by Hansen et al., 1993). This allows for easy expansion to population biomass as a key metric (see review by Hansen et al., 1993). This simplification of computational methods was largely due to hardware/software available at the time. However, it is noted (even in the seminal work of Kitchell et al., 1977) that individual metrics (e.g. body mass) respond to environmental dynamics more quickly than population metrics (e.g. population size) (Sibly et al., 2012) and are likely more valuable output. With the advent of accessible computational power, explicit modelling of individual bioenergetic dynamics through DEB models has become an area of extensive research (Sibly et al., 2012, Grimm and Railsback, 2005, Martin et al., 2012, etc).

Once a bioenergetic model can predict growth and reproduction of an individual, an individual-based model (IBM) can be used to predict growth and reproduction of a population of individuals (Grimm and Railsback, 2005). Very simply put, an individual-based model

simulates every individual in the population and population dynamics emerge from the interactions among individuals and their environment (Vidal, 2007). Hence, the linkage of the DEB and IBM frameworks provides a methodology for linking across levels of biological organization.

Currently, there are several published IBMs for the model freshwater invertebrate, *D. magna*, all with different strengths. The goal of the current work is to combine these approaches to maximize the particular value of each model. Martin et al. (2013) provided an excellent DEB-IBM through thoroughly modeling *D. magna* individual bioenergetics but also using a dynamic environment to influence conditions and DEB rates for each individual. This DEB-IBM construct has also been well supported as a model to explore effects of energetic stressors on populations (Martin et al., 2014) and as a key demonstration of the use of free open-source software (NetLogo, Wilensky, 1999; Martin et al., 2012). The spatially-explicit design of the *D. magna* DEB-IBM model of Martin et al. (2012) additionally provided flexibility to add a dimension of complexity and realism through spatial manipulation. Preuss et al. (2009) provided an approach that focused less on organismal energetics and more on a key intra-species interaction—crowding. Their population model was an important advancement for an organism that has strong density-dependent population dynamics under many conditions (e.g. Lampert, 2005). The modelling approach developed by Preuss et al. (2009) provided an additional avenue for a more explicit spatial approach but could be improved by a generic individual-based energetic sub-model (such as DEB) to further explore interactions between density impacts and chemical stressors.

These two modeling approaches can be merged to maximize the strengths of each—the DEB-IBM approach of Martin et al. (2013, 2014) provides the software platform and the

bioenergetic framework while the crowding IBM of Preuss et al. (2009) provides a behavioral/spatial dynamic that is highly relevant to *D. magna*. Beyond the logical and mathematical strength of the above models, they both also produce output that matches experimentally observed population dynamics of *D. magna*.

The primary objectives of the current research were to: (1) combine the strengths of the above modeling approaches for a unique *D. magna* DEB-IBM that closely reflects experimental conditions commonly employed in laboratory toxicity testing, and (2) compare model output of individual- and population-level metrics against observed populations of *D. magna*. A secondary goal was to demonstrate how the current DEB-IBM could be applied to existing toxicity data for a model toxicant, the fungicide pyraclostrobin. Finally, the model is discussed with regard to recent applications of energetic models in ecotoxicology and risk assessment and future areas of continued development and testing.

Methods:

***D. magna* Laboratory Population Dynamics:**

To evaluate the performance of the DEB-IBM we compared model output to laboratory *D. magna* populations. Experimental populations of *Daphnia magna* (purchased from Aquatic BioSystems) were housed in moderately hard synthetic freshwater (US EPA, 2002) in one, two, and three-liter glass beakers and observed for 40 days. Five 1L chambers were started with five neonates (< 24 hours old), one 2L container was started with seven adults and 68 neonates, and one 3L container was started with > 171 neonates. The 2 and 3L chambers were started at higher densities to explore effects of different starting population sizes and size-class distributions.

Ninety percent water changes were performed every other day to avoid need for aeration and water quality degradation. Population sizes and individual organism lengths were recorded during each media change while the old media was removed. Organisms were fed concentrated (3.0×10^7 cells mL^{-1}) *Raphidocelis subcapitata* (formerly known as *Psuedokirschneriella subcapitata* and *Selenastrum capricorutum*, also purchased from Aquatic BioSystems) corresponding to $\sim 1.65 \times 10^5$ cells mL^{-1} , ~ 0.0012 mg Carbon mL^{-1} , or 0.5% of experimental media by volume (as concentrate) on each water change. Temperature was stable at 20°C and lighting was cool fluorescent with a 16 hour-on, 8 hour-off cycle.

At each water change, digital images were recorded (approx. 10) from directly above the experimental chambers. A ruler placed under the beakers was used to set the scale of the images. Image J (Version ij150, 2016) was used to count the number of individuals and measure lengths (eye spot to base of spine). The number of lengths measured per replicate was not consistent due the nature of daphnid movement during photography, but every effort was made to obtain lengths for 25% of total population size. Program R (Version 3.1.1, R Core Team, 2016) was used for data inspection and analysis.

Table 1. Concentrations of ion constituents in moderately hard water used for *D. magna* experiments.

Salt	Concentration
Calcium Sulfate (CaSO_4)	60 mg l^{-1}
Magnesium Sulfate (MgSO_4)	60 mg l^{-1}
Sodium Bicarbonate (NaHCO_3)	96 mg l^{-1}
Potassium Chloride (KCl)	4 mg l^{-1}

Pyraclostrobin Chronic Toxicity Experimental Setup:

One important application of the DEB-IBM developed here is for predicting the effects of toxicants on *D. magna* populations. Data from standardized toxicity tests (OECD Test Number

211) on the fungicide, pyraclostrobin, were used only for development and demonstration purposes. Briefly, single *Daphnia magna* individuals were exposed to 0, 4, and 8 $\mu\text{g L}^{-1}$ of the strobilurin pyraclostrobin in 50 mL of media, and fed concentrated (3.0×10^7 cells mL^{-1}) *Raphidocelis subcapitata* (formerly known as *Psuedokirschneriella subcapitata* and *Selenastrum capricorutum*, purchased from Aquatic BioSystems) corresponding to $\sim 2.31 \times 10^5$ cells mL^{-1} , ~ 0.00168 mg Carbon mL^{-1} , or 0.7% of experimental media by volume (as concentrate) on each water change (every third day). Temperature was approximately 21°C and organisms were on a complete dark phase to limit influence of algal activity on pyraclostrobin concentration. Acetone was used as a carrier for pyraclostrobin; 0.1% v/v, and showed no effect during pilot and experimental tests. Daphnid length from base of spine to eye spot at 21 days was the metric of interest to explore sublethal effects at these relevant concentrations (Cui et al., 2016).

Exposure based difference between lengths at day 21 were used to calculate the proportional change in DEB parameters. Due to the mechanism of action of pyraclostrobin (interruption of mitochondrial respiration and ATP generation; Bartlett et al., 2002) and evidence of strobilurin effect on metabolic rate (Warming et al., 2009) DEB parameter \dot{k}_M , as per Jager et al. (2012), was adjusted by each exposure treatment's DEB parameter proportional change.

DEB-IBM Model for D. magna:

Model development was conducted in NetLogo (Versions 5.3.1, Wilensky, 1999) and R (R Core Team, 2016) simultaneously. Generally, functions were explored in R prior to implementation in the NetLogo environment.

Using simplified DEB functions from Kooijman (2010, and Jager and Zimmer (2012)) and using DEB parameters from the 'add_my_pet' (http://www.bio.vu.nl/thb/deb/deblab/add_my_pet/index.html) database for female *D. magna*, a

DEB-IBM was created in NetLogo (Wilensky, 1999). Stochasticity as parameter variability was not explicitly included in sub-models to isolate impact of spatial heterogeneity that may result in stochastic outcomes. To emulate experimental conditions, I created a 3-dimensional environment representing an experimental chamber holding 1000mL of media and phytoplankton food sources—an expansion of Martin et al.’s (2013) model—where individual daphnids were impacted not only by the local food quantity, but also by their local density (e.g., Preuss et al. 2009), what I refer to here as the “Neighborhood Effect.”

Below is a pseudo-code in simplified NetLogo syntax describing the order of submodels and procedures in each daily timestep. In general, the patch conditions of stressor and algae were manipulated first, then daphnid parameters were updated. Updated parameters were used to then grow, reproduce, potentially die, and then lastly, move.

```

to go
  ask patches [
    ifelse time-to-apply-stressor [
      set stressor random-normal mean sd
    ] [
      set stressor stressor * decay-rate
    ]

    ifelse count daphnia-here >= 1 [
      set algae (algae - (ingestion-rate * count daphnia-here))
    ] [
      set algae random-normal mean sd
    ]
  ]

  ask daphnia [
    calculate-neighborhood-effect
    calculate-f
    calculate-ingestion-rate
    calculate-dL
    grow
    calculate-reproductive-output
    reproduce
    die?
    move
  ]
end

```

Output and input to the model were flexible and could be adjusted based on specific, desired outputs (mean size versus histogram of all sizes or magnitude and mode of action of stressors). One of the major goals of the current modeling effort was to continue the “generic” framework presented by Martin et al. (2013) that allows a modeler to specifically address needs of their individual organisms or systems (e.g. behavioral characteristics or experimental chamber size/shape) while still maintaining a fairly constant model ‘core’ (DEB-IBM).

Submodel Section:

DEB Growth Model

Growth of organisms was assumed to follow the von Bertalanffy growth function (VBG) with rapid early growth that tapers to a maximum limit (von Bertalanffy, 1938). Via dynamic energy budget parameters, growth can be modeled in this fashion with a few functions.

$$f = \frac{[food]}{[food] + K} \quad \text{eq. 1}$$

$$L_{\infty} = \frac{f \dot{v}}{g k_M} \quad \text{eq. 2}$$

$$\dot{r}_B = \frac{k_M g}{3(f + g)} \quad \text{eq. 3}$$

$$\frac{d}{dt}L = \dot{r}_B (L_{\infty} - L) \quad \text{eq. 4}$$

where f is the functional response value, expressed as a relative value (0-1) with 0 indicating starvation and 1 *ad libitum* food availability. K is the half-saturation constant for the given food type at a concentration that corresponds with an f of 0.5. It is worth noting that this hyperbolic function is the core and essential connection between an organism and its environment in the DEB framework (see Beaudoin et al. (2015) for a sensitivity analysis of DEB parameters). L_{∞} is the maximum length attained by an organism at a given functional response value, f , with

standard DEB parameters \dot{v} , g , and \dot{k}_M (eq. 2). \dot{v} is an abstract DEB parameter and is interpreted as energy conductance with units of length time⁻¹. By definition, \dot{v} is surface-area-specific maximum assimilation rate divided by maximum energy density (J per l^3). As only energy density can be measured, estimates for other parameter values are derived by solving the full DEB models. Conceptually, a moiety moving at a given rate (assimilation rate) through a media of a given density (energy density) would have a velocity—this is the conceptual driver for \dot{v} as assimilation processes require that food items move across membranes and barriers. g is the energy investment ratio, and while it remains fairly abstract, it is more easily explained as the ratio of the energetic cost of structure divided by the maximum energetic density of somatic structure multiplied by the ratio of energy allocated to non-reproductive processes. \dot{k}_M is a somatic maintenance rate coefficient that represents the volumetric somatic maintenance rate divided by the volumetric energetic cost of soma.

The functions described above (Jager et al., 2012) are simplifications of a ‘full DEB’ model and one of the major assumptions that allow this simplification is that if the reserve compartment (Figure 2 below) has constant inputs and outputs, allocation to structure (and accordingly reproduction) and maintenance costs will remain constant and growth will follow the generalized form of a von Bertalanffy curve (von Bertalanffy, 1938). For organisms that do not have large changes in body shape (isoforms) during their lifetime this model performs very well. For my purpose of modeling *Daphnia magna* growth over an experimentally relevant time period, this simplification is reasonable and affords more allocation of computational power/effort to environmental or behavioral complexities.

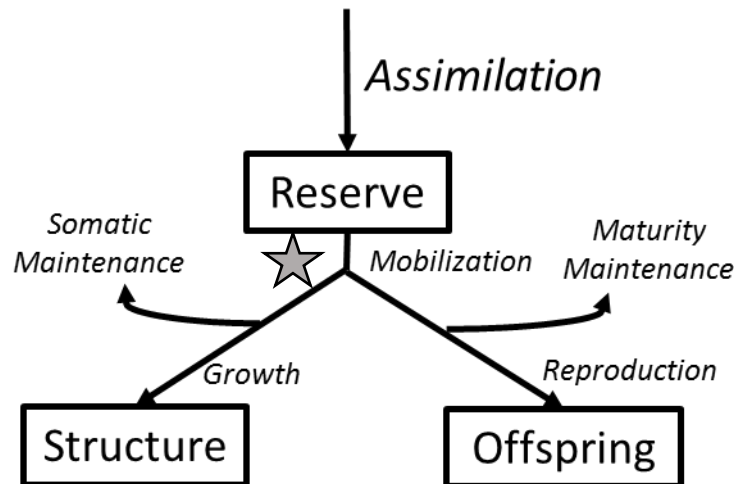


Figure 2. Simplified schematic of DEB system model. Additional simplifications allow truncation at mobilization node (star).

For a more complete listing of parameters used in the complete and sub- models, see Table 2.

Modeling Juvenile Starvation Mortality

Starvation is a function of a critical mass threshold, animal condition (f), and physical length (as compared to volumetric length). Using Martin et al.'s (2013b) critical mass of 0.4 of maximum attained volume as a threshold for unavoidable, *per capita* mortality as inspiration, the function:

$$\frac{1}{f/L_{phys}} * 0.4 \quad \text{eq. 5}$$

was used to define a threshold for mortality as a function of organism size and 'condition'. As the current model does not contain the "full DEB" parameter 'reserve,' eq. 5 acts as a combination of the physical size threshold (0.4 of maximum attained size) and the scaled reserve condition of the organism ($1-e$). Unavoidable per capita probabilistic mortality (parameterized at

0.35) was calculated using similar functions as Martin et al. (2013b). As such, starvation based mortality was probabilistically determined by an ‘if’ statement (eq. 6):

$$if\ random - float\ 1 < \left(\frac{1}{f} * 0.4 \right) * \left(1 - (1 - 0.35)^{\frac{1}{timestep}} \right) [die] \quad eq.6$$

Essentially, this ‘if’ statement controls the code for the starvation threshold (eq. 5) and a mortality constant (0.35 day⁻¹) with a common per capita mortality probability function (as per Martin et al., 2013b) to determine if a shrinking daphnid will die. Starvation mortality takes place during the die? procedure.

Martin et al. (2013b) specifically addressed starvation mortality and starvation recovery as a shortcoming in daphnid population models and a key objective here was to provide this method as a suggested improvement. The core of this suggestion lies in allowing “recovery” due to movement to patches that increase f values and thereby decrease the effect of body size. By not including reserve in this model, the lag time of size effect from shifts in f need to be accounted for. Behaviorally, this would be addressed by movement, and by including this in the size/condition threshold (eq. 5) the model accounts for individual movements to areas of greater resource density.

The Neighborhood Effect on Movement

Under the premise that daphnids tend to aggregate towards areas of high resource density but also avoid con-specifics (Cuddington and McCauley, 1994; Neary et al., 1994; Larsson, 1997; Jensen et al., 2001; Lampert, 2005) the probability of moving to a patch with higher algae density (in the move procedures) was modeled as a hyperbolic curve (see Figure 7 in Lampert (2005)). The explanatory axis of that function is a “crowd” count (number of daphnids in 27mL “neighborhood”) (or converted to mL of container available per daphnid as in Preuss et al. (2009)) and the response is a proportional (0-1) measure of the ‘Neighborhood Effect’

magnitude. The word neighborhood comes from NetLogo syntax, and corresponds to the 27 adjacent and interior cubic patches that a daphnid could inhabit or interact with. As daphnid density decreases (the ‘Neighborhood Effect’ decreases), daphnids move more randomly (i.e. less local competition for resources or less physical contact) and as density increases, the Neighborhood Effect hyperbolic function guides daphnid movement towards areas of higher resource density (and, due to high rates of local ingestion, away from con-specifics). The neighborhood effect ($NE_{Movement}$) using the count of daphnids in the local 27 mL ($CrowdCount$) and the half-saturation constant for movement ($HSC_{Movement}$) was modeled as:

$$NE_{Movement} = \frac{CrowdCount}{CrowdCount + HSC_{Movement}} \quad \text{Eq. 6}$$

The Neighborhood Effect on Reproduction:

Using the work of Preuss et al. (2009) as inspiration for the impact of localized density on reproductive output (brood size decreases as density increases; see Figure 3 below), a hyperbolic function (similar to above) was used to determine the probability of reproducing and the reduction in brood size (assuming reproduction occurs) during the reproduce procedures. The half-saturation constant for reproduction ($HSC_{Reproduction}$) was set at 17.5 daphnids mL⁻¹.

$$NE_{Reproduction} = \frac{CrowdCount}{CrowdCount + HSC_{Reproduction}} \quad \text{Eq. 7}$$

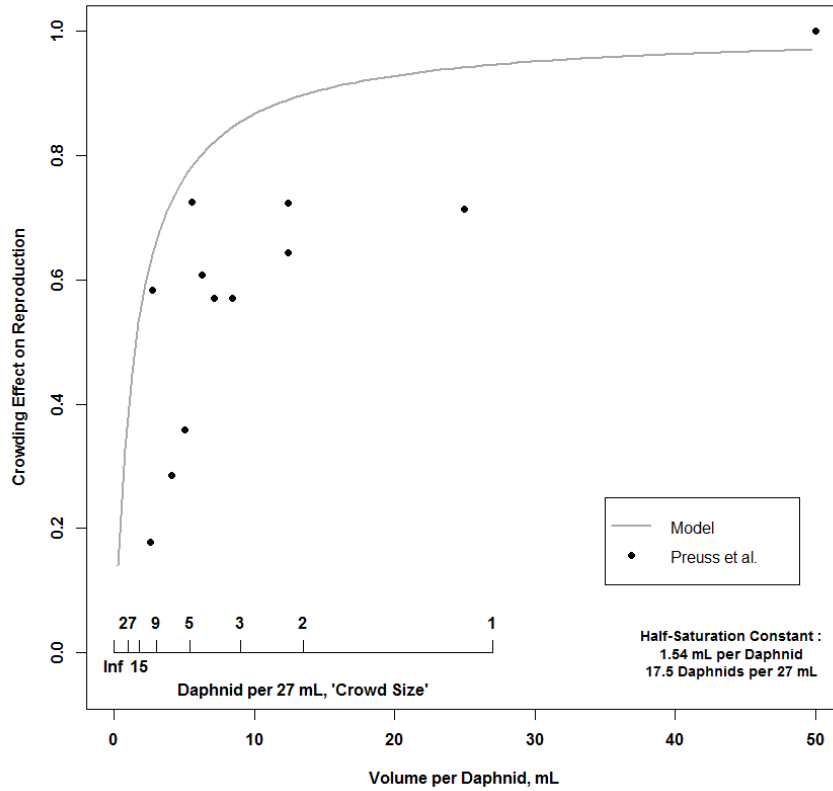


Figure 3. The hyperbolic function used to model the neighborhood effect on *D. magna* reproduction plotted against data published in Preuss et al. (2009) showing reduction in brood size by volume of media per daphnid. Notice inverse x-axes for crowd size and volume per daphnid independent variables. This specific function has a crowd size of 17.5 daphnids mL⁻¹ as a half-saturation constant. Occurrence of a reproductive event is also modeled by using a random number between 0 and 1, and if random number is below modeled $NE_{Reproduction}$ reproduction occurs.

Reproduction as Function of Length:

Cumulative reproductive output was modeled as a function of length, and iterative output only occurs on a ‘pulsed’ frequency (e.g., every 2.5 days for *D. magna*). The iterative magnitude is a function of cumulative reproduction divided by the age of the organism. The function below is from Kooijman (2010; Figure 2.10).

$$CumulativeReproduction = aL^2 + \frac{k_M}{\psi} L^3 - bL^2 \quad \text{Eq. 8}$$

With a and b as fitting parameters adjusted to fit observed data from experimental organisms (See Figure 3 for a demonstration of fitted functions).

To avoid the unknown or generally unavailable L_R term, bL^2 is used as a potentially more flexible replacement. Figure 4 below demonstrates the data used to parameterize a and b from my lab data ('East') and also from published datasets ('Martin' and 'Preuss').

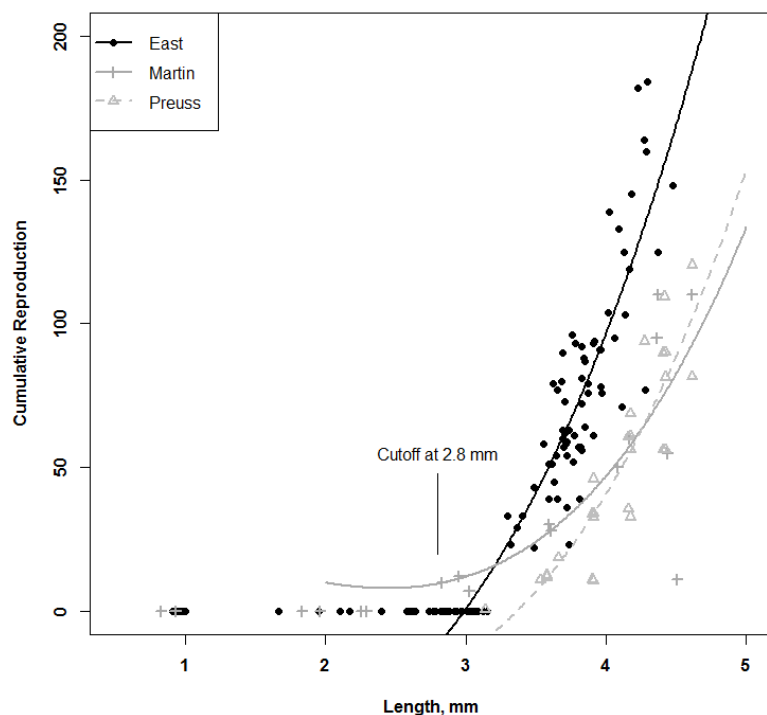


Figure 4. Cumulative reproduction as a function of length from three datasets. Points represent observations from authors East (black dot and line), Martin et al. (2013b) (gray cross and line), and Preuss et al. (2009) (gray triangle and dashed line). Lines are cumulative reproduction functions (Eq. 8) fitted (`{nls}` package) at first reproductive event thresholds 2.8 mm (East and Martin et al.) or none (Preuss et al.). a for lines are -1.599, -10.277, -7.372 and b 58.882, -30.290, 22.473 in order of legend. All three datasets are from similarly designed 21-day experiments with feeding levels $>1.1 \text{ mg C L}^{-1}$ and 1 individual daphnid per 50 to 100 mL of moderately hard media.

Energetic Stressor Effect Submodel:

To apply my *D. magna* DEB-IBM in an ecotoxicological context, I used model formulations from Jager and Zimmer (2012) to determine DEB parameter effects of energetic stressors (sublethal), at an individual level. This method uses the theoretical and quantitative framework of DEB to alter parameters due to exposure. Experimental endpoints (such as length) are used to quantify the shifts in individual model parameters. For demonstrative purposes, strobilurin fungicides act through decreasing ATP generation (Bartlett et al., 2002) and can be modeled as increasing the DEB model parameter: somatic maintenance rate coefficient (k_M). Warming et al. (2009), provided evidence that strobilurin fungicides (azoxystrobin) can increase

metabolic rates of daphnids by as much as 33% at environmentally relevant concentrations. An overall increase in metabolic activity was suggested by Sokolova (2013) as a potential compensatory characteristic of reduced ATP supply. While \dot{k}_M will not increase in the same magnitude as overall respiration rates as the DEB model parameter does not represent the same energetic process, this does support the overall hypothesis that \dot{k}_M will increase alongside empirical metabolic rate observations. In essence, sublethal energetic effects of strobilurin fungicides may be effectively modeled at an individual level by altering DEB parameter \dot{k}_M .

Our research on the effects of pyraclostrobin demonstrate that daphnid length at 21 days can be impacted by concentrations as low as $8 \mu\text{g L}^{-1}$ (Lockett, in prep.). Figure 5 shows that there is a pattern of decline in size at day 21 due to exposure to pyraclostrobin (Fig. 5a). These data can be used in the DEB function framework (Equations 2 and 3 above) to predict changes in allocation processes of individuals (Fig. 5b).

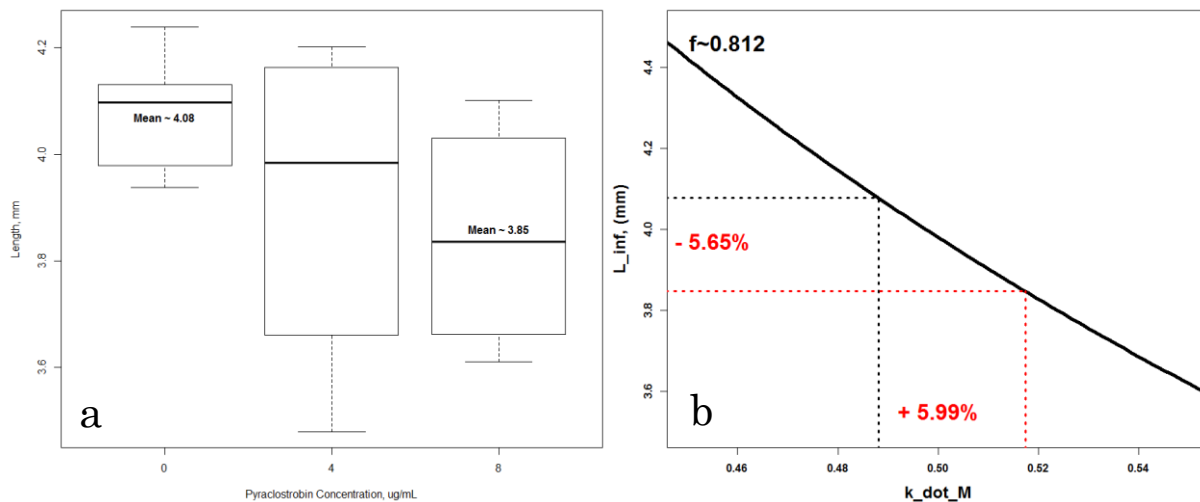


Figure 5a and 5b. Effect of pyraclostrobin on day 21 length of *D. magna* (LEFT) and plot of day 21 length, maintenance coefficient, and DEB-based function at a given food level (RIGHT). Based on the left data, \dot{k}_M can be adjusted to represent individuals that are exposed to pyraclostrobin as per the DEB function visually demonstrated on the right. Using the day 21 size as a final size, an f of 0.812 can be estimated and then corresponding decreases in size (-5.65%) can be related to increases in DEB maintenance rates (+5.99%) due to increased energy allocation due to stressor tolerance activities.

Of note is that this shift of k_M only occurs in the growth functions. Reduced reproduction due to reduced energetic allocation to reproduction processes would be accounted for in the smaller size of organisms and not by adjusting Equation 8 above. Appendix A, Figure A7 demonstrates the quantitative outcome of this principle.

Modeling Stressor Exposure:

In model scenarios with chemical stressors, the stressor was probabilistically distributed but occurring every third day (representing common media change rates) and was modeled with a 2 day half-life breakdown. Thus, individual maintenance rate parameter adjustments were made by the stressor level present in the given patch at the given time rather than an overall application. In addition, to represent potential experimental designs, the chemical stressor was only ‘applied’ for the first 30 days of the 40-day simulation.

Table 2. Table describing model parameters with values for *D. magna* as per sources or fitted by author.

Parameter	Units	Value	Source	Function	Description
K	$\# l^{-3}$	1661.539	Martin et al.	--	Half-Saturation Constant
f	unitless	--	--	$f = \frac{[food]}{[food] + K}$	Functional Response Value
\dot{v}	$L t^{-1}$	0.1584	Martin et al.	--	Energy Conductance
g	unitless	2.44936	Martin et al.	--	Energy Investment Ratio
\dot{k}_M	t^{-1}	0.488075	Martin et al.	--	Somatic Maintenance Rate Coefficient
L	L	--	--	$V = L^{1/3}$	Volumetric Length
L_{phys}	L	--	--	$L_{phys} = L * shape_factor$	Physical Length
$shape_factor$	unitless	0.2637	Martin et al.	$shape_factor = V^{1/3} / L$	Shape Coefficient
L_{∞}	L	--	--	$L_{\infty} = \frac{f \dot{v}}{g \dot{k}_M}$	Asymptotic von Bertalanffy Length
\dot{r}_B	t^{-1}	--	--	$\dot{r}_B = \frac{\dot{k}_M g}{3(f + g)}$	von Bertalanffy Growth Rate
$CrowdCount$	$\#$	variable	--	--	Count of Daphnids in 27mL 'Neighborhood'
$HSC_{Movement}$	$\#$	1.75	East	--	Half-Saturation Constant for Movement Neighborhood Effect
$HSC_{Reproduction}$	$\#$	17.5	East	--	Half-Saturation Constant for Reproduction Neighborhood Effect
$NE_{Movement}$	unitless	--	--	$NE_{Movement} = \frac{CrowdCount}{CrowdCount + HSC_{Movement}}$	Neighborhood Effect on Movement
$NE_{Reproduction}$	unitless	--	--	$NE_{Reproduction} = \frac{CrowdCount}{CrowdCount + HSC_{Reproduction}}$	Neighborhood Effect on Reproduction
a	unitless	--	--	--	Cumulative Reproduction Fitting Parameter
b	unitless	--	--	--	Cumulative Reproduction Fitting Parameter

Results:

Experiment Results:

Experimental *D. magna* populations in one liter chambers showed common patterns of rapid increases during first and second reproductive events around days 9 or 10, with a peak in population size near day 20, and then declining towards an equilibrium between 50 and 100 organisms near day 40 (Figure 6). The two and three liter chambers showed slightly different patterns—the daphnid population in the 3L increased earlier due to the high number of neonates and adults at start, but this population had not approached any sort of equilibrium by 40 days. The daphnid population in 2L did not increase until there was a large die-off around day 7, but then population numbers stayed fairly steady at approximately 120 individuals.

To demonstrate the Neighborhood Effect, mL of water per daphnid data (Figure 7) suggest that an equilibrium condition will be reached (all other conditions being equal) at approximately 15 mL per daphnid and this was used to support a crowding threshold or optimal density of daphnids in a local environment. This daphnid density is also supported by the data of Lampert (2005) and Preuss et al. (2009) that respectively suggested that biomass per unit of volume approaches a plateau and that reduced volume per daphnid is linked to increased mortality and reduced reproductive output.

Daphnid size-class structure in the one liter chambers showed common patterns through the experiment duration (Figure 8). Of note is the generally right-skewed distribution, but more

importantly, the right-ward shift of the peak, demonstrating that new neonate production had declined as the populations approached equilibrium levels near day 40.

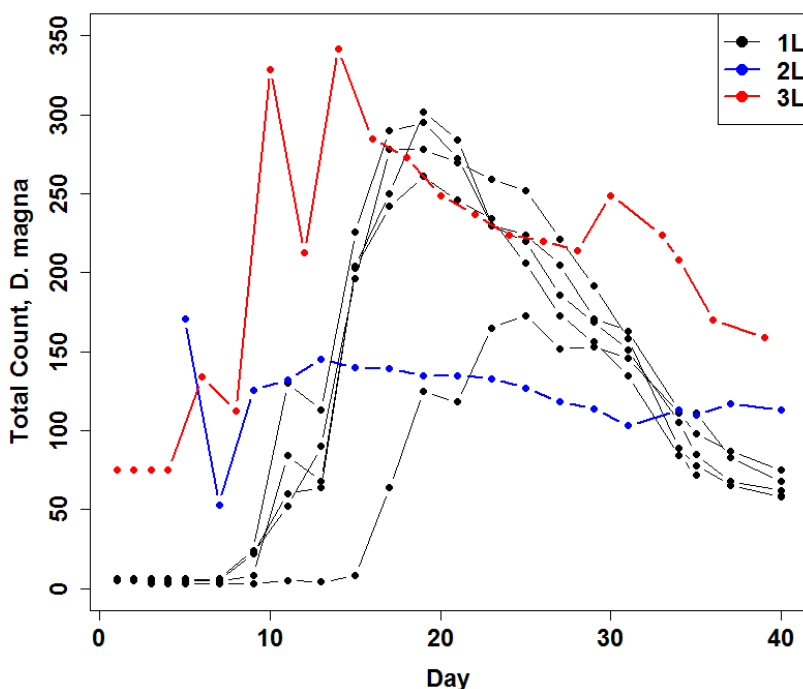


Figure 6. Total *D. magna* counts in 1, 2, and 3 L chambers through 40 days. The two liter chamber was started with more than 170 juveniles that were not counted until the fifth day (minimal mortality was observed until the next observation point). The three liter chamber was started with 68 juveniles and 7 adults. These chambers were set up as comparisons for populations that start at different densities and age structures.

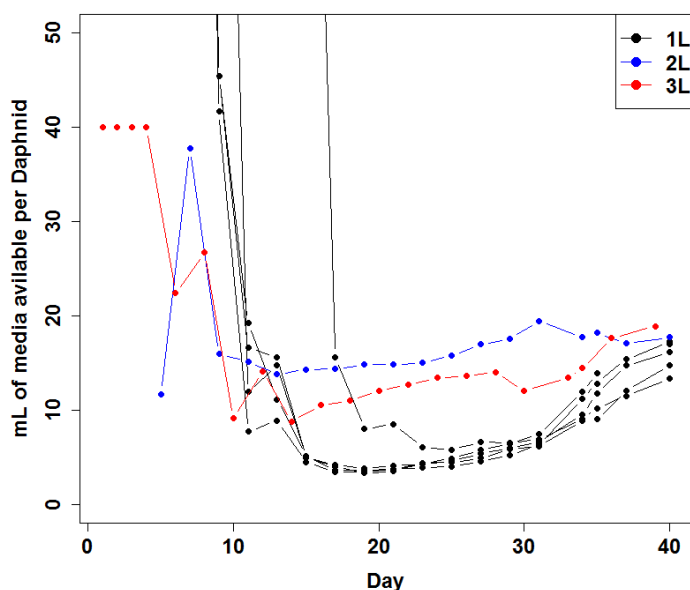


Figure 7. Plot showing mL of media available in experimental chamber per daphnid present. Y-axis is limited to below 50mL to simplify visualization. This plot is included as a comparison to Preuss et al. (2009) and suggests 15mL per daphnid as a target neighborhood size.

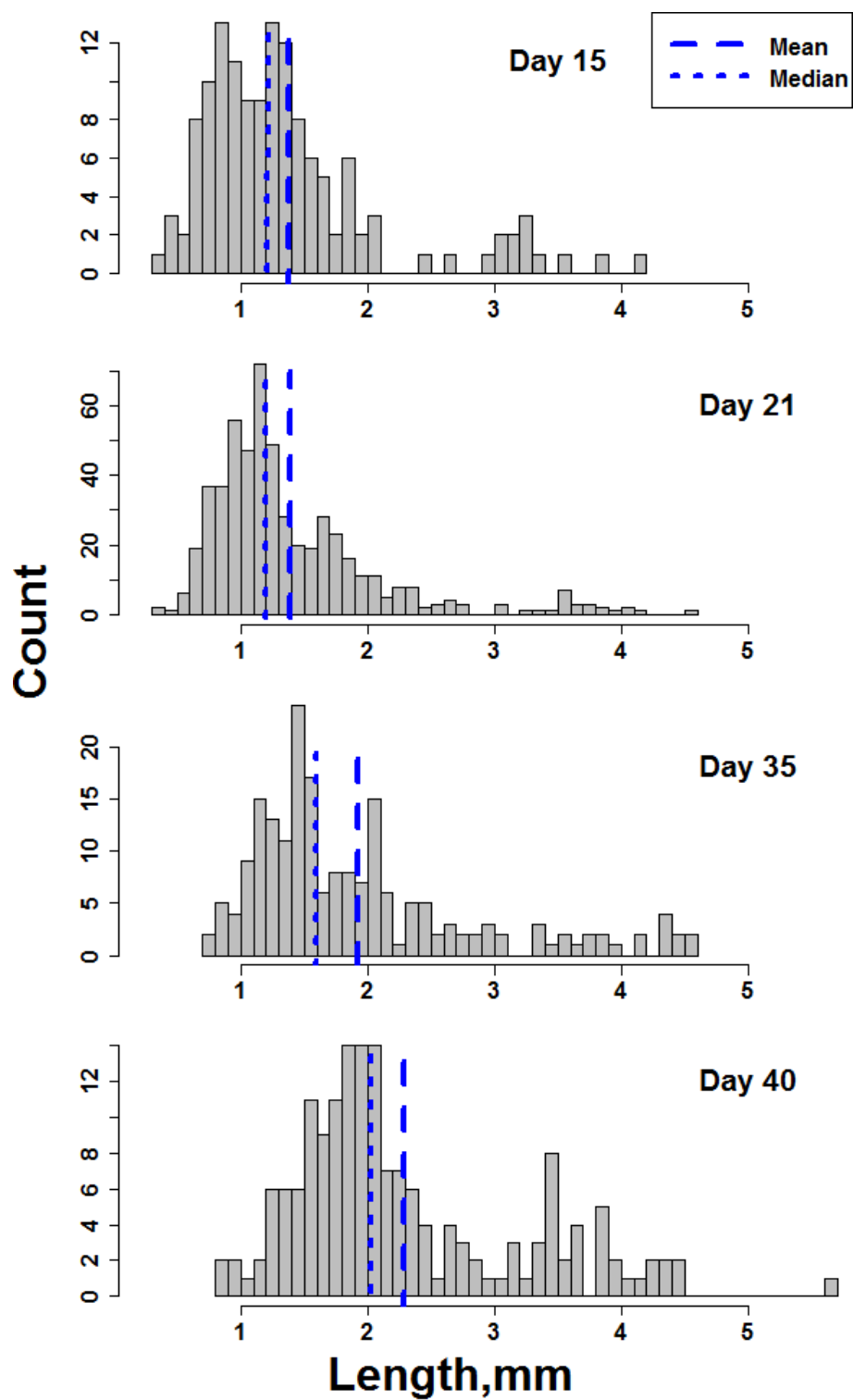


Figure 8. Four histograms of size distributions from 1-liter chamber population data (all five replicates) with mean (blue, dashed) and median (blue, dotted) highlighted. Sizes are in mm and data are presented from days 15, 21, 35, and 40.

Model Output Results:

Population data from the current research (Figure 9a) and from related literature (Martin et al. (2013b) and Preuss et al. (2009) were combined to compare my observations to similar study designs (Figure 9b). Importantly, the population data from the current study showed similar trends in timing and size of population increase, peak, decline, and equilibrium levels compared to both Martin et al. (2013b) and Preuss et al. (2009). Key evidence supporting successful model output is the capture of experimental data (Figure 9c). Model mean (solid line), maxima and minima (gray shading) daphnid population sizes from 50 replicate simulations reasonably captured the size, timing, and variability of experimental observations (Figure 9c). The reproductive function used in these simulations was a ‘combination’ function aimed to fit the early reproduction observed in Martin et al. (2013b) but also the high rate of increase observed in the current data (see Fig. 4 above). Changing the ‘Neighborhood Effect’ function half-saturation constant had clear impacts on model population dynamics (Figure 9d). Increasing the tolerated crowd size for both movement and reproduction lead to a higher mean peak size and increased variability in model output.

Beyond agreeable model fit for population size, model output of maximum, mean, and minimum length reasonably capture the range of observed lengths from experimental organisms (see Figure 10). Modeled mean and median estimates fit less well, but could possibly be improved with further refined parameterization of reproduction, neighborhood effect, and ageing submodels.

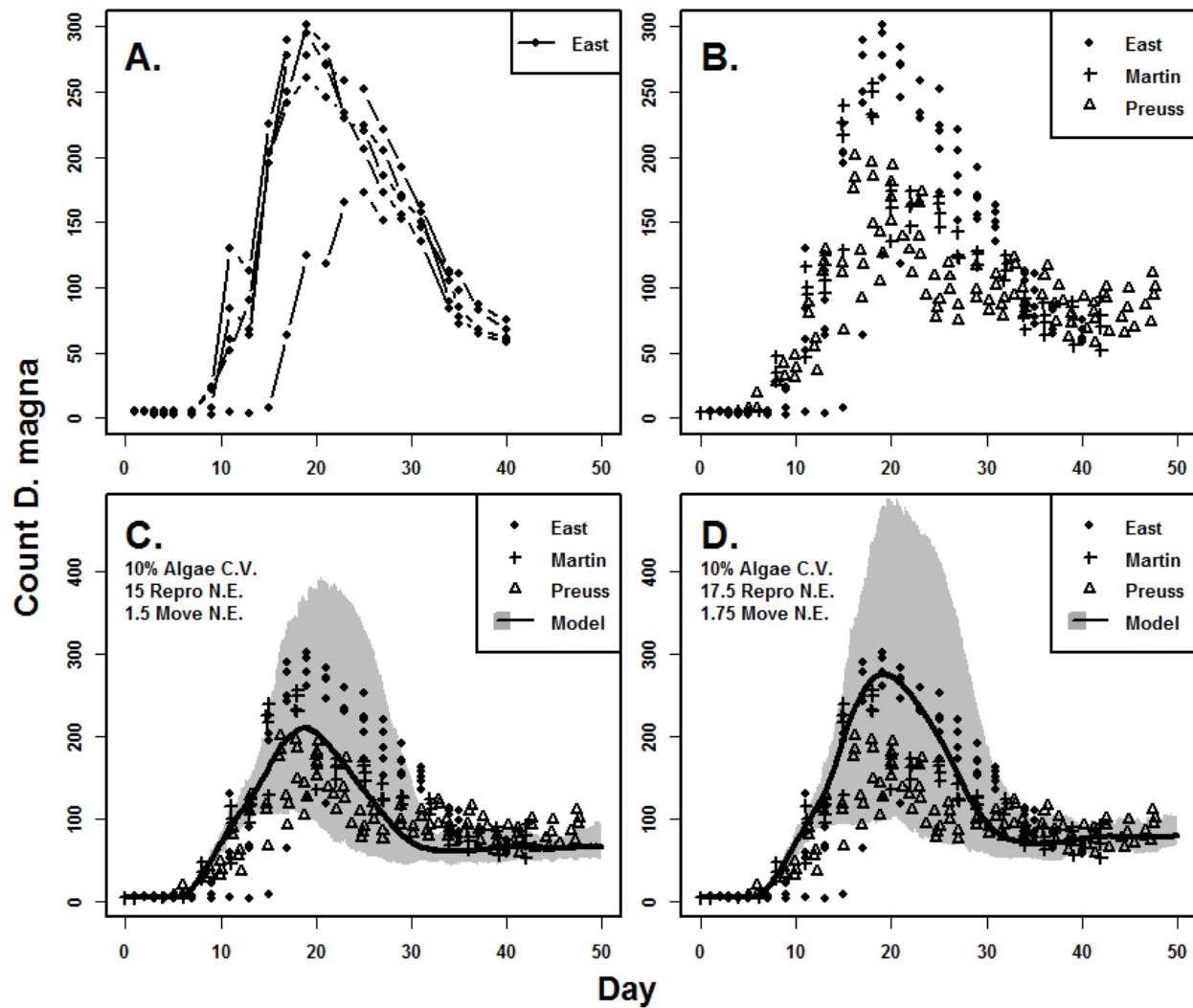


Figure 9a, 9b, 9c, and 9d. Plots of experimental observations (top L and R) and model output (bottom L and R). Top left (a.) shows each replicate (connected points) of one liter populations through 40 days observed by the author. Top right (b.) shows additional datasets published by Martin et al. (2013b) and Preuss et al. (2009). Bottom left (c.) shows the current model plotted against all datasets. Bottom right (d.) shows an additional model output using different 'Neighborhood Effect' model parameters. Solid lines are mean of 50 simulations and gray shading represents maximum and minimum.

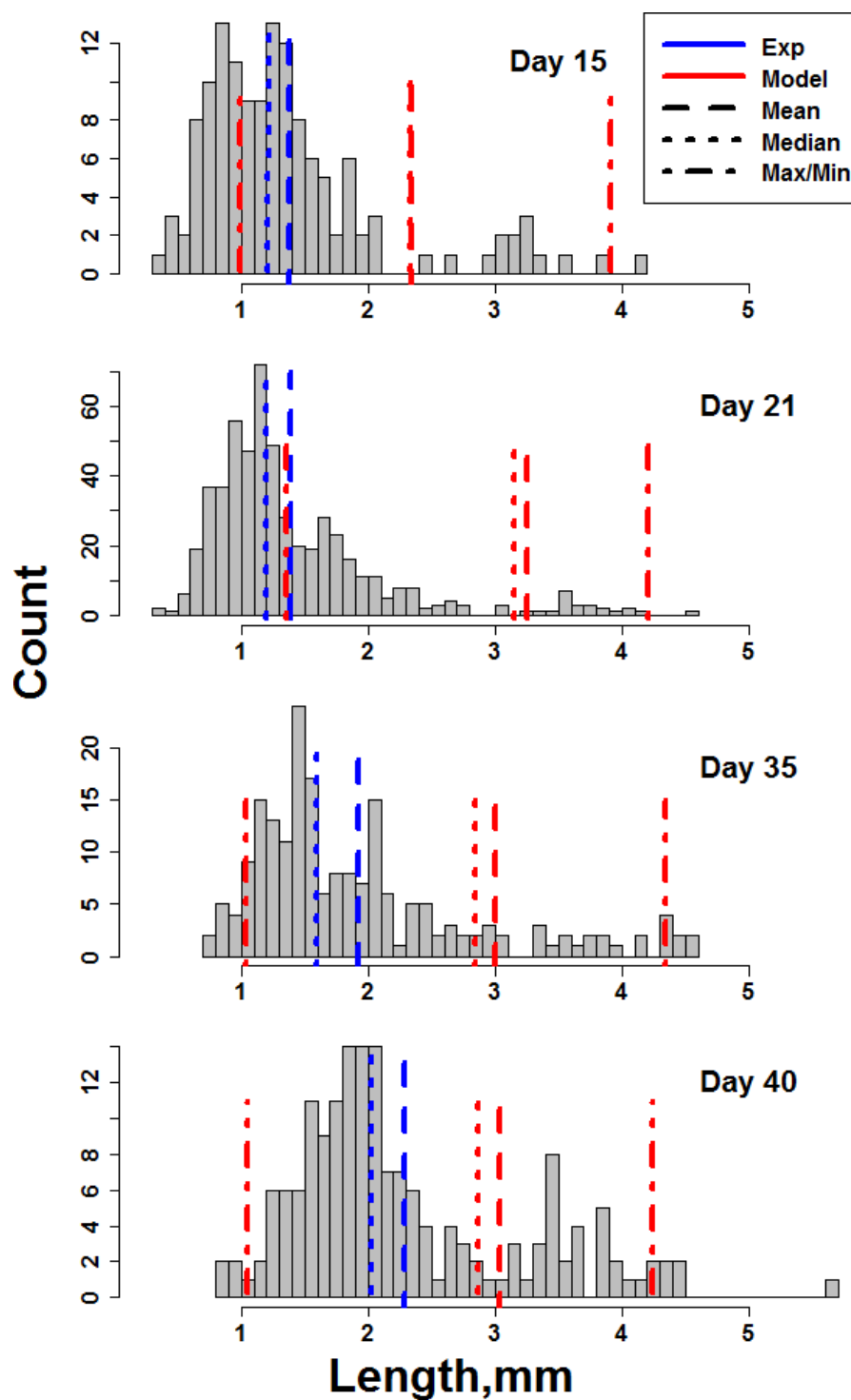


Figure 10. Histograms of lengths (mm) observed in one liter conditions at days 15, 21, 35, and 40 with model output plotted against. Experimental data are summarized by blue lines (dashed for mean and dotted for median) and model data are summarized by red lines (dashed for mean, dotted for median, and dot dash for maximum and minimum). Model data are means of 50 simulation runs.

Modeling Stressor Effects:

Using the pyraclostrobin effect data and exposure patterns outlined above (Fig. 5, Stressor Submodel and Exposure Methods Section), it is clear that adjusting individual energetic parameters can have population level effects (Figure 11). Model output from 50 simulations (each) of populations exposed to a hypothetical concentration eliciting a mean effect of 0%, 6%, or 12% increase in the maintenance coefficient for 30 days ('exposed' every third day with a 2 day half-life) show delayed growth rates and diminished peak sizes. Of note in Figure 11 is the slight rightward shift of population size observations at time points prior to day 21. This suggests that individual increases in maintenance allocation of small amounts (6-12%) can change population peak size and peak timing. Additionally, after day 21, the exposed populations appear to not crash as drastically. This could be due to changes in algae consumption and consequent crowding effects of the exposed populations. However, this moderated decline does not last, and after day 30 (the end of the exposure) the exposed populations do tend to reach the lowest point in 40 days.

See Appendix A, Figure A8a and A8b for distributions of model output for population size and organism size for a range of selected days.

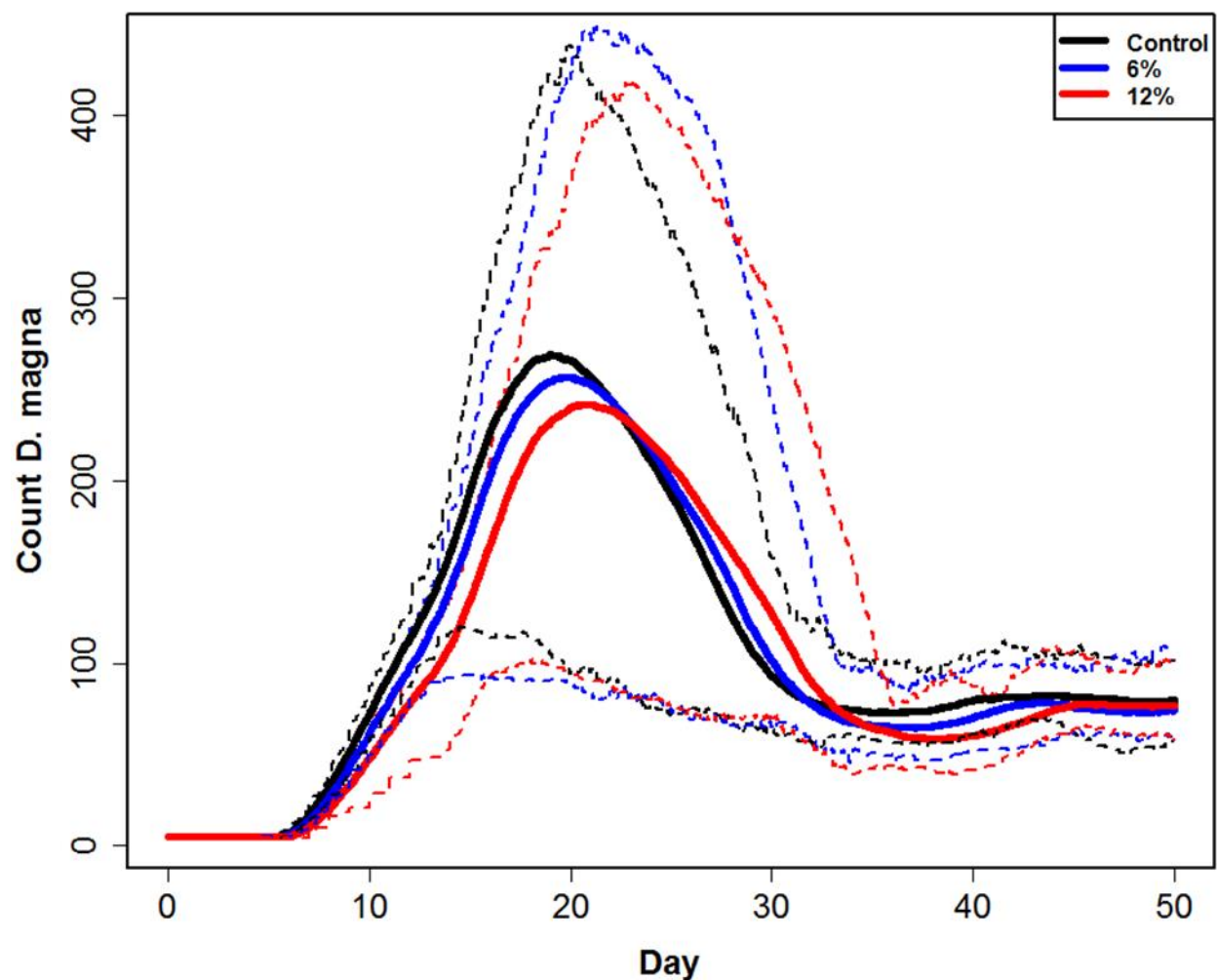


Figure 11. Plot of three model population simulations under a range of stressor exposures. Solid lines are mean and dashed are maximum and minimum of 50 simulations. Stressor exposure was during the first three days and occurred every third day with a 2 day half-life. Exposure in each patch (6% or 12%) was random but normally distributed with a standard deviation of 0.5%.

Discussion:

The key goals of this research were to develop a unique, spatially-explicit DEB-IBM modelling framework and to then compare against observed population dynamics in an effort to ultimately advance population-level risk assessment of chemical stressors. The primary model amendments in the current DEB-IBM were focused on creating a virtual environment that mimicked the spatial arrangement of experimental chambers, resources, organisms, and stressors that reflect common toxicity test designs. The eventual application of the model is to conduct “virtual toxicity tests” and to evaluate model performance against actual toxicity data. Overall, model performance was satisfactory with regard to predicting *D. magna* population dynamics under controlled laboratory conditions and from data from several different sources (this research, Martin et al. 2013b; Preuss et al. 2009). Importantly, the effect of localized density (the ‘Neighborhood Effect’) emerged as a key factor that advances the mechanistic explanation of density-dependent effects on population dynamics of *D. magna*.

The Neighborhood Effect:

The importance of the “Neighborhood Effect” as a way to account for density-dependent effects is strengthened by the fact that regardless of chamber size (1, 2, or 3 liters; Fig. 7), daphnid populations appear to have converged on a density that corresponded to approximately 15 mL per daphnid (1.8 daphnids per 27mL ‘neighborhood’). This therefore suggests (with resource levels being held constant) an optimal or limiting density, regardless of environment size. This is of particular importance as localized, density-dependent population forcing was

hypothesized by the author as a key mechanism that could address the missing post-peak population decline in the model of Martin et al. (2013b, Figure 9).

A maximum biomass level has also been suggested in the work of Lambert (2005) that suggests daphnids fit an Ideal Free Distribution “with costs” (also Larsson, 1997). This can be interpreted as the daphnids selecting a balance between, not only temperature, resource density, and oxygen levels, but also density of competitors. While aggregation in areas of high resource density by daphnids is a commonly observed phenomenon (Cuddington and McCauley, 1994; Neary et al., 1994), it stands to reason that selective pressure could exist to avoid competitors that would maintain existence in close proximity to relatively high resource density locations. Hence, daphnids’ balance of crowding effects and congregation in high resource areas is a key process for the model to capture.

The IBM developed by Preuss et al. (2009) was specifically geared towards addressing crowding as a key mechanism driving population dynamics. Their approach was well supported by experimental data and model output. Specifically, Preuss et al. (2009) described the two forcing processes in their model as resource density and crowding. Resource density is more of a driver at low resources. As resource levels increase, crowding becomes a more prominent driver, and as crowding increases (daphnid density less than 50 ml per daphnid) its importance increases. This is of particular relevance to common experimental conditions, which are often at 50 ml and arguably high resource levels. Based on experimental and model outcomes, Preuss et al. (2009) labeled crowding “as relevant as food supply.” Additionally, Preuss et al. (2009) present model output and data (from Goser, 1997) that suggest crowding can induce or contribute strongly to mortality (Figure 5, Preuss et al., 2009) at densities greater than 5 ml per daphnid, which is equivalent to 5.4 daphnids per 27 mL neighborhood. Their data on brood size

(Figure 2 above and Figure 6 from Preuss et al. (2009) (data from Goser, 1997)) also suggest that there is a strong population dynamic mechanism at densities less than 10ml per daphnid. In relation to the units of the current model—brood size is reduced by 50% at greater than 2.7 daphnids per 27 ml neighborhood.

An additional line of evidence supporting the importance of the Neighborhood Effect arose during the process of parameterization for the current model. Initially, the data from Preuss et al. (2009) and Lambert (2005) were used to define a hyperbolic curve as a possible function to define the relationship between density and crowding effect. This allowed an asymptotic maximum at 1 (100% impact of crowding) and a 50% half-saturation point (could be considered quasi-threshold) that could be parameterized by observed 50% effect data. The initial parameter space for half-saturation constants for reproduction and movement was not well defined. The data from Lambert (2005) suggested a fairly high level of crowding could be withstood (high biomass per unit volume) and the data from Goser (1997) in Preuss et al. (2009) suggested a much lower density.

As shown in Table 1 half-saturation values for movement and reproduction ‘Neighborhood Effect’ functions are quite different. Figures 3 and A5 show that this causes the two functions to have different qualitative shapes. The reproductive ‘Neighborhood Effect’ (Figure 3) is a fairly angular function with a half-saturation constant that is low volume per daphnid or high daphnids per volume. The movement ‘Neighborhood Effect’ (Figure A5) is a fairly smooth shaped function with a half-saturation constant with greater volume per daphnid and lower daphnids per volume. I suggest that these two parameters, $NE_{Reproduction}$ and $NE_{Movement}$, could be this distinctly different due to what are actually quite disparate characteristics. While I named them both ‘Neighborhood Effect,’ they both correspond to

different potential mechanisms. Localized density effects on reproduction comes from observational data from Preuss et al (2009) and Goser (1997) that both imply that density has low impact until a crowded neighborhood causes a steep drop in reproductive output. In converse, localized density effects on movement relates to the balance between resource and con-specific density. The data presented by Lambert (2005) towards this end demonstrate that the range of densities linked to effects is more graded than for reproduction.

To replicate the sharp curve of density effects on reproduction (Preuss et al., 2009) and the gradual effects of density on movement (Lambert, 2005), parameters were initially set an order of magnitude apart. As the data from Preuss et al. (2009) show no effect at 50 ml per daphnid (< 1 daphnid per 27 ml), half-saturation values were initially set at 25 and 2.5 ml per daphnid for movement and reproduction, respectively. These values respectively correspond to 1.08 and 10.8 daphnids per 27 ml in the Neighborhood syntax of NetLogo. Systematically adjusting movement and reproduction parameter values after simulations to attempt to fit data give a satisfactory fit on population size in between 15 and 1.5 and 20 and 2.0 ml per daphnid (1.8 and 18; 1.35 and 13.5 daphnids per 27 ml, respectively).

Of great importance are data supporting the ‘Neighborhood Effect’ parameter values. Figure 6 demonstrates that experimental populations, by day 40 and regardless of experimental chamber size, converged at a density between 15 and 20 ml per daphnid. Firstly, the overlap of model output and data indicates good performance of our model parameterization and the relevance of the ‘Neighborhood Effect’ on reproduction. Secondly, the more nuanced takeaway, is that the data agreement with half-saturation parameter values specific to reproduction may indicate that the ‘Neighborhood Effect’ has a greater or more important impact on reproduction than movement. The experimental populations did not converge near 1.5 ml per daphnid as

implied by the movement half-saturation constant. Lampert (2005) suggests that the impact of con-specifics exists but is not more important than resource density and it may be that in relatively evenly distributed resource environments (experiments) this places the emphasis on reproductive effects.

In summary, experimental and model observations support the mechanisms and parameterizations of localized density-dependent effects (the ‘Neighborhood Effect’) on *D. magna* reproduction and movement patterns.

Starvation Submodel:

Martin et al. (2013b) hypothesized that the observed lack of fit of their model to the post-population peak and equilibrium periods was due to poor performance of starvation sub-models. The model presented here fit best when I included a starvation sub-model that was adjusted to include f in the function. The inclusion of f as a determinant of organism ‘condition’ in addition to shrinkage allows for greater juvenile starvation mortality during periods of high crowding and low resource density. Perhaps more important is that recovery due to movement to areas of greater resource that allow better fit is due to an observable phenomena. After daphnid populations reach peak densities, the ‘Neighborhood Effect’ tends to cause modelled individuals to scatter during periods of population decline. Post-peak movements to areas of increased resource density or reduced con-specific density is a directly testable phenomena. Additionally, this new starvation sub-model adjustment also aligns with the interest of simplifying the number of functions and unique parameters needed to apply DEB individual models to IBM population frameworks.

There is potentially information to be gained from the ‘weird animal’ approach of van Der Meer (2016) to equalize competitiveness between adults and juveniles in their starvation and recovery abilities but this has not yet been applied under this model framework.

Modeling Effects of Chemical Stressors:

Model output for populations exposed to an energetically disruptive chemical stressor suggests that populations are impacted by individual energetics and that this effect can carry over beyond the period of exposure. While there are no population level experiments of the effects of pyraclostrobin (or other strobilurins) with which to compare model results, data does suggest that strobilurins cause mortality and reproductive effects (Ochoa-Acunã et al., 2009 and Cui et al., 2016). Because reproductive effects of strobilurins can be strong (Cui et al., 2016), these would likely translate to population level effects similar to those observed in model output—delay in peak population size and a lower equilibrium. Additionally, Cui et al., (2016) presented data on length that is in agreement with the work of Lockett (in prep) that suggests sub-lethal levels also impact length. Ongoing research to evaluate population-level effects of pyraclostrobin will be helpful in evaluating model performance and use in this context.

Beyond the reasonable model output for chemical stressor exposure, the stressor results also agree with the hypothesis that simplification of DEB model functions would allow for a relatively easy application of individual toxicity test data (Jager and Zimmer, 2012). Data from a relatively coarse energetic metric (length) provided an estimation of energetic allocation disruption at an individual level could then be applied to a robust IBM to explore population level effects in testable and common conditions.

Connecting effects observed in individuals to populations has been the goal of ecotoxicology researchers for some time (see Rohr et al., 2016) and one particular work that supports the current work's methodology and results is Martin et al. (2013a). Reproduction data from individual *D. magna* exposed to 3,4-dichloroaniline were used to adjust DEB reproduction functions within a *D. magna* specific DEB-IBM (Martin et al., 2012). As individual exposures did not result in changes in size (growth and maintenance parameter dependent metrics), a reproduction-specific mechanism of action was determined. Accordingly, cost of embryo survival was reduced as a function of exposure and a series of population simulations were run. For the most part, simulated population size and dynamic timing followed the experimental observations. Additionally, the altered size-class dynamics (due to reproductive effect) were captured by the model when concentrations were higher.

Baveco and de Roos (1996) provide an additional example that is likely the first publication to specifically connect an individual-based population model and individual toxicity data specifically geared towards risk assessment. Earthworms were the target species, predation was a focal ecological interaction, and pulsed pesticide application was the focal chemical risk. Their DEB-based individual energetic model (early work by Kooijman, 1984) accurately connected pesticide reduction in individual growth to population level declines due to single and pulsed exposures. They also applied the model across two species and provided a strong risk assessment policy-oriented synthesis of organism persistence as a function of pesticide half-life and initial exposure through the individual and population model output (See Figure 4, Baveco and de Roos (1996)). It is of note that a similar construct for earthworms has been published more recently (Johnston et al., 2014) that used a different energy budget (still dynamic), but proved accurate in predicting population level effects from individual energetic effect data.

In summary, as the accessibility of DEB and IBMs increases (Grimm and Martin, 2013) there are an increasing number of models (e.g. Beaudoin et al., 2015) that include a large number of complex ecological drivers. While these modeling efforts are inherently important (Koenigstein et al., 2016; Energetics and IBM sections) for their use in understanding population dynamics in the sense of larger ecological processes there is still available room to simplify and improve the core quantitative and software approaches. As is posited in Grimm and Martin (2013), mechanistic effect models (such as DEB-IBMs) provide a framework specifically geared towards quantitatively and mechanistically robust risk and effect predictions. As such, they hold great possibility to change and influence risk assessment policies and methods. This chapter presents one such method of thoroughly, but simply, describing individual metrics that are testable against chemical stressors and expanding that to a similarly testable environment. This provides a framework for exploring new questions and mechanisms of stressors and population level interactions.

Literature Cited:

- Bartell, S., Lefebvre, G., Kaminski, G., Carreau, M., Campbell, K., 1999. An ecosystem model for assessing ecological risks in Québec rivers, lakes, and reservoirs. *Ecological Modelling* 124, 43-67.
- Bartlett, D., Clough, J., Godwin, J., Hall, A., Hamer, M., Parr-Dobrzanski, B., 2002. The strobilurin fungicides. *Pest Management Science* 58, 649–662.
- Baveco, J.M. and A.M de Roos, 1996. Assessing the impact of pesticides on lumbrici populations: an individual-based modelling approach. *Journal of Applied Ecology* 33:1451-1468.
- Beaudoin, R., B. Goussen, B. Piccini, S. Augustine, J. Devillers, F. Brion, and A.R.R. Pery, 2015. An individual-based model of zebrafish population dynamics accounting for energy dynamics. PLoS ONE 10(5): e0125841. doi:10.1371/journal.pone.0125841
- Beketov, M., Liess, M., 2011. Ecotoxicology and macroecology--time for integration. *Environ. Pollut.* 162, 247–54.
- Beketov, M.A., Kefford, B.J., Schäfer, R.B. and Liess, M., 2013. Pesticides reduce regional biodiversity of stream invertebrates. *Proceedings of the National Academy of Sciences*, 110(27), pp.11039-11043.
- Carpenter, SR, Kitchell, JF, Hodgson, JR, Cochran, PA, 1987. Regulation of lake primary productivity by food web structure. *Ecology*. 68(6), 1863-1876.
- Chapman, P., 2002. Integrating toxicology and ecology: putting the “eco” into ecotoxicology. *Marine Pollution Bulletin* 44, 715
- Chen, S., Chen, B., Fath, B., 2013. Ecological risk assessment on the system scale: A review of state-of-the-art models and future perspectives. *Ecological Modelling* 250, 2533.
- Clements, W.H., J.R. Rohr 2009. Community responses to contaminants: Using basic ecological principles to predict ecotoxicological effects. *Environmental Toxicology and Chemistry* 28(9), 1789-1800
- Cuddington, K.M. and McCauley, E., 1994. Food-dependent aggregation and mobility of the water fleas *Ceriodaphnia dubia* and *Daphnia pulex*. *Canadian Journal of Zoology*, 72(7), pp.1217-1226.
- Cui, F., T. Chai, X. Liu, and C. Wang, 2016. Toxicity of Three Strobilurins (Kresoxim-methyl, Pyraclostrobin, and Trifloxystrobin) on *Daphnia magna*. *Environmental Toxicology and Chemistry*, Early Release.
- EPA (2002). Methods for Measuring the Acute Toxicity of Effluents and receiving Waters to Freshwater and Marine Organisms. Fifth Edition. EPA/821/R-02/012. U.S. Environmental Protection Agency, Office of Water, Washington, DC.

https://www.epa.gov/sites/production/files/2015-08/documents/acute-freshwater-and-marine-wet-manual_2002.pdf

EPA, 1998. Guidelines for Ecological Risk Assessment EPA/630/R-95/002F

Faber, J., Wensem, J., 2011. Elaborations on the use of the ecosystem services concept for application in ecological risk assessment for soils. *Science of the Total Environment* 415, 3–8.

Fath, B., Jørgensen, S., Patten, B., Straškraba, M., 2004. Ecosystem growth and development. *Biosystems* 77, 213–228.

Forbes, V. E., P. Calow, V. Grimm, T. I. Hayashi, T. Jager, A. Katholm, A. Palmqvist, R. Pastorok, D. Salvito, R. Sibly, J. Spromberg, J. Stark, R. A. Stillman, 2011. Adding value to ecological risk assessment with population modeling. *Human and Ecological Risk Assessment*. 17:297–299.

Forbes, V., Calow, P., 2013. Developing predictive systems models to address complexity and relevance for ecological risk assessment. *Integrated Environmental Assessment and Management* 9(3), e75–e80.

Gabsi, F., Preuss, T., 2014. Modelling the impact of the environmental scenario on population recovery from chemical stress exposure: A case study using *Daphnia magna*. *Aquatic Toxicology* 156, 221–229.

Gabsi, F., Schäffer, A., Preuss, T., 2014. Predicting the sensitivity of populations from individual exposure to chemicals: The role of ecological interactions. *Environmental Toxicology and Chemistry* 33, 1449–1457.

Goser, B., Ratte, H.T., 1994. Experimental Evidence of Negative Interference in *Daphnia magna*. *Oecologia* 98, 354–361.

Grimm, V. and B. Martin, 2013. Mechanistic effect modeling for ecological risk assessment: Where to go from here? *Integrated Environmental Assessment and Management* 9(3):e59–e63.

Grimm, V., S.F. Railsback, 2005. Individual-based modeling and ecology. Princeton University Press.

Hansen, M.J., Boisclair, D., Brandt, S.B., Hewett, S.W., Kitchell, J.F., Lucas, M.C. and Ney, J.J., 1993. Applications of bioenergetics models to fish ecology and management: where do we go from here?. *Transactions of the American Fisheries Society*, 122(5), pp.1019–1030.

Heugens, E.H.W., Hendriks, A.J., Dekker, T., van Straalen, N.M., Admiraal, W., 2001. A review of the effects of multiple stressors on aquatic organisms and analysis of uncertainty factors for use in risk assessment. *Critical Reviews in Toxicology* 31, 247–284.

Hoekstra, A., Wiedmann, T.O., 2015. Humanity's unsustainable environmental footprint. *Science* 344, 1114–1117.

- Jager, T., Barsi, A., Hamda, N.T., Martin, B.T., Zimmer, E.I. and Ducrot, V., 2014. Dynamic energy budgets in population ecotoxicology: Applications and outlook. *Ecological Modelling*, 280, pp.140-147.
- Jager, T., Zimmer, E., 2012. Simplified Dynamic Energy Budget model for analysing ecotoxicity data. *Ecological Modelling* 225, 74–81.
- Jensen, K.H., Larsson, P. and Hogstedt, G., 2001. Detecting food search in *Daphnia* in the field. *Limnology and Oceanography*, 46(5), pp.1013-1020.
- Johnston, A.S.A., M.E. Hodson, P. Thorbek, T. Alvarez, and R.M. Sibly, 2014. An energy budget agent-based model of earthworm populations and its application to study the effects of pesticides. *Ecological Modelling* **280**:5-17.
- Jusup, M., Sousa, T., Domingos, T., Labinac, V., Marn, N., Wang, Z., Klanjscek, T., 2016. Physics of Metabolic Organization. *Physics of Life Reviews*.
- Kitchell, J.F., Stewart, D.J., Weininger, D., 1977. Applications of a Bioenergetics Model to Yellow Perch (*Perca flavescens*) and Walleye (*Stizostedion vitreum vitreum*). *Journal of the Fisheries Board of Canada*. 34, 1922–1935
- Koenigstein, S., F.C. Mark, S. Gobling-Reisemann, H. Reuter, and H. Poertner, 2016. Modelling climate change impacts on marine fish populations: process-based integration of ocean warming, acidification and other environmental drivers. *Fish and Fisheries* DOI: 10.1111/faf.12155
- Kooijman S. 2010. Dynamic energy budget theory for metabolic organization. 3rd ed. Cambridge, UK: Cambridge University Press.
- Laender, F., Schamphelaere, K., Vanrolleghem, P., Janssen, C., 2008a. Comparing ecotoxicological effect concentrations of chemicals established in multi-species vs. single-species toxicity test systems. *Ecotoxicology Environmental Safety* 72(2), 310–5.
- Laender, F., Schamphelaere, K., Vanrolleghem, P., Janssen, C., 2008b. Validation of an ecosystem modelling approach as a tool for ecological effect assessments. *Chemosphere* 71, 529-545.
- Lampert, W., 2005. Vertical distribution of zooplankton: density dependence and evidence for an ideal free distribution with costs. *BMC biology*, 3(10).
- Larsson, P., 1997. Ideal free distribution in *Daphnia*? Are daphnids able to consider both the food patch quality and the position of competitors?. In *Cladocera: the Biology of Model Organisms* (pp. 143-152).
- Larsson, P., 1997. Ideal free distribution in *Daphnia*? Are daphnids able to consider both the food patch quality and the position of competitors? *Hydrobiologia* 360, 143–152.
- Liess, M, 2002. Population response to toxicants is altered by intraspecific interaction. *Environmental Toxicology and Chemistry*, 21(1), pp.138-142.
- Lockett, L. 2016 (In Prep.). Title, Thesis, Towson University.

- Mace, G.M., 2014. Whose conservation?. *Science*, 345(6204), pp.1558-1560.
- Martin, B., Jager, T., Nisbet, R., Preuss, T., Grimm, V., 2014. Limitations of extrapolating toxic effects on reproduction to the population level. *Ecological Applications*
- Martin, B., Jager, T., Nisbet, R., Preuss, T., Hammers-Wirtz, M., Grimm, V., 2013a. Extrapolating ecotoxicological effects from individuals to populations: a generic approach based on Dynamic Energy Budget theory and individual-based modeling. *Ecotoxicology* 22, 574–83.
- Martin, B., Zimmer, E., Grimm, V., Jager, T., 2012. Dynamic Energy Budget theory meets individual-based modelling: a generic and accessible implementation. *Methods in Ecology and Evolution* 3, 445–449.
- Martin, B.T., Jager, T., Nisbet, R.M., Preuss, T.G. and Grimm, V., 2013b. Predicting population dynamics from the properties of individuals: a cross-level test of Dynamic Energy Budget theory. *The American Naturalist*, 181(4), 506-519.
- McMahon, T.A., Halstead, N.T., Johnson, S., Raffel, T.R., Romansic, J.M., Crumrine, P.W. and Rohr, J.R., 2012. Fungicide-induced declines of freshwater biodiversity modify ecosystem functions and services. *Ecology Letters*, 15(7), pp.714-722.
- Meer, J., 2016. A paradox in individual-based models of populations. *Conservation Physiology* 4, 1-12.
- Neary, J., Cash, K., McCauley, E., 1994. Behavioral aggregation of *Daphnia pulex* in response to food gradients. *Functional Ecology* 8, 377–383.
- Ochoa-Acuña, H., Bialkowski, W., Yale, G., Hahn, L., 2009. Toxicity of soybean rust fungicides to freshwater algae and *Daphnia magna*. *Ecotoxicology* 18, 440–446.
- Orlinskiy, P., Münze, R., Beketov, M., Gunold, R., Paschke, A., Knillmann, S., Liess, M., 2015. Forested headwaters mitigate pesticide effects on macroinvertebrate communities in streams: Mechanisms and quantification. *Science of the Total Environment* 524, 115-123.
- Preuss, T.G., Hammers-Wirtz, M., Hommen, U., Rubach, M.N. and Ratte, H.T., 2009. Development and validation of an individual based *Daphnia magna* population model: the influence of crowding on population dynamics. *Ecological Modelling*, 220(3), 310-329.
- R Core Team (2016). R: A language and environment for statistical computing. R Foundation for Statistical Computing, Vienna, Austria. URL <https://www.R-project.org/>.
- Rasband, W.S., ImageJ, U. S. National Institutes of Health, Bethesda, Maryland, USA, <http://imagej.nih.gov/ij/>, 1997-2016.
- Rohr, J.R., Salice, C.J., Nisbet, R.M., 2016. The pros and cons of ecological risk assessment based on data from different levels of biological organization. *Critical Reviews in Toxicology* 46, 756–84
- Sibly, R., Grimm, V., Martin, B., Johnston, A., Kulakowska, K., Topping, C., Calow, P., Nabe-Nielsen, J., Thorbek, P., DeAngelis, D., 2013. Representing the acquisition and use of energy

- by individuals in agent-based models of animal populations. *Methods in Ecology and Evolution* 4, 151–161.
- Smetanová, S., Bláha, L., Liess, M., Schäfer, R.B., Beketov, M.A., 2014. Do predictions from Species Sensitivity Distributions match with field data? *Environmental Pollution* 189, 126–33.
- Sokolova, I., 2013. Energy-Limited Tolerance to Stress as a Conceptual Framework to Integrate the Effects of Multiple Stressors. *Integrative and Comparative Biology*. ict028.
- Sokolova, I., Frederick, M., Bagwe, R., Lannig, G., Sukhotin, A., 2012. Energy homeostasis as an integrative tool for assessing limits of environmental stress tolerance in aquatic invertebrates. *Marine Environmental Research* 79, 1–15.
- Suter, G., Norton, S., Fairbrother, A., 2005. Individuals versus organisms versus populations in the definition of ecological assessment endpoints. *Integrated Environmental Assessment and Management* 1, 397–400.
- Truhaut, R., 1977. Ecotoxicology: objectives, principles and perspectives. *Ecotoxicology and environmental safety*, 1(2), 151-173
- Vidal, J.M., Fundamentals of Multi Agent Systems (2009).
- von Bertalanffy, L., 1938. A quantitative theory of organic growth (inquiries on growth laws. II). *Human biology*, 10(2), pp.181-213.
- Warming, T.P., Mulderij, G. and Christoffersen, K.S., 2009. Clonal variation in physiological responses of *Daphnia magna* to the strobilurin fungicide azoxystrobin. *Environmental Toxicology and Chemistry*, 28(2), pp.374-380.
- Wilensky, U. 1999. NetLogo. <http://ccl.northwestern.edu/netlogo/>. Center for Connected Learning and Computer-Based Modeling, Northwestern University. Evanston, IL.
- Zimmer, E., Jager, T., Ducrot, V., Lagadic, L., Kooijman, S., 2012. Juvenile food limitation in standardized tests: a warning to ecotoxicologists. *Ecotoxicology* 21, 2195–204.

Appendix A:

Below are figures demonstrating several points of interest that support the above document.

Individual Models:

Figures A1, A2, and A3 demonstrate ageing based mortality (top left), growth (top right), cumulative reproduction (bottom left), and crowd count (bottom left, number of daphnids in 27 mL area) at either high or low food levels, with and without starvation sub models.

Starvation Models:

Key to Figure A4 is that while each organism reaches starvation mortality at the same proportional size, decreased resource levels (lower f) increase the rate at which an organism approaches that proportional size.

Movement Neighborhood Effect Submodel:

Figure A5 shows the relationship to daphnid density and crowd count on movement patterns of individual daphnids.

Reproduction Function Variability:

As seen in Figure A6, there is a wide range of variability in cumulative reproduction as a function of length relationships. I propose that this is a large source of variability and worth of attention in adaptations of this and other DEB-IBM models for experimental organisms.

Metabolic Rate Effect Details:

Reproductive functions include \dot{k}_M and thus, the assumption that energetic stressors increasing this rate will artificially cause the reproduction submodels to increase reproductive output. As this is likely not observed (see Jager and Zimmer (2012; reproductive modes of action are adjusted separately than other single DEB parameters), stressor effect has to be specifically address to the \dot{k}_M values in the growth functions. Figure A7 demonstrates this principle. The yellow line has a 20% increased \dot{k}_M value and this suggests that reproductive output would occur much earlier than normal organisms. More likely is that stressors cause decreases in reproductive output—and this is modeled already by the reduction in size (shift to the left on regular function (black line)).

Model Output Distributions with Stressor Effect:

Figure A8 shows distributions from 50 simulations of population size and organism length.

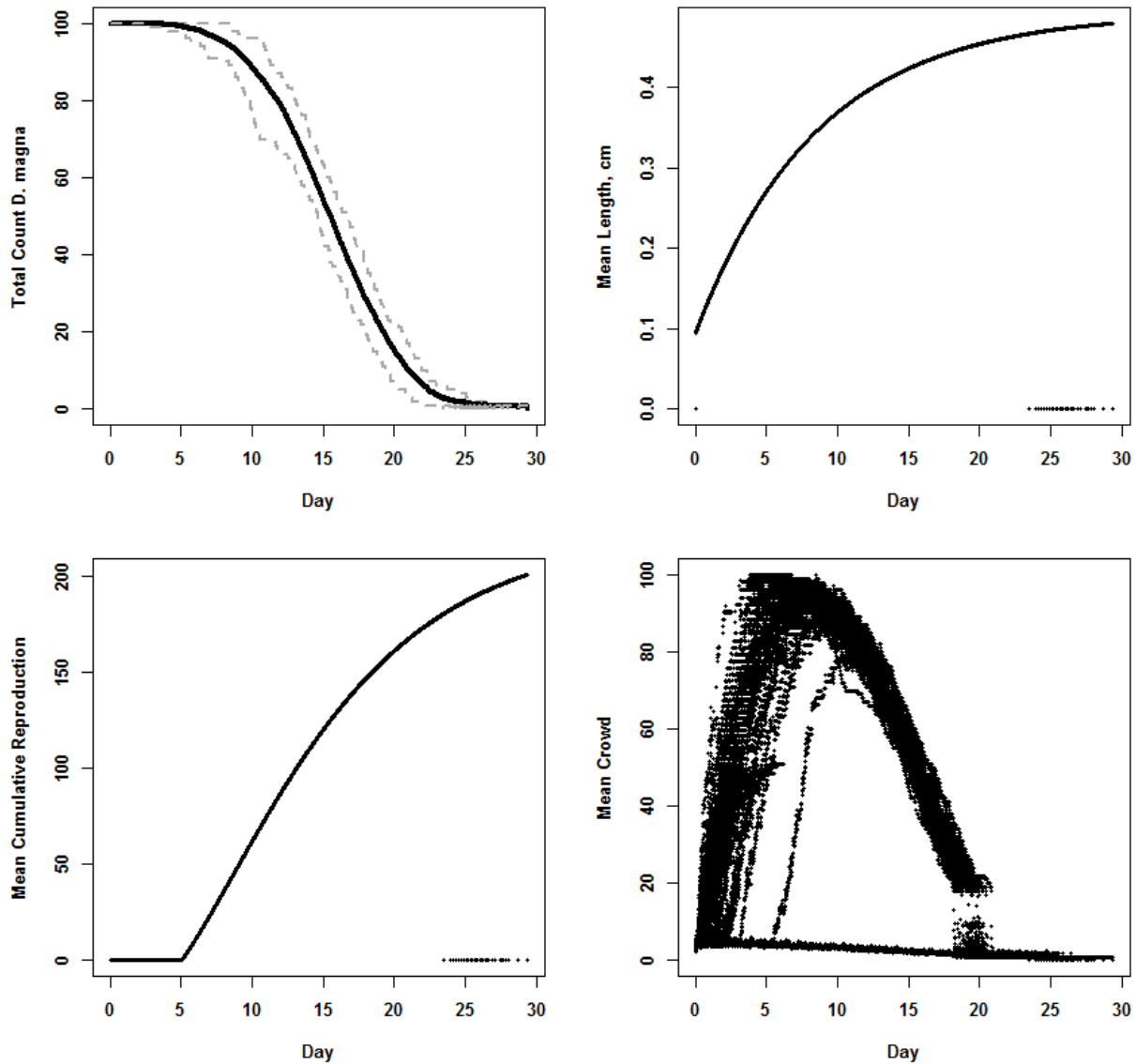


Figure A1. Figures from 50 model iterations to display effect of age-based mortality on a population that is not reproducing (top left), mean individual growth and cumulative reproduction (top right and bottom left), and finally the interrelated relationship between crowding and movement (bottom right). These model runs were performed without any starvation or reproduction sub-models and any mortality or variation is based on age-based death or impact of successful patch choice, algae ingestion rates, and neighborhood crowd counts. Zero values at final days correspond to conditions where there are zero animals remaining and an error is returned during calculation of the mean—this is recorded as a zero.

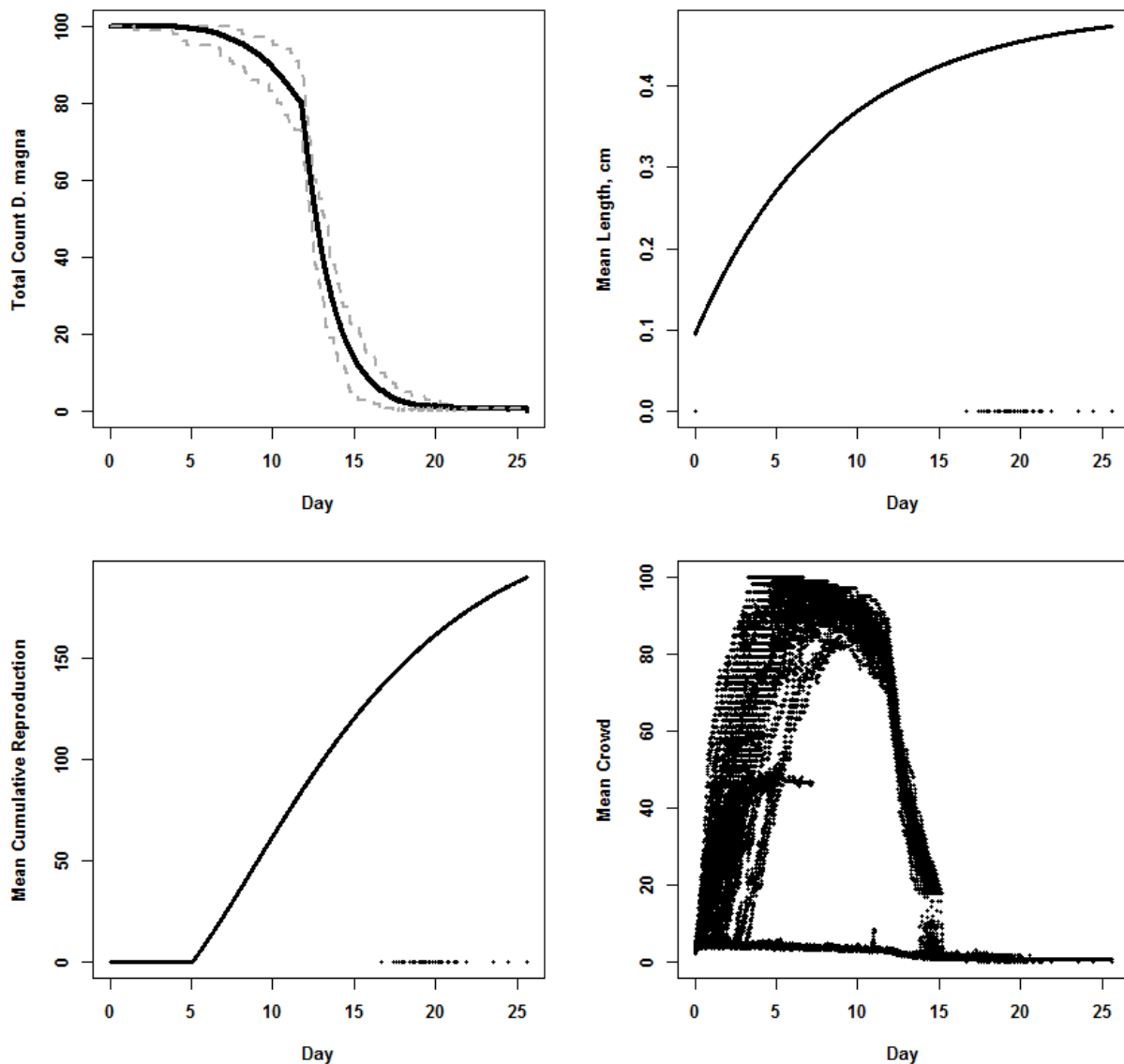


Figure A2. Figures from 50 model iterations to display effect of age- and starvation-based mortality on a population that is not reproducing (top left), mean individual growth and cumulative reproduction (top right and bottom left), and finally the interrelated relationship between crowding and movement (bottom right). Mortality is due to aging and starvation sub-models. Neighborhood effects on movement and reproduction are modeled with crowd count values in bottom right. Zero values at final days correspond to conditions where there are zero animals remaining and an error is returned during calculation of the mean—this is recorded as a zero. Of note: Neighborhood effect drive increased rate of starvation in areas of high ingestion/phytoplankton depletion.

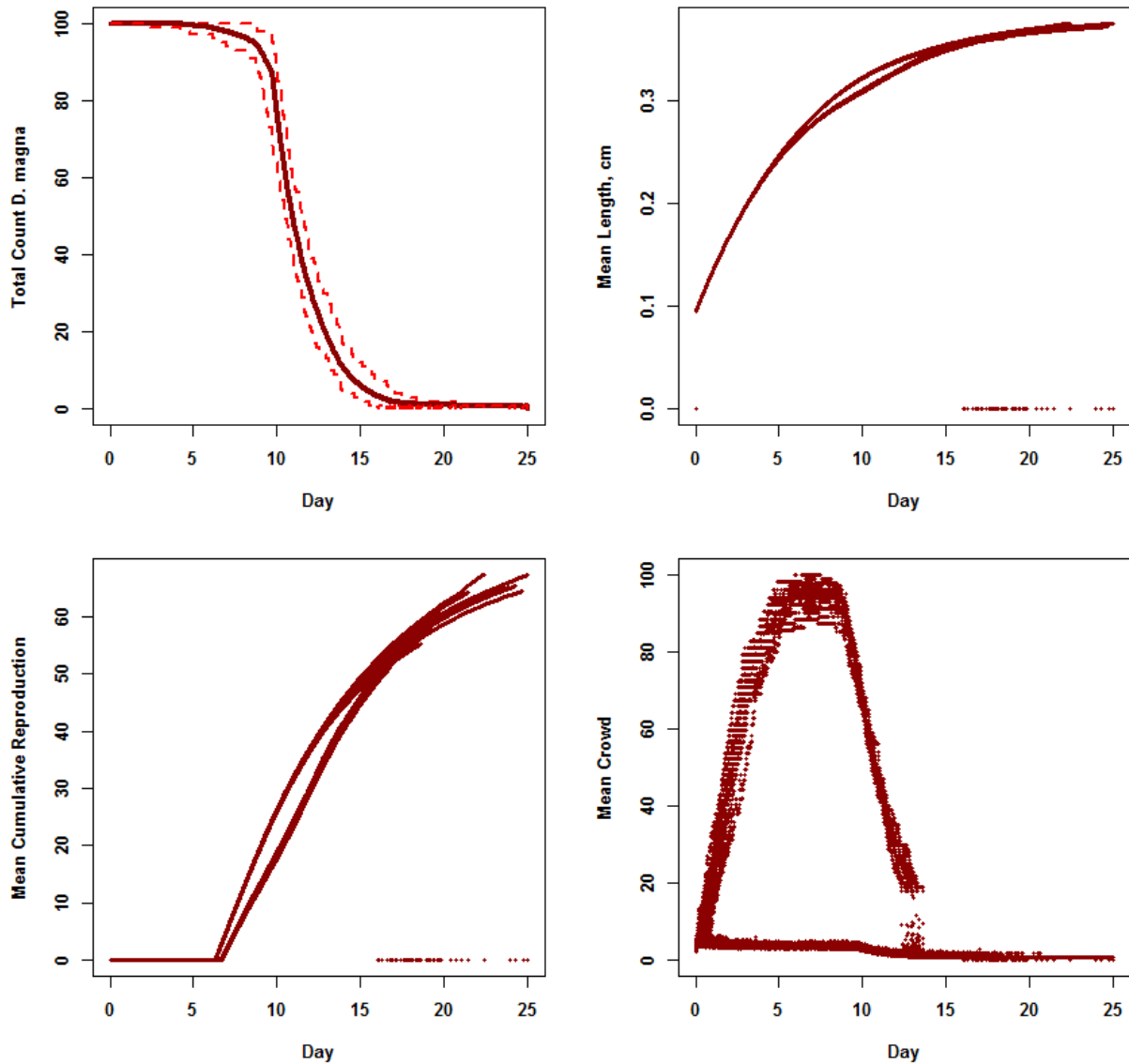


Figure A3. Figure similar to conditions presented above, but with food reduced by an order of magnitude. Of importance is the increase in variability of mean metrics during periods of highest growth and reproduction rates due to increased effects of individual starvation during periods of high energy demand.

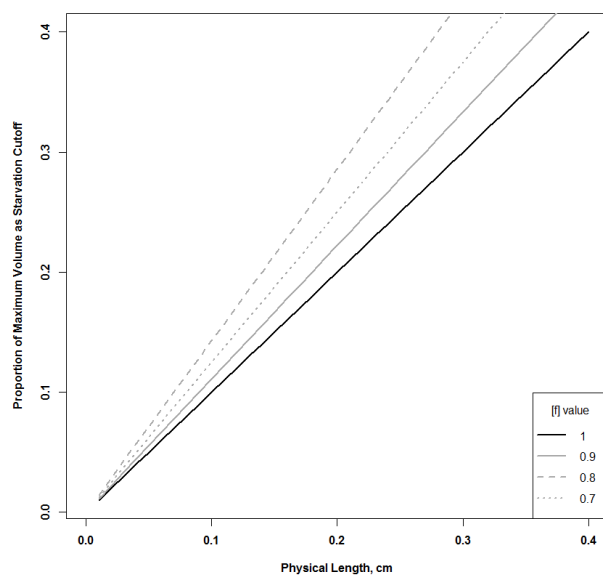


Figure A4. Figure demonstrating function for starvation sub-model that provides volumetric cutoff point. At a constant f value, individuals reach 0.4 (modeled volumetric starvation shrinkage critical mass as per Martin et al.) at their given maximum physical size. Overarching premise being that smaller animals can survive lesser shrinkage events but all individuals approach 0.4 at the same rate (lower f values increase rate of starvation shrinkage tolerance—assuming the organism survives).

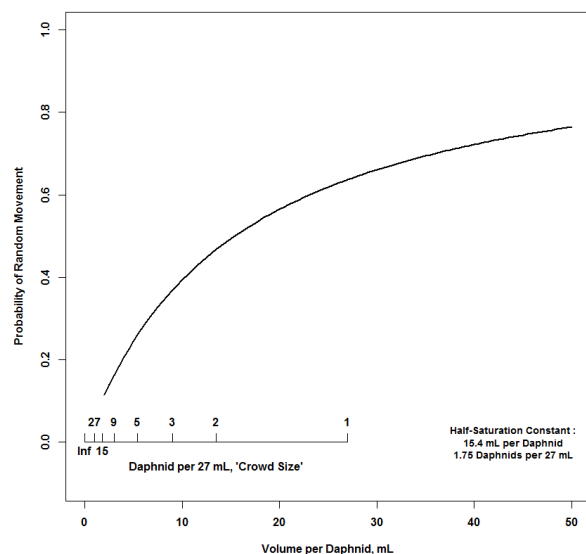


Figure A5. Figure describing hyperbolic function used to model neighborhood effect on *D. magna* movement between patches. Notice inverse x-axes for crowd size and volume per daphnid independent variables. This specific function uses a crowd size of 1.75 daphnids mL^{-1} as a half-saturation constant.

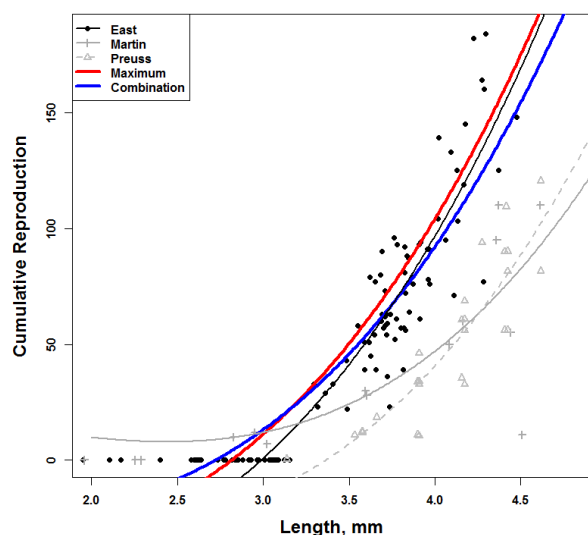


Figure A6. Figure showing fitted curves from data. Equation is as above. Important—these reproduction data are not from the same experiment, but from individual organism per 100mL media in glass jar exp. Feeding rate was $\sim 1.1 \text{ mg C mL}^{-1}$. Media was changed every three days.

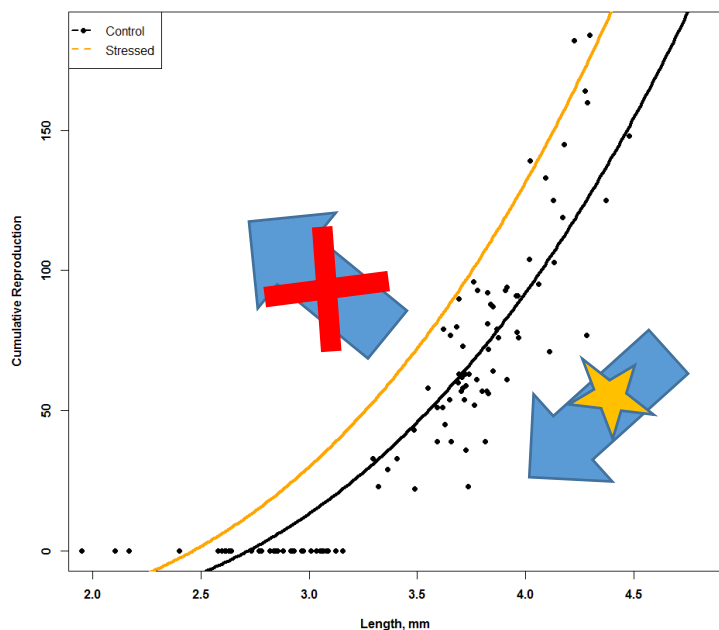


Figure A7. Figure showing incorrect shifting of reproduction curve due to k_{dot_M} shifting. This shift is not needed as animals are going to be smaller and their reproductive output will be smaller.

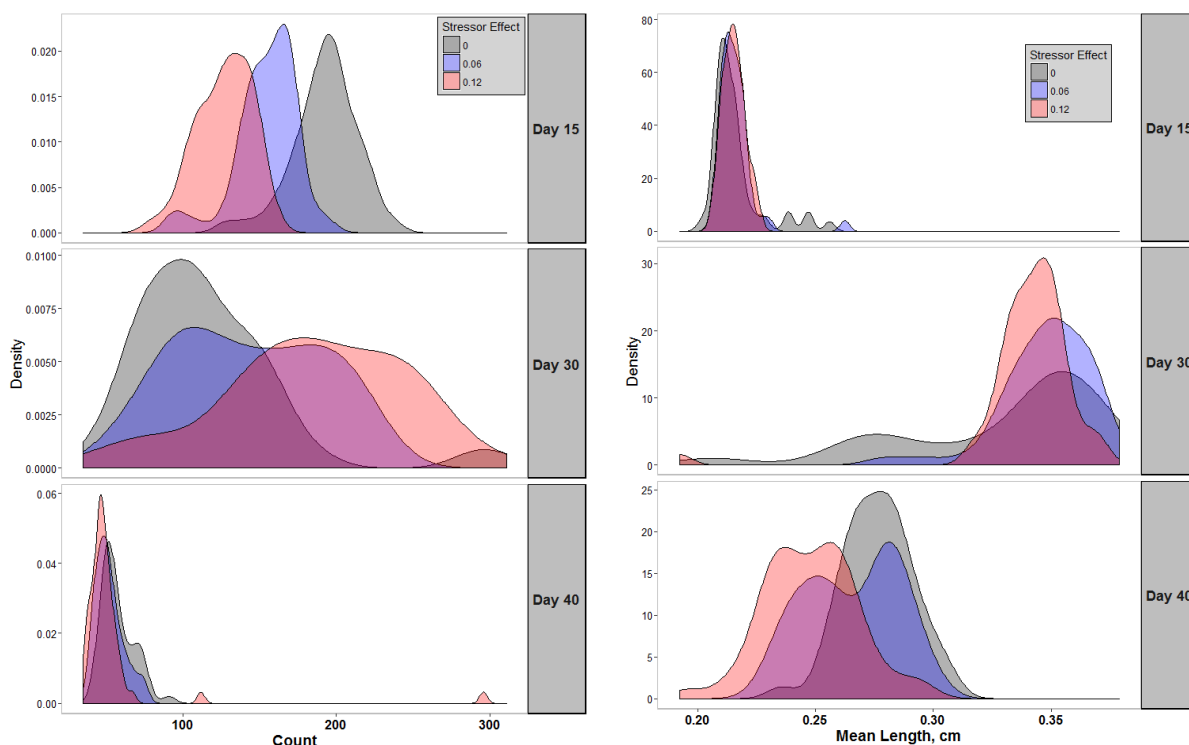


Figure A8a and A8b. Distributions from 50 simulations with a range of stressor effects on somatic maintenance coefficient parameter. Left (a) is population size at days 15, 30, and 40 and right (b) are size distributions on days 15, 30, and 40. Stressor effect magnitudes were 0%, 6%, and 12% and were ended at day 30.

Chapter II.

An Energetic Model Accounting for Morphology and Experimental Characteristics of *Lymnaea stagnalis*

Introduction

As human activities continue to result in the release of chemical stressors that affect biodiversity and ecosystem function (Beketov et al., 2013; McMahon et al., 2012), it is critical to formalize a method to understand and predict the risks of chemical stressors to natural systems (Bradbury et al., 2004; Forbes and Calow, 2002). Ecological Risk Assessments (ERAs) provide the conceptual and, ideally, quantitative approach used to predict risk of chemical effects to natural systems (EPA, 1998, 2004). A key result of an ERA is an estimate of the risk of negative effects to ecological receptors (Suter, 2016). These risk estimates are almost always determined using laboratory based single-species toxicity test data (Suter, 2016). For example, Hayashi et al. (2016) used algal toxicity of herbicides determined in laboratory tests to inform a spatiotemporal model to predict regional ecotoxicity of herbicides in Japan. As discussed in Hayashi et al. (2016) risk estimation requires integrating information on effects and natural conditions. In their work, single algal species, herbicide-toxicity tests were used to inform an estimation of risk under observed stream flow conditions (Hayashi et al., 2016). Integrating these methods and endpoints led to a much more useful understanding of the risk to algae under relevant environmental conditions (Norton et al., 1992). However, as emphasized by Hayashi et al. (2016), there remains room for specificity and improvement in the conceptual and quantitative linkages between environmental conditions, effects on ecological receptors, and risk estimation.

In relation to the limitations presented by Hayashi et al. (2016), Rohr et al. (2016) highlight that metrics from single species toxicity tests typically do not match ecological dynamics due to differences in design, fundamental approaches, and scale. They posit a focus on further developing the quantitative and modeling approaches used by risk assessors to bridge disconnects between data and protection goals while maintaining the strength of research at each level of biological organization (e.g., individuals, populations, communities). Two perspectives that can serve to bridge this gap, are that chemical mode of action is imperative in establishing causative linkages between toxicant exposure and organismal effects (e.g. Ankley et al., 2010) and that population dynamics are vital to understanding the complexities of natural systems (De Laender et al., 2010). A quantitative linkage between causal effects and natural system dynamics, that does not require a large regulatory experimental paradigm shift, would likely revolve around a mathematical model that links these levels of focus (Rohr et al., 2016). For example, a model for zebrafish (*Danio rerio*) by Beaudouin et al. (2015) accounted for nutrient cycling, resource dynamics, and behavioral differentiation between age-classes and sexes, which were crucial in capturing population dynamics. The model of Beaudouin et al. (2015) also provides detailed energetic insights for each modelled individual that could not only capture effects of non-chemical and indirect stressors, but also provide mechanistic linkages for toxicity effect data (Jager and Zimmer et al., 2012; Martin and Grimm, 2013).

Beaudouin et al. (2015) demonstrated a potential method to link organisms of interest and their environment using a flexible and generic model framework. The generic and flexible approach to ERA methods is one of the core requirements that makes ERA valuable across a range of systems and stressors (Norton et al., 1992). The fundamental design of Beaudouin et al. (2015) was related to the generic dynamic energy budget, individual-based model (DEB-IBM)

first presented by Martin et al. (2012). This model has been validated against individual and population data (Martin et al., 2013) and, as described in Grimm and Martin (2013), provides a mechanistic effect framework that not only quantitatively links individuals and populations, but provides the conceptual linkage as well. Specifically, the population dynamics emerge from processes modelled at individual levels. This process-based design holds promise for ERA focused linkage of individual level data and risk estimation at higher levels of biological organization (Jager et al., 2006).

One particular study organism that is relevant to mechanistic effect modeling and regulatory ERA methods is the great pond snail (*Lymnaea stagnalis*) (Charles et al., 2016; OECD, 2016; Ducrot et al., 2014, Zimmer et al., 2012, and Zimmer et al., 2014). *L. stagnalis* has been proposed for use in a reproductive toxicity test for freshwater gastropods (Charles et al., 2016; OECD 2016) and has been used widely in the literature for toxicity testing. Accordingly, there will likely be data generated on an individual level in relation to stressor exposure (Zimmer et al., 2012; Zimmer et al., 2014; Barsi et al., 2014) and then motivation to incorporate that data into ERAs (Ducrot et al., 2014; Cote et al., 2015). Additionally, focus on *L. stagnalis* is due to its ecological relevance and extensive global range (Budha et al., 2010). Specifically, *L. stagnalis* is a generalist herbivore (Elger et al., 2002) that is ecologically relevant to a variety of physical processes (Gutierrez et al., 2003; Elger and Lemoine, 2005). Importantly, *L. stagnalis* also demonstrate individual behaviors that are easily observable and relevant to ecological and stressor interactions (Lukowiak et al., 2008).

As suggestions to improve ERA methods largely rest on the linkage of individual metrics to population/community metrics (Rohr et al., 2016) and *L. stagnalis* has been studied as a model organism to explore individual stressor effects on ecosystems (OECD, 2016; Charles et al.,

2016), there is motivation to design and evaluate an individual energetic model specific to *L. stagnalis* (Ducrot et al., 2010; Ducrot et al., 2010, Zimmer et al., 2012; Zimmer et al., 2014).

Using the conceptual design of Grimm and Martin (2013) and example of Beauduoin et al. (2015), a successful *L. stagnalis* individual-based model (Grimm and Railsback, 2005) would incorporate a suite of relevant behaviors and intra- and inter-specific interactions.

Spatiotemporal patterns of movement towards resources or away from stressors (Elger et al., 2005; Lukowiak et al., 2008) and energetic deposition/cycling (Gutierrez et al., 2003) are likely ecologically relevant foci of an individual-based model of *L. stagnalis*. Modelling these interactions at the individual level would allow a direct connection between stressor data from standardized individual tests (OECD, 2016) and ERA output (Barsi et al., 2014).

Beyond the ecological details potentially relevant to an individual model, *L. stagnalis* present a significant physiological uniqueness worthy of attention. Generally, bioenergetic models of individual growth are simplified to a von Bertalanffy growth pattern (VBG) (von Bertalanffy, 1938). VBG is defined by minimal parameters but captures very significant details regarding individual growth—starting size, growth rate, and asymptotic size. Organisms that follow ‘normal’ VBG easily fit this model as they have high rates of growth rates shortly after birth and then a reduced growth rate as they approach maximum size. *L. stagnalis* do not demonstrate normal VBG under standard diet and laboratory conditions (Zonneveld and Kooijman, 1989; Zimmer et al., 2012; Arambasi et al., 2013; and Zimmer et al., 2014). Instead, this species shows a sigmoidal (‘S’ shaped) growth pattern with low growth rates after birth, but then a period of increased growth rate later in life (Figure 1). In considering individual and population-level models of *L. stagnalis* it is clear that capturing this deviation from common growth patterns is imperative.

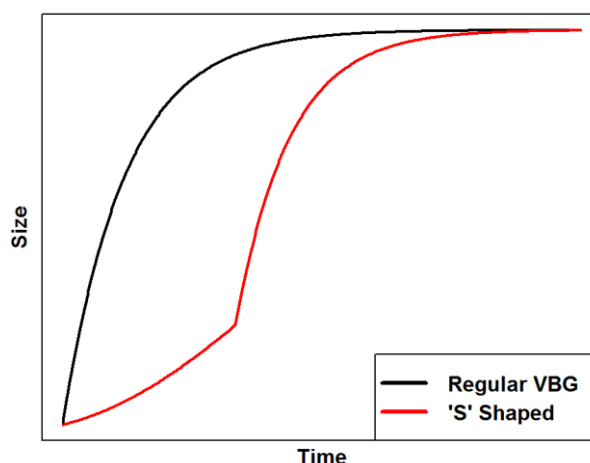


Figure 1. Two hypothetical growth patterns. 'Regular' von Bertalanffy growth (VBG, black) and an example of 'S' Shaped growth (red) observed in *L. stagnalis*. The delay in reaching a more rapid growth rate also leads to a delay in sexual maturity.

As in Chapter 1, in which a Dynamic Energy Budget (Kooijman, 2010) individual-based model (e.g., Martin et al., 2012) (DEB-IBM) was developed and applied for *Daphnia magna*, a similar model for *L. stagnalis* may prove useful and robust in capturing individual and system level dynamics relevant to ecological risk assessment based on standardized test endpoints. Specifically, the goal would be to capture individual growth patterns with enough mechanistic detail to infer impacts of sublethal stressors, independently and in combination, with behavioral and system interactions (Jager and Zimmer et al., 2012; Zimmer et al., 2012). Again, as in the *D. magna* model, adjustments will be needed to create a well performing model of *L. stagnalis* growth at individual and population levels accounting for specific ecological and energetic characteristics (Zimmer et al., 2012; Barsi et al., 2014).

The objectives of this chapter are to (1) refine a simplified DEB-IBM model of individual growth of *L. stagnalis*, (2) include important behavioral characteristics of *L. stagnalis* individuals in the IBM, and (3) evaluate model output against a series of experimental scenarios. Meeting these objectives would demonstrate a model framework that captures mechanisms and

phenomena specific to *L. stagnalis* with the ultimate goal of improving quantitative linkages between levels of study in ecological risk assessments of chemical stressors in aquatic systems.

Methods:

DEB-IBM model:

As in Chapter 1 of this thesis, the overall model approach is a DEB-IBM developed in R (R Core Team, 2016) and NetLogo (Version 5.3.1, Wilensky, 1999). The core of the design is motivated by the work of Martin et al.'s (2012) generic DEB-IBM platform. While the generic platform has great strength in its applicability, some specificity is required to adequately capture the internal and external energetic mechanisms. Specific to *Lymnaea stagnalis*, the observed “S-shaped” growth pattern (Zonneveld and Kooijman, 1989; Zimmer et al., 2012; and Arambasi et al., 2013) that deviates from the common von Bertalanffy pattern (von Bertalanffy, 1938) and their non-random movement pattern in a three dimensional environment. Refinement of the DEB sub-model focused on applying the ‘food limitation’ approach by Zimmer et al. (2012) and linking it to a ‘snail-specific’ IBM movement model that mimicked their wall/surface focused movements.

Using simplified DEB functions (Kooijman's, 2010, (Figure 2.10); Jager and Zimmer (2012)) and using DEB parameters from the ‘add_my_pet’ (http://www.bio.vu.nl/thb/deb/deblab/add_my_pet/index.html) database for *L. stagnalis*, a DEB-IBM was created in NetLogo (Wilensky, 1999). To emulate experimental conditions, we created a 3-dimensional environment representing an experimental chamber holding 1000mL of media and surface located food sources. The surface-located resource represented Romaine lettuce as a

representative of macrophytic vegetation, which is also commonly used in experimentation (Charles et al., 2016; OECD, 2016; Ducrot et al., 2014).

These model refinements were intended to improve the generic framework of Martin et al. (2012) by increasing the number of factors that influence individual energetic state. Accordingly, model output for individuals (and populations) will emerge from an increased number of mechanisms and potentially improve output across an increased range of ecological conditions (Grimm and Martin, 2013).

DEB and Juvenile Assimilation Lag Sub-Model:

The initial functions of the DEB growth sub-model were based on growth of organisms assuming adherence to the von Bertalanffy growth function with rapid early growth then tapering to a maximum limit (von Bertalanffy, 1938). Via dynamic energy budget parameters we can model growth in this fashion with a few functions:

$$f = \frac{[food]}{[food] + K} \quad \text{eq. 1}$$

$$L_{\infty} = \frac{f \dot{v}}{g \dot{k}_M} \quad \text{eq. 2}$$

$$\dot{r}_B = \frac{\dot{k}_M g}{3(f + g)} \quad \text{eq. 3}$$

$$\frac{d}{dt}L = \dot{r}_B (L_{\infty} - L) \quad \text{eq. 4}$$

where f is the functional response value, expressed as a relative value (0-1) with 0 indicating starvation and 1 *ad libitum* food availability. K is the half-saturation constant for the given food type at a concentration that corresponds with an f of 0.5. L_{∞} is the maximum length attained by an organism at a given functional response value f with standard DEB parameters \dot{v} , g , and \dot{k}_M (eq. 2). \dot{v} is an abstract DEB parameter and is interpreted as energy conductance with units of

length time⁻¹. By definition, \dot{v} , is surface-area-specific maximum assimilation rate divided by maximum energy density. g is the energy investment ratio, defined as the ratio of the energetic cost of structure divided by the maximum energetic density of somatic structure multiplied by the ratio of energy allocated to non-reproductive processes. \dot{k}_M is a somatic maintenance rate coefficient that represents the volumetric somatic maintenance rate divided by the volumetric energetic cost of soma.

In other implementations of DEB-IBM, the functional response value (f) was a product of the whole environment—resources per container volume (Martin et al., 2012). In Chapter 1, f values were modeled by the amount of resources in the patch containing the individual organism (e.g. resources per mL) to improve the detail of the individual energetic model. However, an *L. stagnalis*-specific adaption of this model was a combination of these two approaches (individual vs. container). Individual f values were determined by the concentration of resources in the container unless the individual was in a patch that contained lettuce. If the snail was directly in a patch containing lettuce its f value was set to 1. This was required due to the use of a simplified DEB model. This DEB model was simplified by removing a ‘reserve’ compartment that helps the starvation sub-model. Without this ‘reserve’ compartment, individuals that spend normal periods of time away from food items would die prematurely. This methodology is supported by DEB parameterization experiments that model food level as constant (Zimmer et al., 2012 and Zimmer et al., 2014) even though food level has clear—though small—fluctuations. i.e., DEB model parameters are fitted with this coarse approach in mind.

The food-limitation (or neonate assimilation lag) sub-model for *L. stagnalis* growth hypothesized and tested by Zimmer et al. (2012) was used to model individual deviation from VBG patterns (see Figure 1 above). The food-limitation model is driven by the hypothesis that

young snails cannot physically chew lettuce food items due to a small mouth opening or that they physically cannot reach the lettuce at the same rate as adult/juvenile snails. From a mechanistic standpoint, assimilation of energy has a lag period before it reaches levels observed in adult or sub-adult *L. stagnalis*. Within the quantitative framework, this is performed by adjusting the f value downward until an organism reaches a pre-determined size, at which point the f value becomes the original ‘non-lag’ value. The functions below were used in concert with the DEB functions above to model this adjustment:

$$f(L) = af_0 \frac{L}{L_m} \quad \text{with } L < L_f \quad \text{eq. 5}$$

$$L_m = \frac{\dot{v}}{gk_M} \quad \text{eq. 6}$$

with L_f being the length at which normal growth is observed (and the neonate assimilation lag period ends), a being a ‘food quality’ parameter that is largely used to fit the model to observations that different foods cause reductions in growth rate (Zimmer et al., 2012), f_0 is the “regular” functional response value (eq. 1 above), L is the length, and L_m is the maximum (non f -influenced) length.

Reproduction as Function of Length:

Cumulative reproductive output was modeled as a function of length, and iterative egg production only occurred on a ‘pulsed’ frequency (e.g., 1-2 events per week for *L. stagnalis*, (personal communication, Evy Reatgui-Zirena and Charles et al., 2016). The iterative magnitude is a function of cumulative reproduction divided by the age of the organism. The function below is from Kooijman (2010; Figure 2.10).

$$CumulativeReproduction = aL^2 + \frac{k_M}{\dot{v}}L^3 - bL^2 \quad \text{Eq. 7}$$

With a and b as fitting parameters adjusted to fit observed data from experimental organisms (data from ‘add_my_pet’ database used). To avoid the unknown or generally unavailable L_R term, bL^2 was used as a potentially more flexible replacement (See Kooijman, 2010, Figure 2,10). Figure 2 below demonstrates the data used to parameterize a and b published datasets (Zimmer et al., 2012 and Zimmer, 2013). See Table 1 for a summary of parameters, sources, and descriptions used in this model.

Spatially-Explicit Behavioral Model:

In a fashion similar to Chapter 1 above, a DEB-IBM of *L. stagnalis* was created in NetLogo (Wilensky, 1999) of a 3-dimensional environment (with a variable volume) designed to replicate an experimental chamber with lettuce patches on the surface of the media and walls that provide surface for movement.

Below is a pseudo-code in simplified NetLogo syntax describing the order of procedures (submodels) in each daily timestep. In general, the patch conditions of stressor and lettuce were manipulated first, then the snails update parameters, grow, reproduce, potentially die, and then move lastly.

```

to go
  ask patches [
    ifelse time-to-apply-stressor [
      set stressor random-normal mean sd
    ] [
      set stressor stressor * decay-rate
    ]

    ifelse count snails-here >= 1 [
      set lettuce (lettuce - (ingestion-rate * count snails-
here))
    ] [
      set lettuce random-normal mean sd
    ]
  ]
  ask snails [
    calculate-f

```

```

        calculate-ingestion-rate
        calculate-dL
        grow
        calculate-reproductive-output
        reproduce
        die?
        move
    ]
end

```

Of particular importance to this model is the design of the “walk” pattern of *L. stagnalis*. Casual observation suggests that the snails are either on the lettuce patches or a surface (wall or bottom) of the 3-dimensional chamber and they must move toward the surface to breath. As such, snails probabilistically leave the wall and rise to the surface where they can search for lettuce or move to other walls. The pseudo-code in simplified Netlogo syntax demonstrates how this procedure operates. Within the overall schedule of procedures during a timestep, “draw_walls” occurs during setup phases and “move” and “wobble” occur during the later individual stages of the timestep (after growth and reproduction procedures).

```

; setup procedure occurs prior to go procedure
to setup
to draw_walls [
    ask patches with [ coordinates = max ] [
        set id wall
    ]
]
end

; go procedure here (as above)

to move [
    ask snails [
        ifelse random 100 > 80 [
            move-to patch with [zcor = max-zcor]
        ][
            wobble
        ]
    ]
]

to wobble [
    ask snails [
        ifelse patch-ahead [id] = wall [
            move-to patch-ahead

```

```

    ] [
    turn random direction
    wobble
    ]
  ]
]

```

As experimental work with snails generally is for a short period of their lifespan and not explicitly focused on populations (Charles et al., 2016), this model is largely focused on the growth and behavior of individuals over a similarly short timespan. While reproductive behavior was modeled (and offspring produced) populations were not simulated as the timeframe to observed emergent dynamics of *L. stagnalis* (≥ 1 year) was greater than typical laboratory experimental design (1-2 months).

Table 1. Table of parameters, sources, and descriptions for *L. stagnalis*.

Parameter	Units	Value	Source	Function	Description
K	$\# l^{-3}$	3.08	Zimmer et al.	–	Half-Saturation Constant
f_0	unitless	–	–	$f = \frac{[food]}{[food] + K}$	Functional Response Value
f	unitless	–	–	$f(L) = af_0 \frac{L}{L_m}$ with $L < L_f$	Functional Response Value
\dot{v}	$L t^{-1}$	0.2161	Zimmer et al.	–	Energy Conductance
g	unitless	0.1176	Zimmer et al.	–	Energy Investment Ratio
\dot{k}_M	t^{-1}	0.4882	Zimmer et al.	–	Somatic Maintenance Rate Coefficient
L	L	–	–	$V = L^{1/3}$	Volumetric Length
L_{phys}	L	–	–	$L_{phys} = L * shape_factor$	Physical Length
L_m	L	–	–	$L_m = \frac{\dot{v}}{g\dot{k}_M}$	Maximum Possible Length
$shape_factor$	unitless	NA	Zimmer et al.	$shape_factor = V^{1/3} / L$	Shape Coefficient
L_∞	L	–	–	$L_\infty = \frac{f\dot{v}}{g\dot{k}_M}$	Asymptotic von Bertalanffy Length
\dot{r}_B	t^{-1}	–	–	$\dot{r}_B = \frac{\dot{k}_M g}{3(f + g)}$	von Bertalanffy Growth Rate
$\alpha_{Lettuce}$	unitless	1.4225	Zimmer et al. East	$f(L) = af_0 \frac{L}{L_m}$ with $L < L_f$	Food Quality Parameter
L_f	L	0.8687	Zimmer et al.		Length at end of Food Limitation

Results:

To meet the first objective to refine the individual DEB model to capture growth of *L. stagnalis*, data from Zimmer et al. (2014) was used to estimate an f value. Then using other parameters from the same data set, growth of an individual was modeled through a 350 day ‘lifespan.’ Figure 2 demonstrates that the juvenile assimilation lag model seems to model growth of *L. stagnalis* through its full lifespan quite well. Of note is the somewhat abrupt change at the L_f point (approximately day 150 in Figure 2). This is due to the lack of variability around the point where assimilation lag ends in the model and fitting model parameters from mean values rather than distributions. It is possible that inclusion of stochasticity in the L_f parameter could be used to improve this abrupt change, but this was not evaluated here.

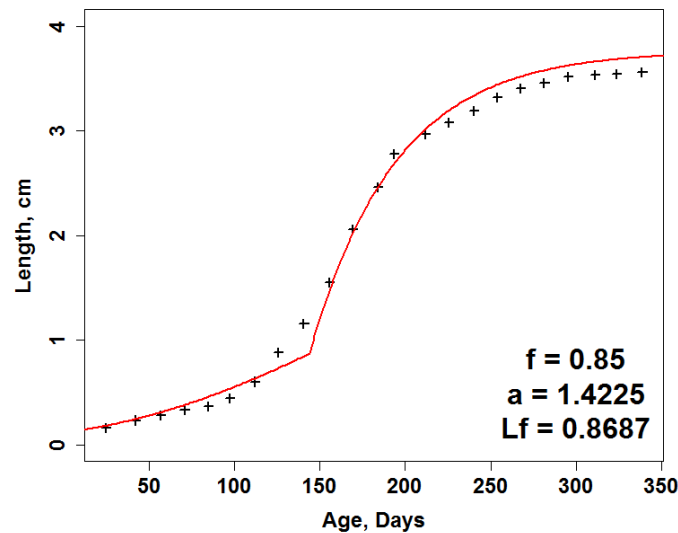


Figure 2. Juvenile assimilation lag model (red line) fit against growth data (black crosses) from Zimmer et al. (2014). Final size data and parameters (Table 1) were used to estimate an f value of 0.85 and in combination with food quality parameter (a) and length at regular assimilation (Table 1) the model fits data well.

After confirmation of the individual growth model, several conditions were simulated in the DEB-IBM to evaluate model output. Specific conditions included amount of food, timing of

food application, and shape and size of the environment. Final metrics of interest were shell length (cm) and f value as they are indicators of organism and system energetic state. All data presented are from 50 simulation runs and data were collected on day 250. The goal of these simulations was to evaluate whether the *L. stagnalis* model functions and metrics could capture predictable changes in system-wide energetic manipulations.

Food amount and application frequency have differential but important effects on individual snails (Figures 3a and 3b). Food amount has the largest effect on mean size and f value, but timing of resource input has an interesting effect on mean f value. Decreased food input frequency appears to increase the variation of mean f values of snails. This poses an interesting insight into toxicity test experimental design and individual stressor response energetics that would not be captured in traditional metrics like organism size (see Figure 3a). Increased variability in organism condition (f value) may present increased variability in stressor response.

Due to the spatially-explicit detail at which individual movement was modelled, it was hypothesized that, at constant food levels, environment shape could influence snail energetics. Two container shapes—‘shallow’ and ‘narrow’ were tested (Figure 4a and 4b). It was hypothesized that a shallow environment would improve the energetic state of the organisms in that less time would elapse between movements from the bottom to top of the environment. The ‘narrow’ environment was to test the increased density of lettuce patches, but increased distance between upper and bottom portions of the environment. Two additional environments—two cubes—of differing size were also tested to explore the effect of food density in relation to the environment.

Much as in the food level and application frequency, environmental shape may have nuanced impacts on energetic metrics (Figure 5). Figure 5a shows that median (of 50 simulations) lengths are ranked: 'Shallow' > 'Large' > 'Small' > 'Narrow' but that the distributions of responses are quite overlapped. This ranking is likely due to the increased number of snails with elevated f values in the 'Shallow' and 'Large' scenarios (Figure 5b). Clearly the interplay between environment shape and its effect on food location is of great importance to organisms with specific walk/search patterns.

In summary, these results suggest that energetic sub-models and spatially-explicit sub-models were successful in application and expected output. These results also display the strength of a flexible but specific framework in exploring impact of experimental design.

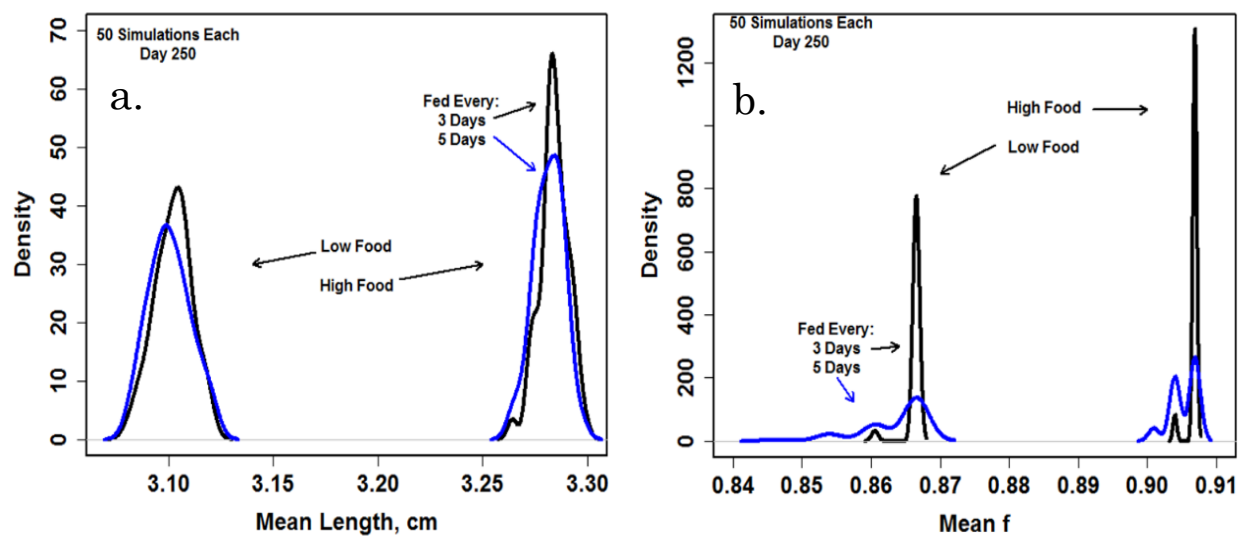


Figure 3a and 3b. Density plots of responses ((a.) mean length, cm, and (b.) mean f value) of four simulation conditions manipulating resource level and timing of application. 50 simulations were run for each conditions and data was collected on day 250. High food was 30 cm² lettuce per L and low was 20 cm² lettuce per L. Lettuce was applied every three or five days.

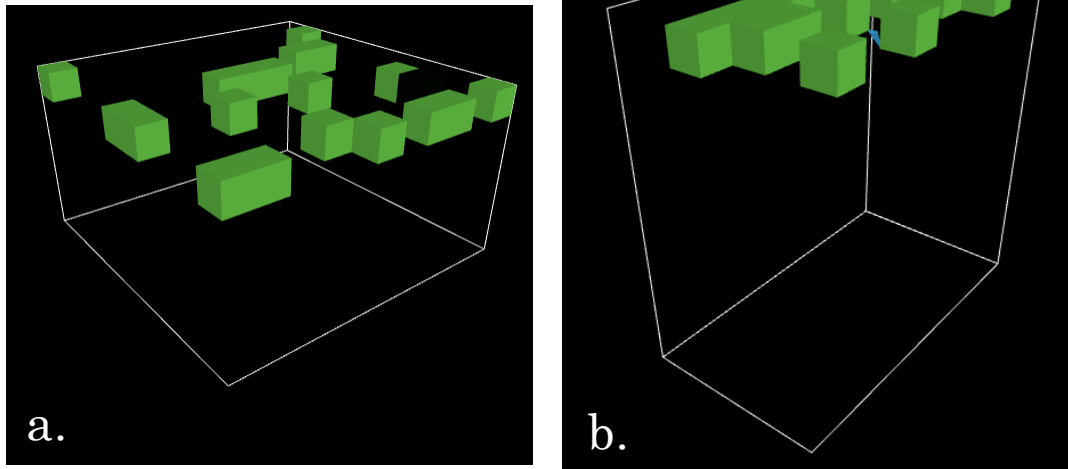


Figure 4a and 4b. Two simulated environment shapes used to simulate growth of snails. (a.) is ‘shallow’ with an area of 796 cm^3 and dimensions of $11 \times 11 \times 6 \text{ cm}$ and (b.) is ‘narrow’ with an area of 796 cm^3 and dimensions of $11 \times 6 \times 11 \text{ cm}$. Green patched are single cm^2 patches containing lettuce.

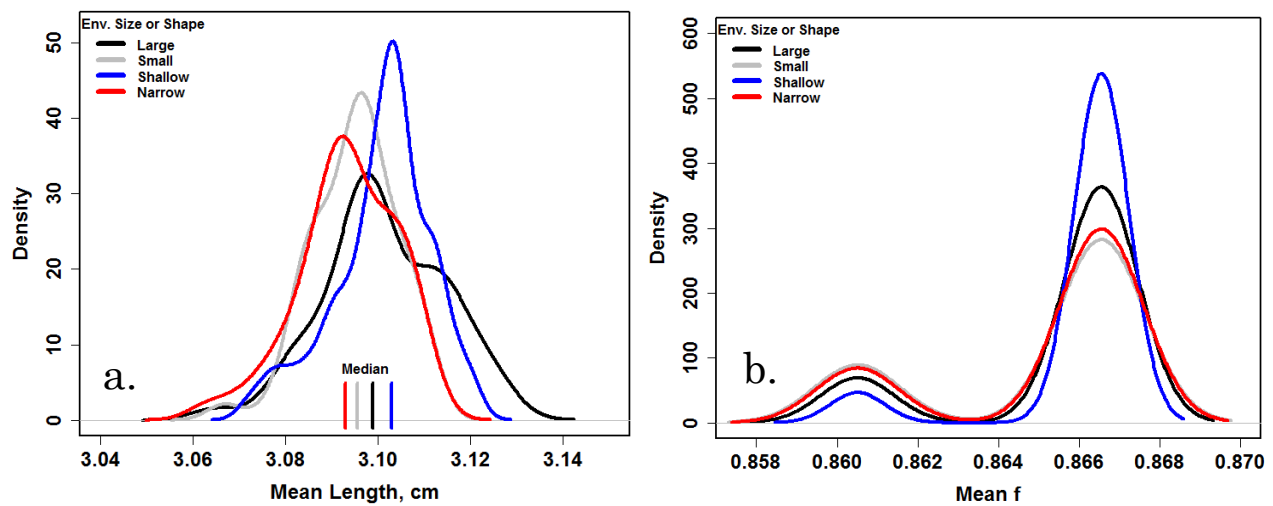


Figure 5a and 5b. Density plots of responses ((a.) mean length, cm, and (b.) mean f value) of four simulations with varied environment shape or size. 50 simulations were run for each condition and data was collected on day 250. ‘Large’ is a cube of 1331 cm^3 , ‘small’ is a rectangle 396 cm^3 , ‘shallow’ is a rectangle 726 cm^3 , and ‘narrow’ is a rectangle 726 cm^3 . Dimensions (x,y,z or length,width,depth) of ‘shallow’ were $(11,11,6) \text{ cm}$ and ‘narrow’ were $(11,6,11)$.

Discussion:

Mechanistic effect models are proposed as a means to improve both the output and value of ecological risk assessment of chemical stressors (Rohr et al., 2016 and Grimm and Martin, 2013). These models will require well performing and robust individual energetic models to provide confidence predictions of larger system dynamics (Sibly et al., 2013 and Grimm and Martin, 2013). The research presented in this chapter was intended to contribute to efforts to increase confidence in a single organism model (*L. stagnalis*) through specific details of bioenergetics but also spatially-explicit phenomena. Model output for individual growth matches published datasets (Figure 2) (Zimmer et al., 2012 and Zimmer et al., 2014) and anticipated energetic effects of resource level and spatial variation are produced when the full model is run.

Juvenile Assimilation Lag:

While most experimental designs for *L. stagnalis* do not incorporate the full lifespan of the organism (Charles et al., 2016), there are recent efforts to explore effects of chemical stressors and diet types on juvenile or neonate stage snails (Fidder et al., 2016, Reatgui-Zirena et al., 2016) and a model with increased detail would improve confidence in predicting these conditions. Additionally, it is important that the juvenile assimilation lag period arises from a reasonably testable mechanism. If a lettuce diet is unavailable to juvenile or neonate snails (Zimmer et al., 2012), more accessible diet items could be presented and growth patterns could be observed to test this mechanism (Reatgui-Zirena et al., 2016). Additionally, due to the flexibility of the function used to account for juvenile assimilation lag, the magnitude of assimilation lag for different diet items could be explored. The $a_{Lettuce}$ parameter could be fitted

to growth patterns under different diet conditions. As presented in Zimmer et al. (2012) this is a key consideration for models geared towards sub-lethal energetic effects of chemical stressors. The work of Fidler et al. (2016) and Reatgui-Zirena et al. (2016) also corroborate with the hypothesis that increased detail at individual levels increases confidence of overall understanding of stressor mechanisms and effects.

While the juvenile assimilation lag period is the chosen mechanism for this model, there is work that posits another mechanism and quantitative approach. *L. stagnalis* were one of the first organisms modelled using the dynamic energy budget (Zonneveld and Kooijman, 1989) and the core message was that two parameter sets were required to model the full lifespan of *L. stagnalis*. Juvenile snails appeared to allocate energy at different rates than adult snails. Zimmer et al. (2014) returned to this work as a contrast to the earlier Zimmer et al. (2012). The two approaches being ‘food-limited’ and ‘metabolic-acceleration’ with food-limited as described under the moniker ‘juvenile assimilation lag’ in this research and metabolic acceleration being a more complicated approach. Metabolic acceleration (as in Zimmer et al., 2014) requires shifting DEB parameters at given sizes to account for the increased rate of allocation of food items as the snails age. As shown in Zimmer et al. (2014), this model provides a ‘smoother’ fit in relation to Figure 2 of this research, but does not appear to fit better across the lifespan of the snails.

As there has not been work to specifically address which of these methods is more correct, I prefer the simpler juvenile assimilation lag (food limitation) model. As the metabolic acceleration models are fitted from observed data and as are juvenile assimilation lag methods, the timing of parameter shifts are both arguably arbitrary. Additionally, the metabolic acceleration model requires a ‘full DEB’ model, which introduces an additional series of calculations and can increase computational costs required to run model simulations. Lastly,

both models are mechanistic, so in the absence of supporting evidence, the simpler juvenile assimilation lag model is preferred.

Spatially-Explicit Behavioral Model:

Improvement of an organism specific individual-based model requires an appropriate level of detail of internal processes (see above) but also an appropriate level of detail in the external interactions between individuals and the environment (Sibly et al., 2013, Grimm and Martin, 2013). This becomes very clear when an increased level of complexity is desired. In the work of Beauduoin et al. (2015), individual zebrafish were modelled through sex, age, and location specific sub-models. Their well-performing model suggests that for organisms with specific resource or habitat needs for specific sexes or age classes (such as zebrafish), this level of detail is required. The energetic backbone of the model of Beuaduoin et al. (2015), provides additional support, as the biomass dynamics observed are best fit by the spatially-explicit energetic interactions between different sex and age-class zebrafish and their prey items.

A well performing ecotoxicology model that accounts for complexity of multiple species will require strong individual models (Grimm and Martin, 2013) and I suggest that the current model framework can serve as an initial effort. As *L. stagnalis* represents an important regulatory (OECD, 2016) and ecological organism (e.g. Gutierrez et al., 2003) there is value in this specific and detailed approach. Linking internal and external at the individual and organismal level provides the platform upon which linkage of intra- and inter-population/community models can be built. At the intra-individual level, this requires generic but flexible approaches such as a DEB model with juvenile assimilation lag to account for

organism specific adjustments. Spatiotemporal dynamics of resources and abiotic conditions can then be accounted for at an individual level by organism specific but generic ‘walk’ patterns.

In summary, this chapter presents a *Lymnaea stagnalis* specific DEB-IBM that accounts for several unique characteristics of *L. stagnalis* growth and behavior. Specifically, a refined simplified DEB-IBM model of individual growth accounting for juvenile assimilation lag and a detailed model of movement patterns was described. Evaluation of model output demonstrated that the model performed as expected and incorporation of juvenile assimilation lag and detailed behavioral characteristics was important to model output. The model demonstrated a conceptual and quantitative framework specific to *L. stagnalis* that could potentially be useful to improve ecological risk assessment of chemical stressors.

Literature Cited:

- Arambašić, M.B., Pašić, M., Ristanović, D., Kalauzi, A. and Kojić, L., 2013. Pond Snail *Lymnaea stagnalis* L.: The Implication for Basic and Applied Research. *World Applied Sciences Journal*, 25(10), pp.1438-1448.
- Barsi, A., Jager, T., Collinet, M., Lagadic, L. and Ducrot, V., 2014. Considerations for test design to accommodate energy-budget models in ecotoxicology: A case study for acetone in the pond snail *Lymnaea stagnalis*. *Environmental toxicology and chemistry*, 33(7), pp.1466-1475.
- Beketov, M.A., Kefford, B.J., Schäfer, R.B. and Liess, M., 2013. Pesticides reduce regional biodiversity of stream invertebrates. *Proceedings of the National Academy of Sciences*, 110(27), pp.11039-11043.
- Bradbury, S.P., Feijtel, T.C. and Leeuwen, C.J.V., 2004. Meeting the scientific needs of ecological risk assessment in a regulatory context. *Environmental science & technology*, 38(23), pp.463A-470A.
- Budha, P.B., Dutta, J. & Daniel, B.A. 2010. *Lymnaea stagnalis*. The IUCN Red List of Threatened Species 2010: e.T155475A4782225. <http://dx.doi.org/10.2305/IUCN.UK.2010-4.RLTS.T155475A4782225.en>. Downloaded on 30 November 2016.
- Charles S., V. Ducrot, D. Azam, R. Benstead, D. Brettschneider, K. De Schamphelaere, S. F. Goncalves, J. W. Green, H. Holbech, T. H. Hutchinson, D. Faber, F. Laranjeiro, P. Matthiessen, L. Norrgren, J. Oehlmann, E. Reategui-Zirena, A. Seeland-Fremer, M. Teigeler, J.P. Thome, M. T. Kaplon, L. Weltje, L. Lagadic, Optimizing the design of a reproduction toxicity test with the pond snail *Lymnaea stagnalis*. 2016. *Regulatory Toxicology and Pharmacology*, 81:47-56
- Côte, J., Bouétard, A., Pronost, Y., Besnard, A.L., Coke, M., Piquet, F., Caquet, T. and Coutellec, M.A., 2015. Genetic variation of *Lymnaea stagnalis* tolerance to copper: A test of selection hypotheses and its relevance for ecological risk assessment. *Environmental Pollution*, 205, pp.209-217.
- Ducrot V., C. Askem, D. Azam, D. Brettschneider, R. Brown, S. Charles, M. Coke, M. Collinet, M.L. Delignette-Muller, C. Forfait-Dubuc, H. Holbech, T. Hutchinson, A. Jach, K. L. Kinnberg, C. Lacoste, G. Le Page, P. Matthiessen, J. Oehlmann, L. Rice, E. Roberts, K. Ruppert, J. E. Davis, C. Veauvy, L. Weltje, R. Wortham, L. Lagadic, 2014. Development and validation of an OECD reproductive toxicity test guideline with the pond snail *Lymnaea stagnalis* (Mollusca, Gastropoda), *Regulatory Toxicology and Pharmacology*, 70(3):605-614
- Ducrot, V., Péry, A.R. and Lagadic, L., 2010. Modelling effects of diquat under realistic exposure patterns in genetically differentiated populations of the gastropod *Lymnaea stagnalis*. *Philosophical Transactions of the Royal Society B: Biological Sciences*, 365(1557), pp.3485-3494.

- Ducrot, V., Teixeira-Alves, M., Lopes, C., Delignette-Muller, M.L., Charles, S. and Lagadic, L., 2010. Development of partial life-cycle experiments to assess the effects of endocrine disruptors on the freshwater gastropod *Lymnaea stagnalis*: a case-study with vinclozolin. *Ecotoxicology*, 19(7), pp.1312-1321.
- Elger, A., Barrat-Segretain, M., Amoros, C., 2002. Plant palatability and disturbance level in aquatic habitats: an experimental approach using the snail *Lymnaea stagnalis* (L.). *Freshwater Biology* 47, 931–940.
- Elger, A., Lemoine, D., 2005. Determinants of macrophyte palatability to the pond snail *Lymnaea stagnalis*. *Freshwater Biology* 50, 86–95.
- Fidder, B.N., Reátegui-Zirena, E.G., Olson, A.D. and Salice, C.J., 2016. Energetic endpoints provide early indicators of life history effects in a freshwater gastropod exposed to the fungicide, pyraclostrobin. *Environmental Pollution*, 211, pp.183-190.
- Forbes, V.E. and Calow, P., 2002. Extrapolation in Ecological Risk Assessment: Balancing Pragmatism and Precaution in Chemical Controls Legislation. *BioScience*, 52(3), pp.249-257.
- Grimm, V., S.F. Railsback, 2005. Individual-based modeling and ecology. Princeton University Press.
- Gutiérrez, J.L., Jones, C.G., Strayer, D.L., Iribarne, O.O., 2003. Mollusks as ecosystem engineers: the role of shell production in aquatic habitats. *Oikos*. 101:79-90.
- Hayashi, T.I., Imaizumi, Y., Yokomizo, H., Tatarazako, N. and Suzuki, N., 2016. Ecological risk assessment of herbicides in Japan: Integrating spatiotemporal variation in exposure and effects using a multimedia model and algal density dynamics models. *Environmental Toxicology and Chemistry*, 35(1), pp.233-240.
- Jager, T. and Zimmer, E.I., 2012. Simplified dynamic energy budget model for analysing ecotoxicity data. *Ecological Modelling*, 225, pp.74-81.
- Jager, T., Heugens, E.H. and Kooijman, S.A., 2006. Making sense of ecotoxicological test results: towards application of process-based models. *Ecotoxicology*, 15(3), pp.305-314.
- Kooijman S.A.L.M. 2010. Dynamic energy budget theory for metabolic organization. 3rd ed. Cambridge, UK: Cambridge University Press.
- Lukowiak, K., Martens, K., Rosenegger, D., Browning, K., Caigny, P., Orr, M., 2008. The perception of stress alters adaptive behaviours in *Lymnaea stagnalis*. *Journal of Experimental Biology* 211, 1747–56.
- Martin, B., Zimmer, E., Grimm, V., Jager, T., 2012. Dynamic Energy Budget theory meets individual-based modelling: a generic and accessible implementation. *Methods in Ecology and Evolution* 3, 445–449.
- McMahon, T.A., Halstead, N.T., Johnson, S., Raffel, T.R., Romansic, J.M., Crumrine, P.W. and Rohr, J.R., 2012. Fungicide-induced declines of freshwater biodiversity modify ecosystem functions and services. *Ecology Letters*, 15(7), pp.714-722.

- Norton, S.B., Rodier, D.J., van der Schalie, W.H., Wood, W.P., Slimak, M.W. and Gentile, J.H., 1992. A framework for ecological risk assessment at the EPA. *Environmental toxicology and chemistry*, 11(12), pp.1663-1672.
- OECD (2016), *Test No. 243: Lymnaea stagnalis Reproduction Test*, OECD Publishing, Paris. DOI: <http://dx.doi.org/10.1787/9789264264335-en>
- R Core Team (2016). R: A language and environment for statistical computing. R Foundation for Statistical Computing, Vienna, Austria. URL <https://www.R-project.org/>.
- Reátegui-Zirena, E.G., Fidder, B.N. and Salice, C.J., 2016. A cost or a benefit? Counterintuitive effects of diet quality and cadmium in *Lymnaea stagnalis*. *Ecotoxicology*, pp.1-11.
- Rohr, J.R., Salice, C.J., Nisbet, R.M., 2016. The pros and cons of ecological risk assessment based on data from different levels of biological organization. *Crit. Rev. Toxicol.* 46, 756–84
- Sibly, R., Grimm, V., Martin, B., Johnston, A., Kulakowska, K., Topping, C., Calow, P., Nabe-Nielsen, J., Thorbek, P., DeAngelis, D., 2013. Representing the acquisition and use of energy by individuals in agent-based models of animal populations. *Methods in Ecology and Evolution* 4, 151–161.
- Suter II, G.W., 2016. *Ecological risk assessment*. CRC press.
- van der Meer, J., Klok, C., Kearney, M.R., Wijsman, J.W. and Kooijman, S.A.L.M., 2014. 35years of DEB research. *Journal of Sea Research*, 94, pp.1-4.
- von Bertalanffy, L., 1938. A quantitative theory of organic growth (inquiries on growth laws. II). *Human biology*, 10(2), pp.181-213.
- Wilensky, U. 1999. NetLogo. <http://ccl.northwestern.edu/netlogo/>. Center for Connected Learning and Computer-Based Modeling, Northwestern University. Evanston, IL.
- Zimmer, E., Jager, T., Ducrot, V., Lagadic, L., Kooijman, S., 2012. Juvenile food limitation in standardized tests: a warning to ecotoxicologists. *Ecotoxicol Lond Engl* 21, 2195–204.
- Zimmer, E.I., 2013. The pond snail under stress: interactive effects of food limitation, toxicants and copulation explained by Dynamic Energy Budget theory. Doctoral dissertation, Vrije Universiteit.
- Zimmer, E.I., Ducrot, V., Jager, T., Koene, J., Lagadic, L. and Kooijman, S.A.L.M., 2014. Metabolic acceleration in the pond snail *Lymnaea stagnalis*?. *Journal of Sea Research*, 94, pp.84-91.
- Zonneveld, C. and Kooijman, S.A.L.M., 1989. Application of a dynamic energy budget model to *Lymnaea stagnalis* (L.). *Functional Ecology*, pp.269-278.

Chapter III.

Modelling Experimentally Observed Indirect Energetic Facilitation between Co-occurring *Lymnaea stagnalis* and *Daphnia magna*.

Introduction:

The overall goal of ecotoxicological research is to provide data, tools, and insights that can inform and improve ecological risk assessment. As highlighted recently, however, there is an important disconnect between ecotoxicology study endpoints and ecological risk assessment (ERA) outcomes (Rohr et al., 2016). This disconnect is largely due to the mismatch of experimental endpoints and environmental protection goals. Most data used to inform ERAs is obtained from individual-level toxicity tests while society is most interested in protecting populations, communities, and ecosystems (Rohr et al., 2016). Given that expanding regulatory testing protocols to include specifically evaluating population and community-level metrics is unlikely to occur (OECD, 2016; OECD, 2012), the most practical way forward is to improve methods that link individual-level effects to effects at higher levels of biological organization. To this end, a robust and flexible quantitative linkage might provide a means of predicting effects of chemical stressors on ecological systems within the constraints of current testing guidelines (Jager, Heugens, and Kooijman, 2006; Jager and Zimmer, 2012; Forbes et al., 2011; Grimm and Martin, 2013; and Rohr et al., 2016).

Much of the recent focus on linking results from toxicity tests to natural systems in the context of ERAs has been built on a premise of organismal energetic costs of exposure to

chemical stressors. These energetic costs at individual-levels are represented by shifts in energy allocation patterns that can drive subsequent changes in population dynamics (e.g. Sokolova, 2013; Nisbet et al., 2000, Congdon et al., 2001, Baas et al., 2010, Kooijman, 2001). One specific framework of energetic assimilation and allocation is the Dynamic Energy Budget Theory of Metabolic organization (DEB) (Kooijman, 2010). The DEB theory has a sophisticated and robust mathematical framework (Jusup et al., 2016) and has been implemented for a number of species (see ‘add_my_pet’ database at <http://www.bio.vu.nl/thb/deb/deblab/add_my_pet/>; Lika 2011a; and Lika 2011b). Additionally, recent research (e.g. Jager and Zimmer (2012) in concert with Kooijman 2001 above) specifically demonstrates the connection of stressor effects to a DEB-based organismal model that is individual based. DEB additionally has a foundation in ‘first principles’ (Jusup et al., 2016), is supported by a large and growing database (Kooijman, 2010 and ‘add_my_pet’ database), and allows focus towards mechanistic stressor effects at individual levels (Jager and Zimmer, 2012). Hence, developing and implementing DEB models is an excellent starting point to establish mathematical linkages between individual-level data and higher levels of biological organization.

While the large body of DEB modeling has revolved around models of controlled laboratory settings for model parametrization, there have been several that link indirectly or directly to field data. Martin et al. (2012) and Zimmer et al. (2014) are good examples of parameterizing a DEB model from controlled conditions of food and environment. Both *Daphnia magna* and *Lymnaea stagnalis* are common toxicity test model organisms and accordingly, data obtained for these species ideally can lead to models that perform well under conditions common to toxicity tests. Moving beyond simple experimental conditions, however, requires more understanding of the environment and inter- intra-species variability of DEB

model parameters. Cardoso et al. (2006) demonstrated that linking model results from laboratory settings and field-observed data can provide insight into the variability in model parameters under varying environmental conditions. Potentially more important, is to parameterize a DEB model from laboratory-observed data and to then accurately predict organism energetics under field-observed conditions. To some extent, this is the ultimate objective for ecological modelers. For example, Ren and Schiel (2008) developed and parameterized a DEB model of oyster growth under lab conditions and were able to accurately predict oyster growth in the field under naturally varying food and temperature conditions.

These examples provide additional support for a DEB-based modelling framework for applications in ecotoxicology. Additionally, the above examples lay the groundwork and provide working examples of increasing model system complexity. As outlined in Rohr et al. (2016), multi-species models could be useful because they directly relate to higher levels of biological organization which are relevant to environmental regulation and management. Beyond regulatory relevance, multi-species models commonly take methodological and conceptual constructs (Park et al., 2008 and Vinebrooke et al., 2004) that are designed to explicitly account for indirect interactions between system members. This interaction-dependent framework of multi-species models that leads to emergence of population and community dynamics from interactions, processes, and contexts at lower levels of organization has been a strength and goal of many current ERA modelling methods (Chen et al., 2013; Jager et al., 2006, Rohr et al., 2016). However, we are not aware of any efforts that have attempted to use DEB models to explore multi-species systems or, specifically, the energetic interaction of one species with another (in greater complexity than phytoplankton dynamics such as Ren and Schiel (2008)). In an effort to explore a new avenue of ecotoxicology research, but remain based in

ERA and regulatory relevant organisms, I developed a multi-species DEB-IBM that is a combination of the *D. magna* and *L. stagnalis* DEB-IBMs presented in Chapters 1 and 2 of this thesis. These species do not directly compete for resources nor is one a predator to the other. Accordingly, their energetic interactions are likely to be entirely indirect but of high potential relevance to exploring effects of stressors at population- and community-level (Congdon et al., 2001).

As the two model organisms, *D. magna* and *L. stagnalis*, and their interaction, are seldom studied together in relation to ecotoxicology (Sanchez and Tarazona, 2002), below is an introduction to what I hypothesize is their main route of interaction—indirect energetic facilitation (Steiner et al., 2005 and Davidson et al., 1984). I hypothesize that *L. stagnalis* will generally increase daphnid population size through ‘mobilization’ of energy in lettuce that would normally be unavailable to daphnids. Additionally, the increased nutrient and elemental complexity of waste products will likely produce altered phytoplankton dynamics that may influence daphnid population dynamics.

Indirect energetic facilitation is explained by two different potential mechanisms: 1.) Diffusion of competitors—in which a high diversity of competitors leads to suppression of shared resources and/or 2.) Specialization by one competitor causes a shift in resource abundance that effectively reduces prior competitive interactions (Steiner et al., 2005). As suggested in Steiner et al. (2005) distinguishing between these two can be fairly complex. For instance, the seminal work on indirect facilitation by Davidson et al. (1984) between rodents, ants, and two seed types clearly demonstrated that the specialization of the rodent diet for larger seeds removed pressure on smaller seeded plants and therefore supported a greater density of ants. Their experimental exclusion of rodents increased the ratio of large seeds to small seeds and

subsequently decreased the resources available to the ants—decreasing ant density. This is largely an example of the second mechanism presented above. The work of Steiner et al. (2005) demonstrated a scenario closer to the first mechanism—culturing 4 types of zooplankton together produced very different biomass dynamics than culturing each zooplankter individually. Elevated consumer diversity increased individual zooplankter biomass stability which, consequently, drove an overall positive increase in zooplankton biomass through time. While the largest evidence was for the diffusion type of facilitation based on biomass patterns, observed phytoplankton size distribution changes indicate that diet specialization and competitive exclusion may have played a role (Steiner et al., 2005).

In relation to the system I have described (*D. magna* and *L. stagnalis*), I hypothesize that diet specialization (similar to the ant-rodent example of Davidson et al (1984)) will be the greatest mechanism of indirect energetic facilitation of *D. magna* by *L. stagnalis*. As these species likely co-occur in natural lakes or ponds as a zooplankter and macrophyte grazer and are both model organisms for energetic, toxicity, and regulatory studies (Kooijman, 2010; OECD, 2016; and OECD, 2012) a model framework focused on the indirect energetic interactions of these species would be valuable. This chapter presents experimental and model methods and results to introduce and explore a relatively understudied energetic interaction in relation to mechanistic effect models to ultimately improve ecological risk assessments of chemical stressors. The main objectives were to experimentally test whether indirect energetic facilitation occurs from *L. stagnalis* to *D. magna* and to develop a multi-species DEB-IBM that could effectively simulate the energetic interactions between *L. stagnalis* and *D. magna*.

Methods:

Experimental Design

Experimental populations of *Daphnia magna* (purchased from Aquatic BioSystems and cultured in-house) and *Lymnaea stagnalis* (from a culture originating at Texas Tech University, the Institute of Environmental and Human Health) were housed in standard synthetic freshwater (moderately hard) (US EPA, 2002) in one-liter glass jars ($n = 30$) and observed for 40 days. Daphnid populations were started with 5 neonates (0-24 hours old) and the treatments with snails each contained one snail (approximately 2 cm terminus to terminus shell length and age approximate 180 days). 90% water changes were performed every third day and population sizes and individual snail and daphnid lengths were recorded during each media change while the old media was removed. Organisms (if part of algae or lettuce containing treatments) were fed concentrated (3.0×10^7 cells mL^{-1}) *Raphidocelis subcapitata* (formerly known as *Psuedokirschneriella subcapitata* and *Selenastrum capricorutum*, also purchased from Aquatic BioSystems) corresponding to $\sim 1.65 \times 10^5$ cells mL^{-1} , ~ 0.0012 mg Carbon mL^{-1} , or 0.5% of experimental media by volume (as concentrate) and 1 cm^2 rinsed romaine lettuce on each water change. Temperature was stable at 20°C and lighting was a cool fluorescent with a 16 hour on, 8 hour off cycle.

At each water change, digital images were taken from directly above the experimental chambers. A ruler placed under the beakers was used for scaling. Image J (Version ij150, 2016) was used to count the number of individuals and measure lengths, which was taken as eye spot to base of spine in daphnids or terminus to terminus of snail shells. The number of lengths gathered per replicate was not always the same due the nature of daphnid movement during photography,

but a minimum of 25% of total population size was achieved for most sampling events.

Additionally, specific effort was made to gather lengths of the largest daphnid individuals for as long as reasonable confidence existed that they were the starting individuals (28 days). Program R (Version 3.1.1, 2016) was used for data manipulation and figure generation.

Treatments:

Treatments in the experiment were intended to represent a gradient of both energetic quantity and quality (or complexity). Figure 1 below outlines the connection between *D. magna*, *L. stagnalis*, and their respective primary experimental resources, algae and lettuce. The treatments included in this experiment were intended to highlight the contribution of the arrows to organismal interactions. The treatment with the lowest amended energy and low energetic quality was called ‘LD.’ LD referred to lettuce and *Daphnia* and was code for the treatment of only applying lettuce and 5 neonate daphnids to the experimental chambers. Lettuce was changed at each water change to prevent rotting. The ‘AD’ treatment represents an increase in energetic quality and included algae and *Daphnia* and was the treatment most akin to a control population in common experimental conditions. The next more energetically complex and energy rich treatment was ‘ASD.’ ASD designated treatments included algae, *Daphnia*, and a single snail. This treatment was to isolate the potential consumption of algae by *L. stagnalis*. The converse treatment was the ‘SLD’ treatment and included snails, lettuce, and *Daphnia* and was used to isolate snail contributions to *D. magna* without the influence of algae. ‘ASLD’ was the most energetically complex and rich treatment and included algae, a single snail, lettuce, and *Daphnia*. Although it is a vast simplification, ASLD also represents the closest approximation to

what would be present in actual, multi-species systems. Each treatment included 6 replicates and all were monitored and fed (or lettuce just refreshed—LD treatment) concurrently.

Conceptually, my hypothesis regarding energetic complexity and energetic content is that the increasing order of the treatments would be: LD < AD < ASD < SLD < ASLD.

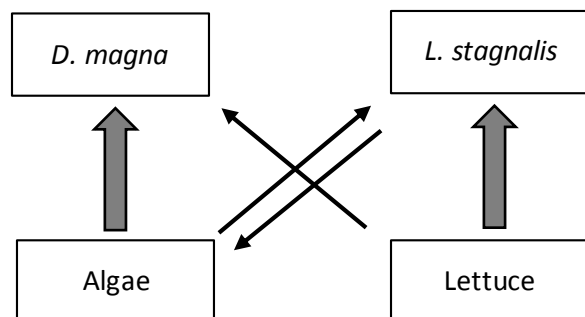


Figure 1. Conceptual diagram of the potential interactions between organisms and resources. Arrow width indicates hypothesized importance of connection. Treatment LD represents the arrow from lettuce to *D. magna*, treatment AD represents the arrow from algae to *D. magna*, ASD represents the arrows between algae, *D. magna* and *L. stagnalis*. SLD represents the arrows between lettuce, *D. magna* and *L. stagnalis*. ASLD encompasses all arrows.

Table 1. Treatment system members and corresponding code labels.

Treatment	Code
Lettuce <i>D. magna</i>	LD
Algae <i>D. magna</i>	AD
Algae <i>L. stagnalis</i> <i>D. magna</i>	ASD
Lettuce <i>L. stagnalis</i> <i>D. magna</i>	SLD
Algae Lettuce <i>L. stagnalis</i> <i>D. magna</i>	ASLD

Energetic Sampling and Quantification:

To test my hypotheses about the ranking of the treatments and begin to develop model parameters for these treatments, carbon content of the water and the daphnids was collected periodically throughout the monitoring period as an estimate of system and individual-level consolidation of overall energy (after Glazier and Calow, 1992 and Frost et al., 2008). Suspended and settled carbon was determined from samples collected from the upper half ('pelagic') and the bottom ('benthic') of the jars on days 2, 21, 30, and 40. Carbon concentration was determined using several methods, one to determine total carbon and another to isolate algae sourced carbon. Algae sourced carbon methods relied on absorbance at 682nm to determine the algae content based on comparison to a standard curve of known lab sourced algae. Through the known carbon content of the lab algae, an algae-based carbon concentration could then be calculated. Total suspended particulate carbon was determined by a sulfuric acid based spectrophotometric method (Albalasmeh et al., 2013 and Reatgui-Zirena et al., 2015). Briefly, water samples were evaporated completely and, along with a tripalmitin standard curve, were suspended in sulfuric acid and chloroform (5:1 ratio) and placed in a 200C oven for 30 minutes. Absorbance at 340nm by the charred carbon in the remaining sulfuric acid was compared against the tripalmitin standard curve to calculate total carbon (mg ml^{-1}) (Reatgui-Zirena et al., 2015).

Carbon, nitrogen, and sulfur content of the daphnids was determined by an Elementar brand 'varioEL' CNS elemental analysis instrument in the Urban Environmental Biogeochemistry Lab at Towson University. Daphnids for elemental analysis were collected on day 39 and were the 5 largest and 5 smallest individuals in each replicate. Daphnids were measured for length using scaled imagery and imageJ and then dried overnight in a 60C oven. Samples were pooled to meet sample size limitations of the instrument. Results from this

instrument were proportion of sample mass as the selected element (e.g. sample mass was 30% carbon indicating that the dry weight of the organism was 30% carbon).

Model Methods:

The model used to explore these energetic conditions/treatments was a combination of the *D. magna* and *L. stagnalis* NetLogo (Wilensky, 1999) based DEB-IBM (Kooijman, 2010, Martin et al., 2012) models of Chapters 1 and 2 (see Figure 2) with a sub-model focused on the ‘conversion’ of carbon contributed by snail waste to an equivalent number of algae cells. The magnitude or efficiency of this conversion has been termed ‘facilitation factor’ and represents a new parameter from those presented in prior chapters.

Similar to my experimental conditions, all model runs started with 5 neonates and one snail approximately 180 days old (~2cm), with algae levels and lettuce levels consistent with the specific treatment. Simulations were run for 40 days in the same fashion as the experiments.

See Chapter 1, Table for parameters specific to *D. magna* and Chapter 2, Table 1 for parameters specific to *L. stagnalis*.

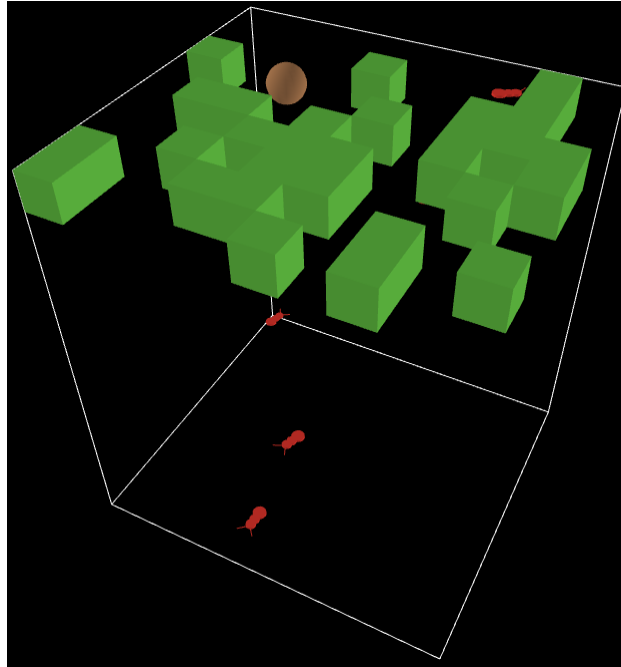


Figure 2. Figure showing three dimensional environment of the multi-taxa DEB-IBM. Green cubes represent patches with lettuce, the brown sphere is the snail, and the red 'bugs' are the daphnids. Algae is not shown, but is in all the patches that are not green.

Facilitation Sub-model:

The new development needed in this model was the quantitative approach to capture the movement of energy from snails to daphnids. Conceptually, this was modelled by the size and condition (f) of the snail that then contributes carbon to the system. The snail-contributed carbon content was then converted to a number of algae cells by a mass of carbon cell^{-1} relationship previously determined and a 'facilitation factor' to control the efficiency of this energy transfer. Note, this is a conceptual and model simplification to relate snail-contributed carbon to consumable energy units (alga) available to daphnia.

Quantitatively, linear models were used to predict algae-based carbon by snail length (Figure 3). On a per patch basis, the sum length of all the snails present (generally 0 or 1) and the maximum snail f value were used to calculate algal contribution to that patch. The linear model slope was multiplied by the sum snail length to predict the magnitude of contribution by the size

of the snail(s) present. The y-axis intercept was multiplied by the f value to shift the linear relationship up or down depending on the condition of the snail. That concentration of algae-based carbon was then converted to a number of cells per unit volume as per in-house lab value of 7.0×10^{-9} mg C cell⁻¹ and multiplied by a facilitation factor to create a new algae concentration for that patch containing snails.

Figure 4 demonstrates that my algae-based carbon content was well predicted by observations of total carbon ($r^2 = 0.78$). Based on the linear model parameters, a reasonable level of 37.5% of the total carbon observed in all facilitated treatments had been consistently ‘converted’ to chlorophyll-containing sources. This provides support for the hypothesis and modeling approach that carbon enrichment in experimental treatments is directly related to algae cell enrichment.

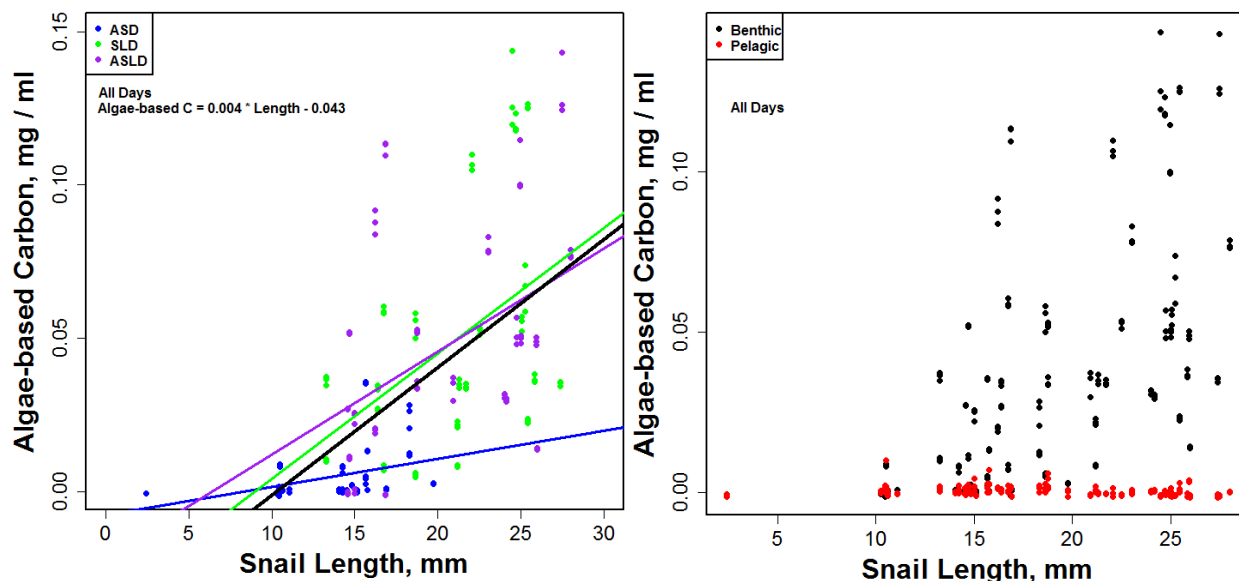


Figure 3. Scatterplots of algae-based carbon as a function of snail length. Data were from experimental observations. ‘All days’ means that data from sampling events on days 2, 21, 30, and 40 were combined in these plots. As shown on **right**, majority of algae-based carbon was present in benthic samples so (as on **left**) the linear model used to predict snail carbon contribution to algae cells was from benthic samples. The function is $\text{mg / ml algae-based C} = 0.0004 * \text{snail length (mm)} - 0.043$ and had a r^2 value of 0.3699.

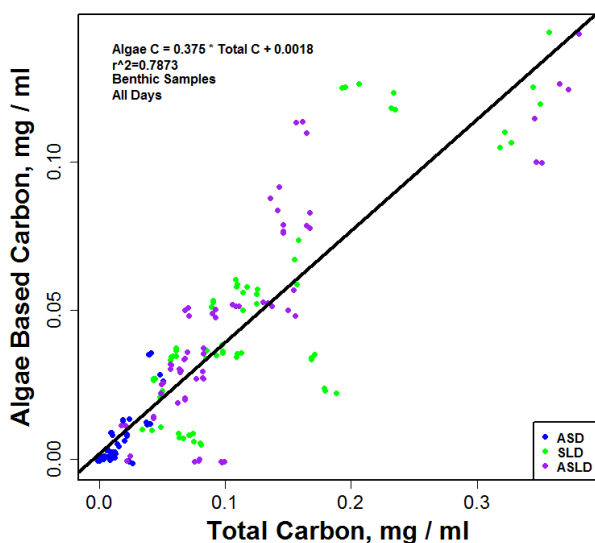


Figure 4. Figure demonstrating the linear relationship between algae-based carbon and total carbon. Key metric is the slope of 0.375, indicating that approximately, 37.5% of total carbon was from chlorophyll containing sources.

Results:

Experimental Results:

Population Level:

Patterns of *D. magna* population dynamics through 40 days in each treatment follow similarly shaped trajectories (Figures 5 and 6). All populations had a period of slow growth during the initial neonate development, a period of rapid population growth and then decline. However, the data suggest differential influence of energetic treatments on daphnid population dynamics. Specifically, it was interesting to note that the ‘LD’ treatment did support a small daphnid population without any experimental addition of resources other than lettuce—which is not directly available to daphnids. The treatment did, however, have the lowest peak size. The next lowest population peak size was the ‘SLD’ treatment. Again, this treatment did not have any resource addition that was daphnid-specific—the only addition was lettuce for the snails. The other treatments had similar peak size magnitude, but the dynamics before and after the peak differed. Those treatments with snails and algae (ASD and ASLD) had distinct peaks, sharp declines, and then a period of slower decline. The ‘AD’ treatment (normal experimental conditions) showed only a steady increase and then a period of slower decline.

Outside of the difference in population size dynamics, there were differences in length (age-class) distributions through time and by treatments. Most of the treatments had the expected right-skewed and multi-modal patterns of many populations with short, but distinct generation times (Figures 7, 8, and 9). However, the lack of right-skewness in the LD treatment agreed with the low population size and lack of a sharp peak/decline indicative of an ageing population. Additionally, of note is that the SLD treatment was the only treatment to maintain a

fairly distinct right-skewness and peak near 1mm through day 40. All others appeared to have a fairly central peak or at least a peak that was moving to the right through time—indicative of decreasing reproduction and increasing ratios of large to small daphnids.

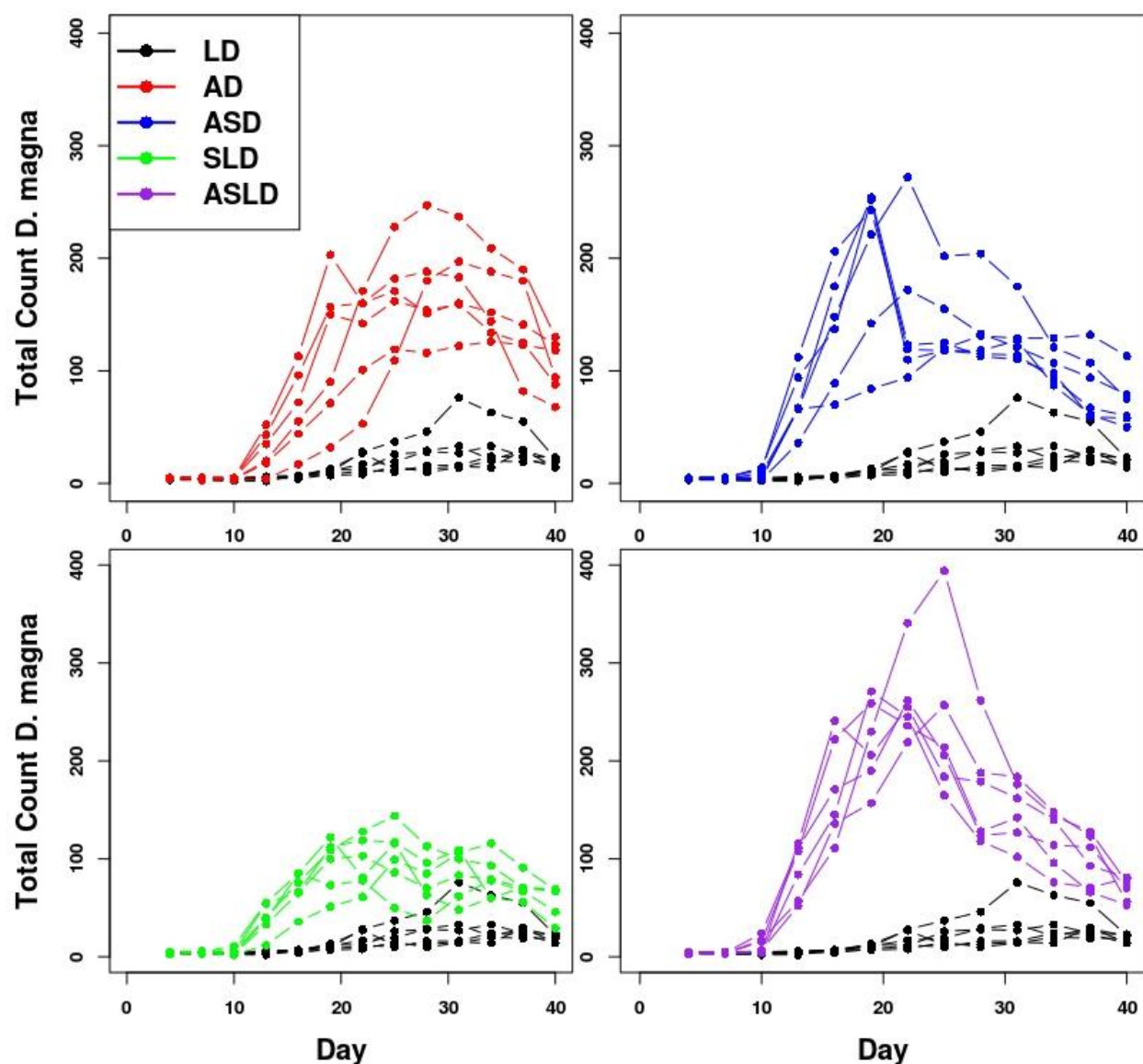


Figure 5. *D. magna* population size of each replicate and treatment through time. Replicates are points connected by lines. Each plot has the 'LD' treatment for consistent comparison. All data from day 40 has 10 individuals added to account for sampling of individuals on day 39.

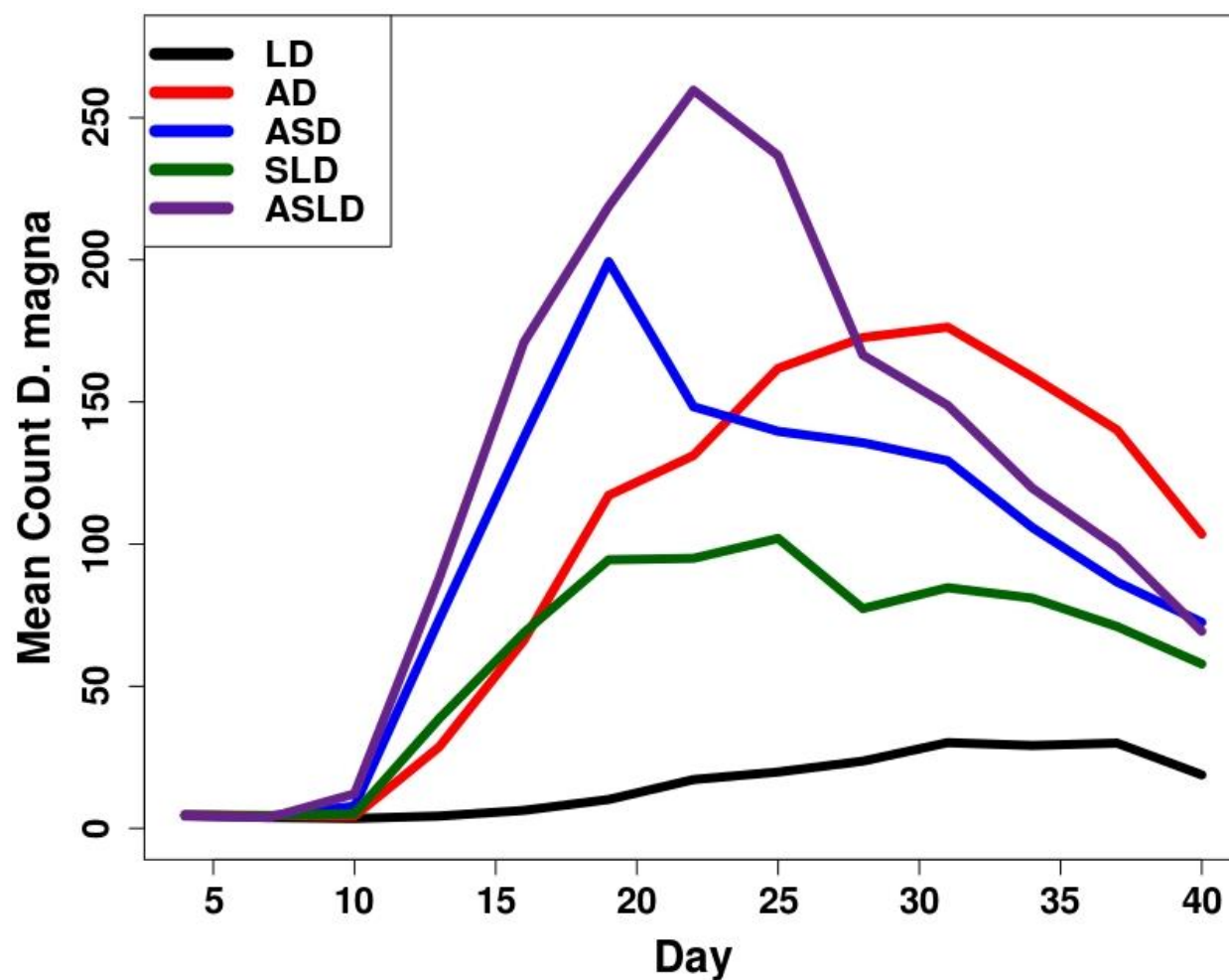


Figure 6. Mean of replicates per treatment *D. magna* population sizes through time. Confidence intervals were removed for ease of comparison across treatments. All data from day 40 has 10 individuals added to account for sampling of individuals on day 39.

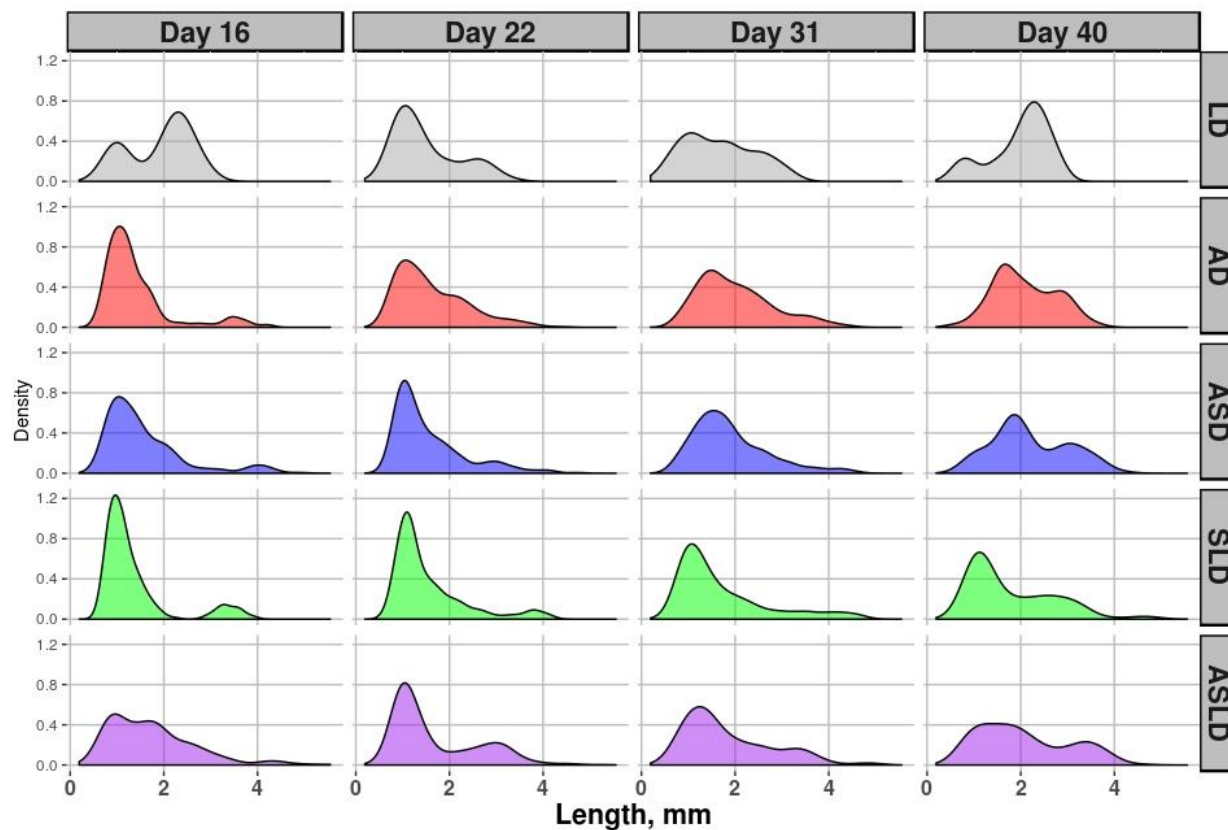


Figure 7. Density plots of *D. magna* lengths of combined replicates by treatment and selected days. Five largest and five smallest individuals were removed from all treatments on day 39.

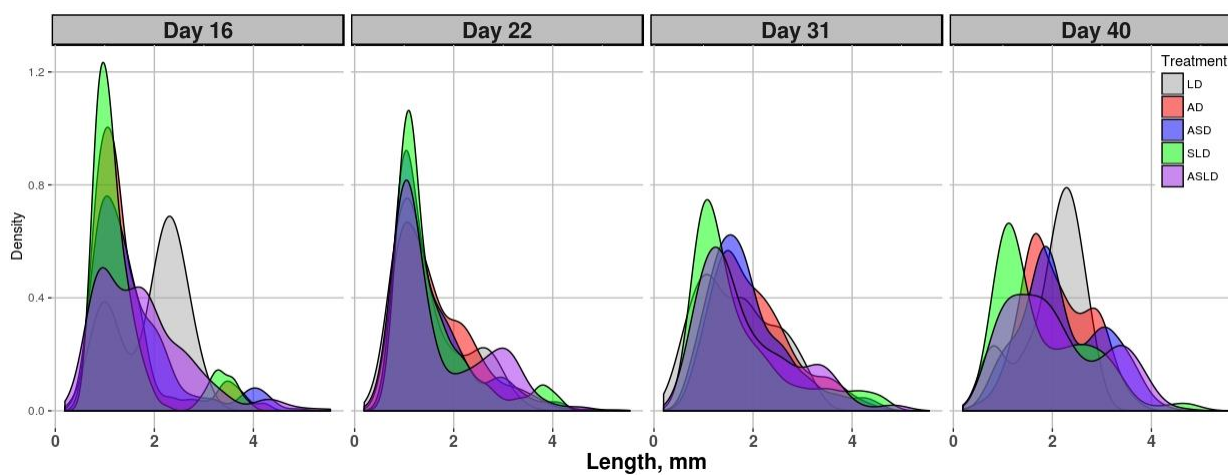


Figure 8. Data from Figure 4 above, presented with treatments overlaid to demonstrate the between treatment differences at the selected timepoints. Five largest and five smallest individuals were removed from all treatments on day 39.

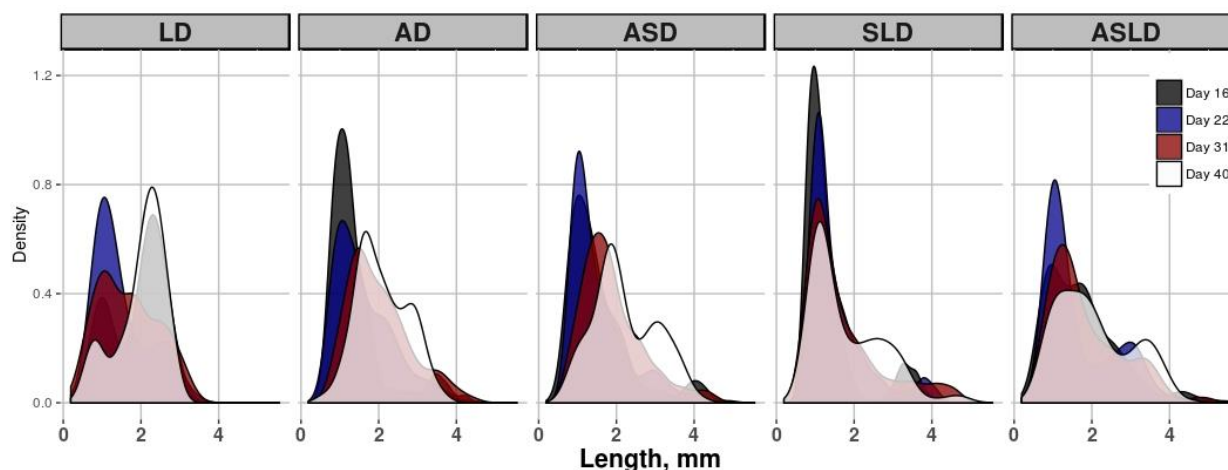


Figure 9. Data from Figure 4 presented by treatment with timepoints overlaid to demonstrate the change in age class distribution through time within treatments. Five largest and five smallest individuals were removed from all treatments on day 39.

Individual Results:

In an effort to connect observed population dynamics with properties of individuals, data from individuals was collected and presented below. Maximum length observed in each replicate for the first 28 days of the experiment was collected and used to fit VBG models to explore the effect of facilitation on individuals (Figure 10). Pilot studies (and Chapter 1 above) suggested that mortality of the initial five neonates is fairly low through the first month and it stands to reason that the largest observed size would be one of the starting individuals. The goal was to demonstrate the difference between individual growth patterns due to the different treatments and, as hypothesized, mean length at day 28 was approximately ranked by energetic ‘quantity and quality’ in increasing order of $LD < AD < ASD < SLD < ASLD$ (Figure 6). The DEB framework provides quantitative evidence that an increase of energetic assimilation and/or allocation can be observed in increased final size (Kooijman, 2010, see eq. 2 in Chapters 1 and 2 above). Visually, this is seen by the approximately ‘parallel’ von Bertalanffy growth patterns

between treatments LD, AD, ASD, and ASLD. Treatment SLD does not appear to follow the ‘parallel’ pattern and this is highlighted by the listed von Bertalanffy growth function parameter (k) values (Figure 10).

In order to further explore the observed growth patterns, a suite of energetic metrics were collected. Daphnids had a satisfactory mass by length relationship that follows expected third power rules, but also there appeared to be some individuals that showed greater deviation (Figure 11). Additionally, the individuals with greater deviation appeared to be from common treatments (Figure 12). It also is clear, due to the clumping of the points, that treatments had contributed to what might be considered energetically different organisms—not just individuals. Of particular note is the large length, but small mass (relatively) of the SLD treatment individuals (green points, Figure 12) that further highlights their deviation from expected patterns.

Beyond mass and length, elemental proportions (C, N, and S) were collected and there were some apparent trends between treatments (Figure 13). N and S measurements were particularly weak and were likely influenced by the limit of detection of the instrumentation and limited mass of sub-adult samples. Carbon, however, showed a positive trend of enrichment in the hypothesized order of energetic quantity and complexity. Again, of note, was the slight deviation of the SLD treatment. In relation to Frost et al. (2008), this observed enrichment may potentially indicate more than just organism condition, as impact of bacterial infections altered C balance in their daphnids.

Additionally, when plotted against mass or length (Figure 14) proportion of each element showed potential treatment-related patterns. C and N appeared to approach linearity with a positive slope while S appeared to either be non-linear or slightly negatively linear.

Again, the SLD treatment appeared to either fall between the AD and ASD treatments (rather than ASD and ASLD as hypothesized) or, as in the case of N, as a potentially completely different relationship.

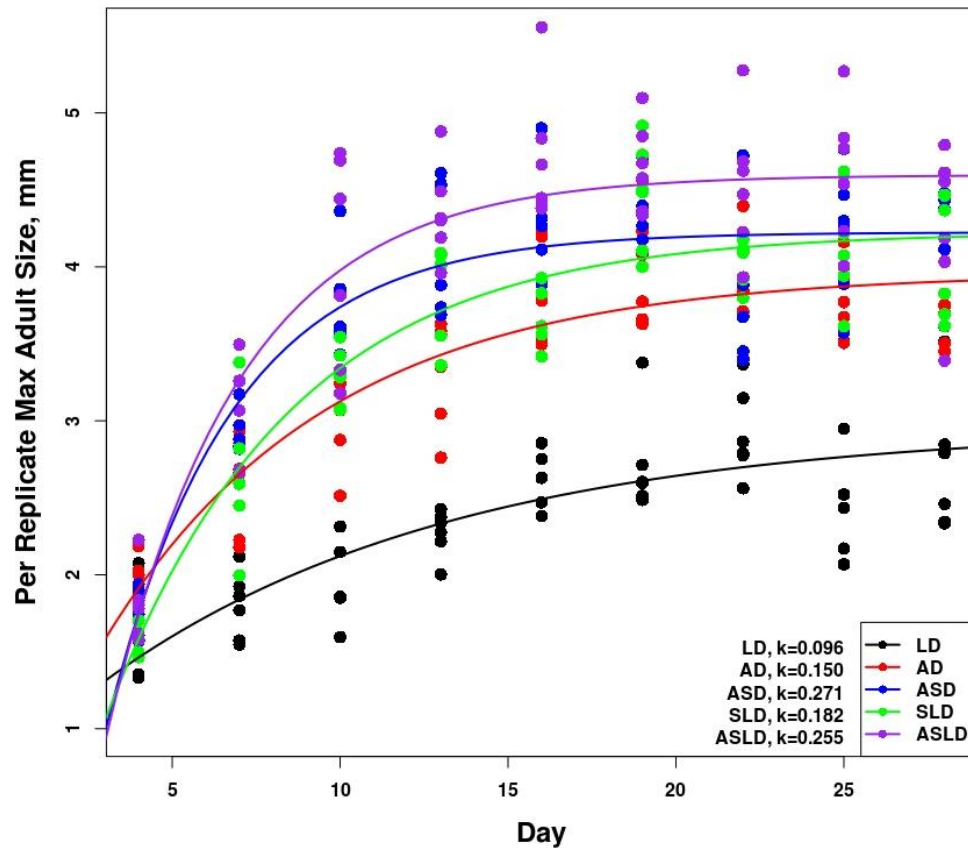


Figure 10. Maximum size measured in each replicate prior to day 28. Fitted von Bertalanffy functions are plotted against data and growth rate parameters (k) are highlighted for each treatment.

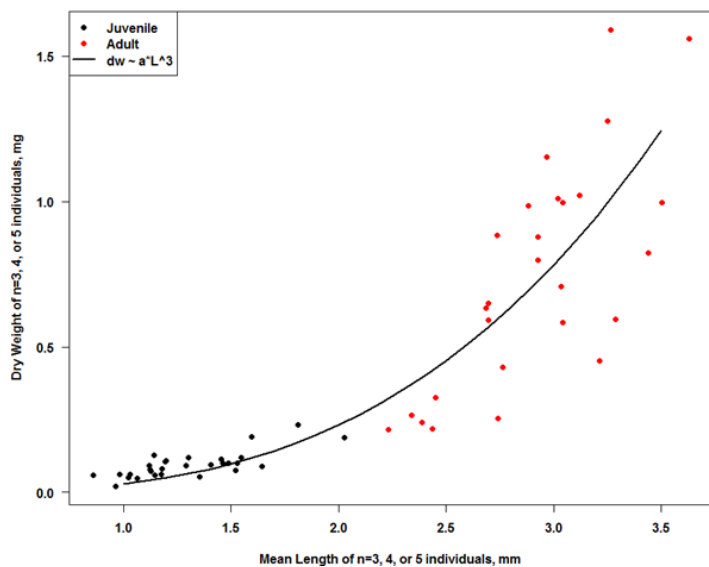


Figure 11. Scatterplot of dry weight (mg, n=3, 4, 5) predicted by mean length (mm, n=3, 4, 5) with fitted length³ function and colors to indicate age-classes.

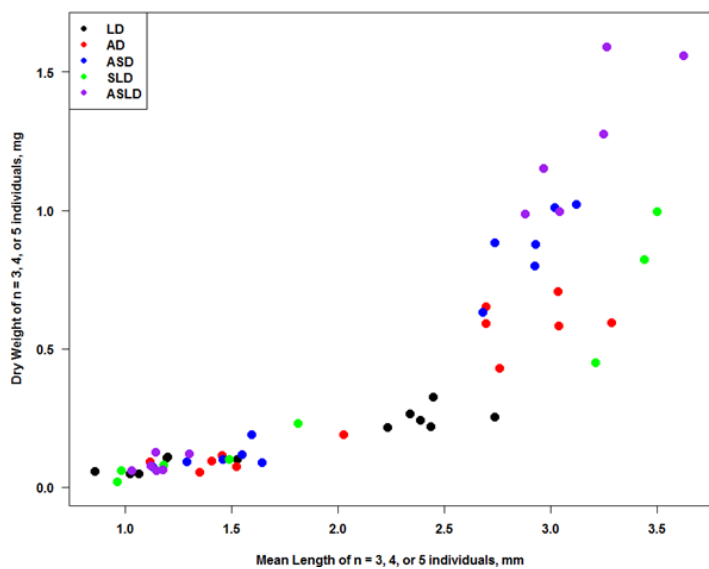


Figure 12. Data from Figure 11 above, but with colors indicating grouping by treatment. Of particular note is the deviation of the SLD (green) data.

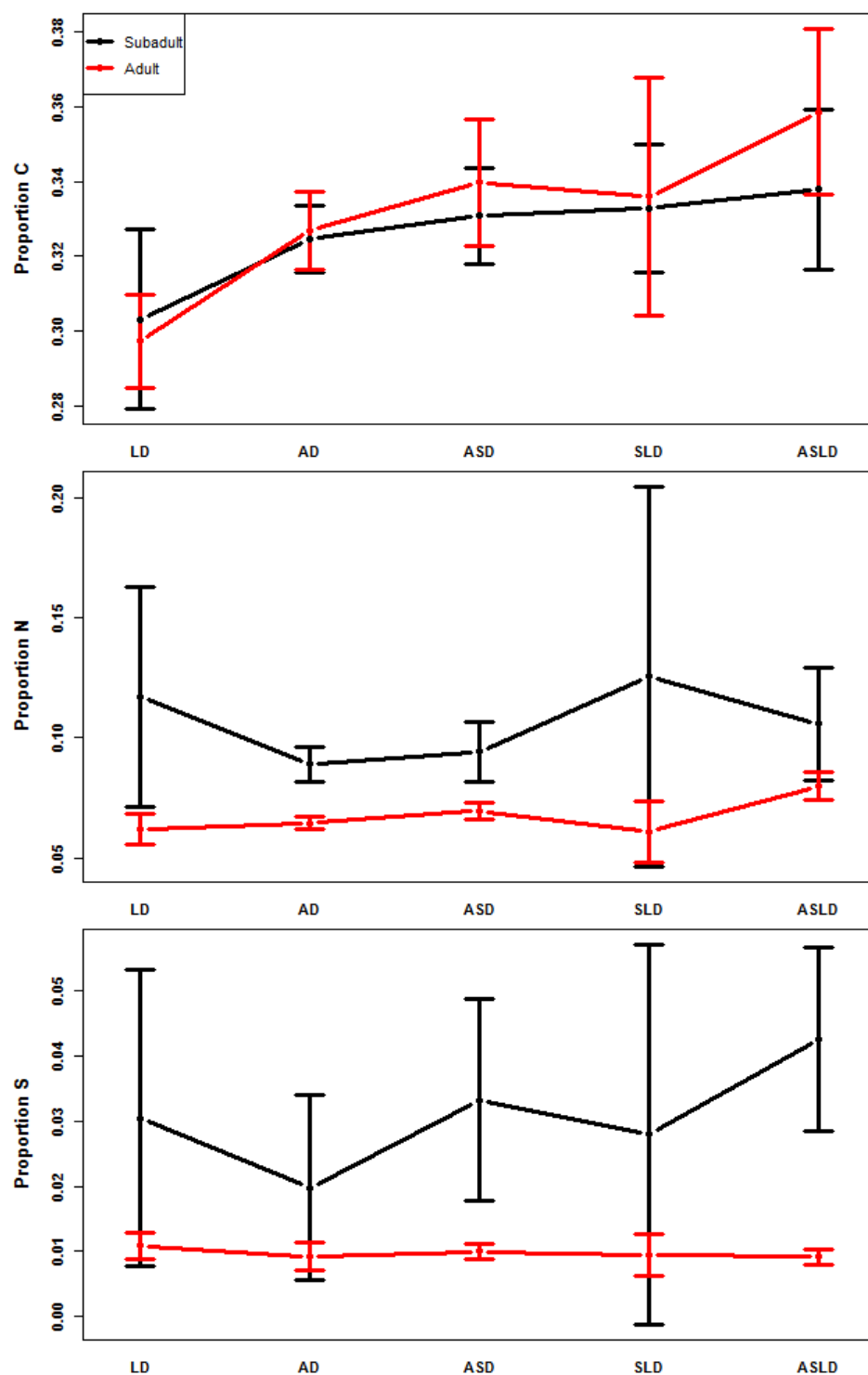


Figure 13. Variability and trends of elemental proportion (C, N, and S; by mass) for daphnia from each treatment and age class. Large variability in subadult age classes is attributed to small sample size.

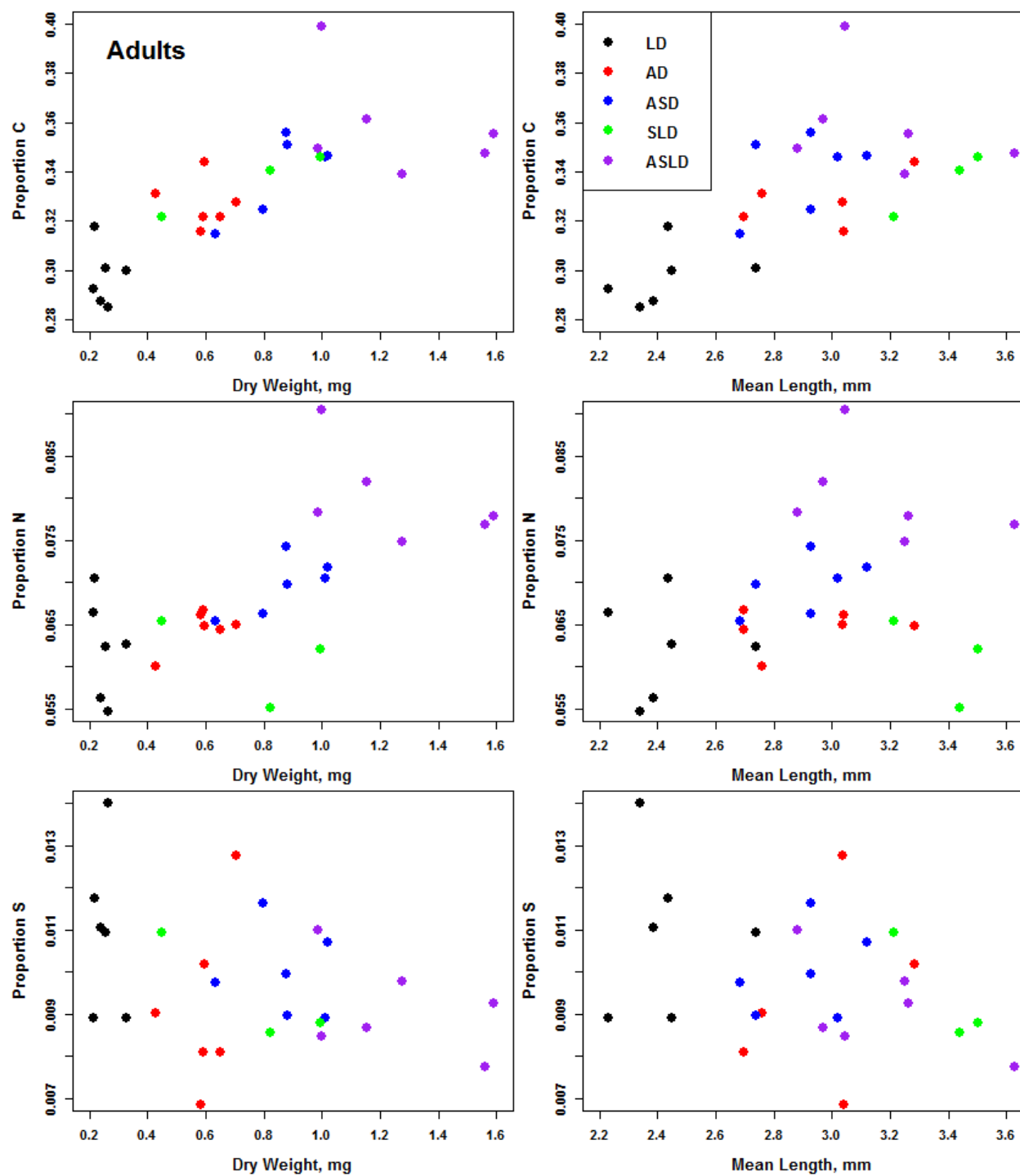


Figure 14. Scatterplots demonstrating grouping of treatments in elemental proportions of daphnia plotted against size metrics (length and dry weight) in the adult age class.

Environmental Energetics:

To explore the hypothesis that the energy of the system was driving the differentiation between the daphnid population and individual metrics, suspended carbon concentration was collected and evaluated (Figure 15). The strongest patterns were the physical descent of the carbon (highest levels in benthic samples) and the enrichment or dilution of carbon through time. That gravity influenced carbon distribution was not surprising given the contribution of snail waste to this carbon pool. Dilution or enrichment of carbon was also demonstrated by the temporal dynamics of C in treatments with snails. As the ASD treatment snails did not show any definitive growth through time (Figure 16)—the temporal decline in benthic total carbon in the ASD treatments (Figure 15, top center) showed that if snails were not fed, they did not contribute to C enrichment of the system and that the dilution of the water samples suggests that C had been allocated to other processes (daphnids' growth, metabolism, snail metabolism, heat loss, etc). The temporal enrichment of benthic total carbon (Figure 15, top center, SLD and ASLD treatments) was supported by the growth displayed in Figure 16 of the SLD and ASLD treatments (plotted against von Bertalanffy growth functions).

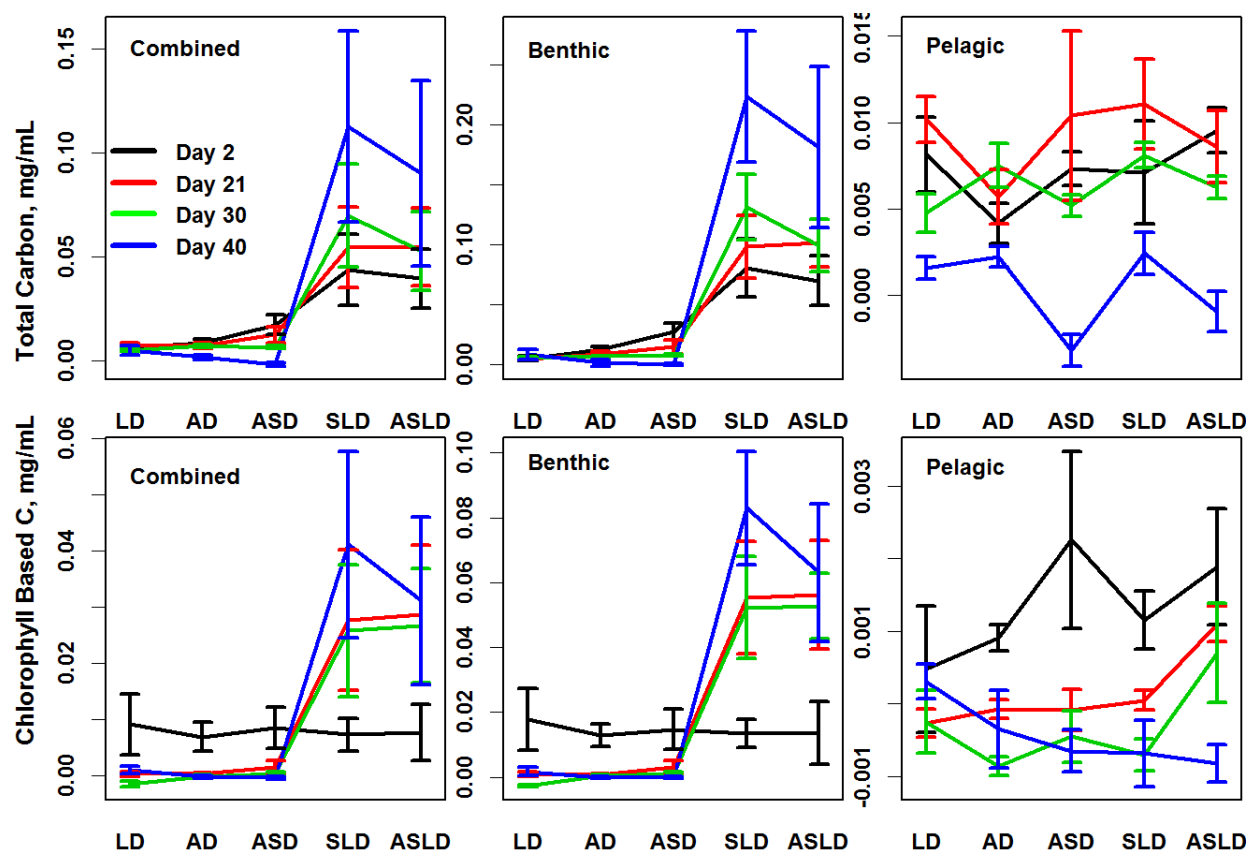


Figure 15. Total (top panel) and chlorophyll sourced (bottom panel) carbon concentrations (mg mL^{-1}) by treatment (x-axis), day (colors), and location (combined, benthic, and pelagic, L to R).

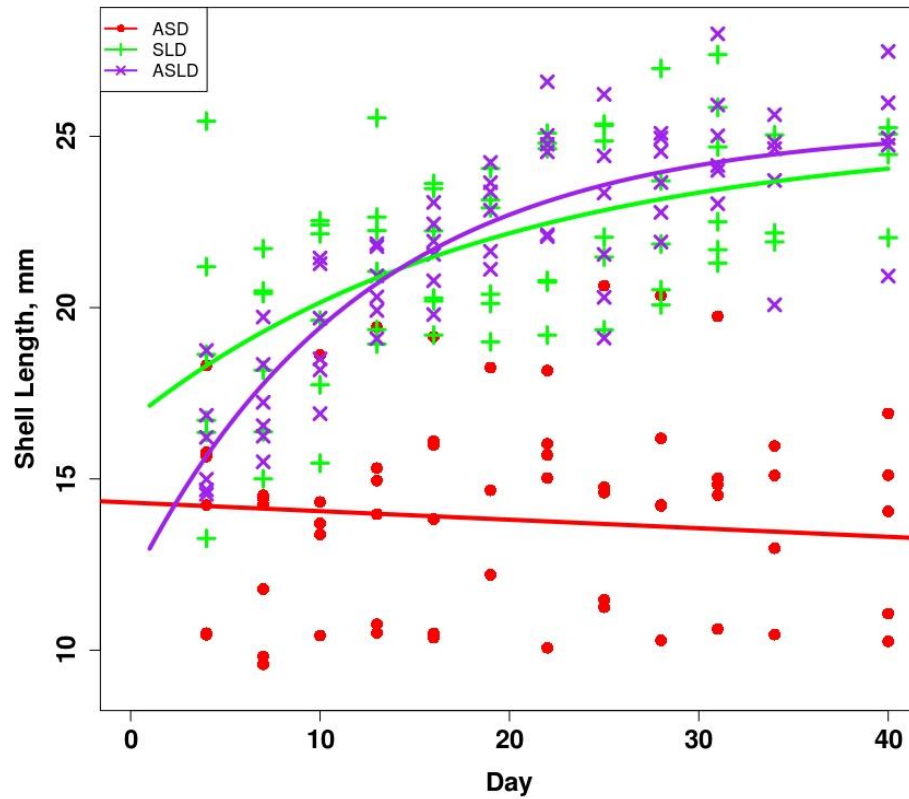


Figure 16. Shell length of *L. stagnalis* individuals in each replicate through time with fitted functions plotted against (von Bertalanffy (SLD and ASLD) and linear (ASD)). Two points from ASD treatment were removed as they were clearly measurement errors (lengths of < 5 mm). Variability is due, in part, to measurement error from using digital photographs to avoid directly handling organisms. Apparent trends are considered accurate regardless of reduced precision.

Model Output:

Three different scenarios were modelled in an attempt to match three of the experimental treatments. The LD and AD treatment were not modelled as conditions similar to AD are presented in Chapter 1 and, as of yet, a sub-model of the direct contribution of carbon/energy sources from LD (lettuce alone) has not been determined. In the scenarios modelled (ASD, SLD, and ASLD), parameters and feeding levels are those presented in Chapters 1 (*D. magna*) and Chapter 2 (*L. stagnalis*). Accordingly, the ASD treatment was modelled by limiting the lettuce amount but keeping algae normal (10^5 cells ml^{-1}). In this scenario, snail individuals did not show growth—similar to the experimental observations (see Figure 16 above). The SLD treatment was modelled by limiting the algae amount, but keeping lettuce at normal levels ($20 \text{ cm}^2 \text{ l}^{-1}$). In this scenario, algae levels were 2 orders of magnitude lower than normal and resulted in f values in daphnia less than 0.5. The ASLD treatment was modelled by keeping algae and lettuce levels normal. In all three scenarios, a non-facilitated group of simulations were run alongside facilitated simulations. The intent was to demonstrate the impact of the experimental condition (ASD vs SLD vs ASLD) alone and then show the impact of facilitation under those conditions.

Modelled ASD simulation output generally captured experimental ASD daphnid population dynamics through 40 days (Figures 17 and 21a). ASD model output also showed that the model predicted no impact of facilitation due to the lack of snail growth and carbon contribution (Figure 17). A similar observation was made in the experimental data (Figure 21a). While the mean modelled daphnid counts do not perfectly match the data, there is a large overlap—indicating that the facilitation observed in the ASD experimental treatments was fairly minimal (Figure 21a).

Model output that demonstrates facilitation is required for growth of a daphnid population in absence of amended algae would support both objectives of this chapter: 1.) Existence of facilitation and 2.) Facilitation can be modelled through a simple quantitative method. In the modelled SLD scenario (Figure 18), facilitation supported persistence of the daphnid population (compare black mean and red minimum line). This supported the surprising SLD experimental observations—daphnid populations can exist and grow without experimentally applied daphnid-specific food items, provided snails were present to facilitate algal growth (Figures 5 and 6). Again, as the mean model and experimental trends do not match well, there is clearly room for model improvement, nevertheless, it is clear that the model captures the essence of the energetic interaction overall.

Additional support for my hypothesis and quantitative structure could come from model output showing increased facilitation influence on daphnid populations from increased snail activity. Using conditions of increased snail resources, the model captured the observed population dynamics of the ASLD treatment quite well (Figure 19). Note that the model predicted a small, but consistent increase of mean population peak due to the increased facilitation in the ASLD treatment (Figure 20a in relation to 20b). The experimental ASLD treatment showed an increase in peak size over the AD ('control') treatments. Additionally, a key observation was the low overlap of maximum and minimum lines between treatments during peak population densities (Figure 21b). This was different than the observation that AD and ASD experimental data show large overlap of maximum and minimum daphnid population sizes (see Figure 21a). Clearly, the model was able to capture the range of experimental observations, but also capture reasonably accurate predictions of mean dynamics.

The model's performance across the three highlighted treatments (ASD, SLD, and ASLD) demonstrates its performance overall (Figure 20a, 20b, and 20c). Clearly, mean model output captured timing and size of daphnid populations quite well under a range of facilitation levels (ASD and ASLD). Additionally, the relatively simple quantitative methodology (snail waste converted to algae cells) appeared to explain the observed persistence of daphnid populations in the experimental treatment without amended algae (SLD).

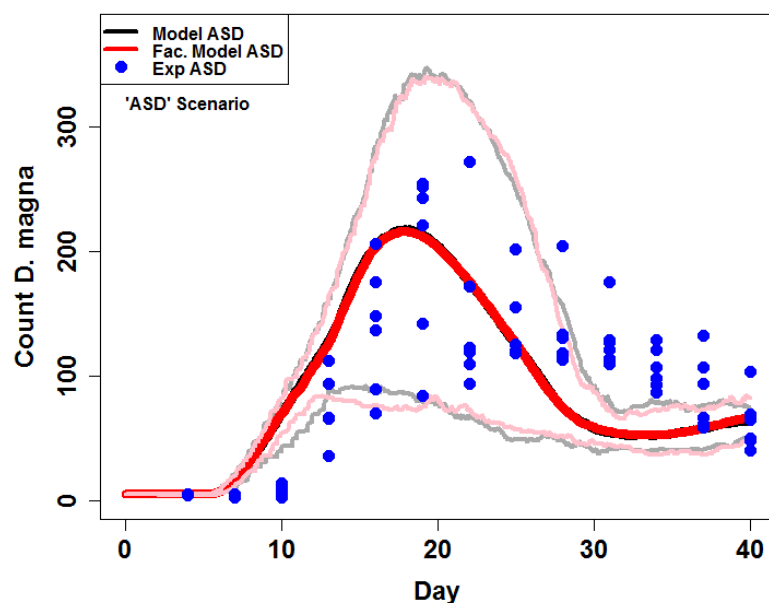


Figure 17. Model output (red and black lines) against experimental output (blue points) for the ASD scenario. Dark lines are means and light lines are maximum and minimum. Model data are of 50 simulations with algae levels set to normal and lettuce to minimum.

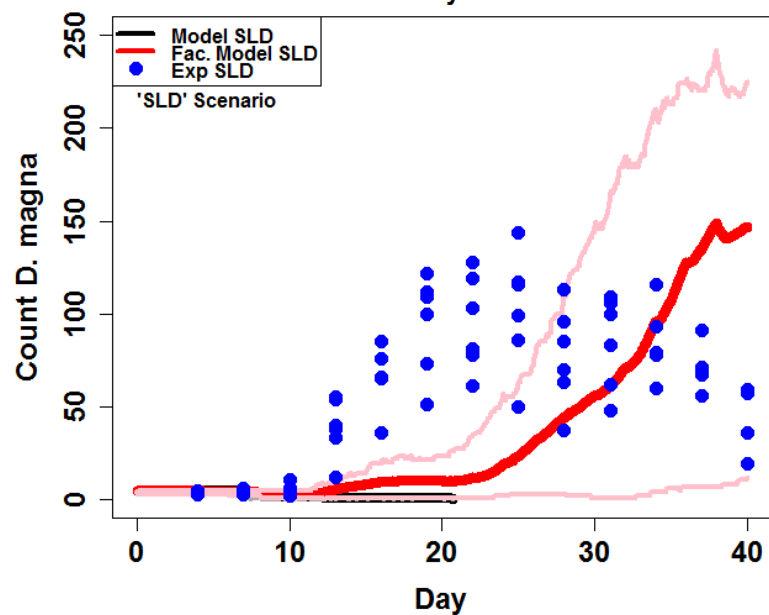


Figure 18. Model output (red and black lines) against experimental output (blue points) for the SLD scenario. Dark lines are means and light lines are maximum and minimum. Model data are of 50 simulations with algae levels set to normal and lettuce to minimum.

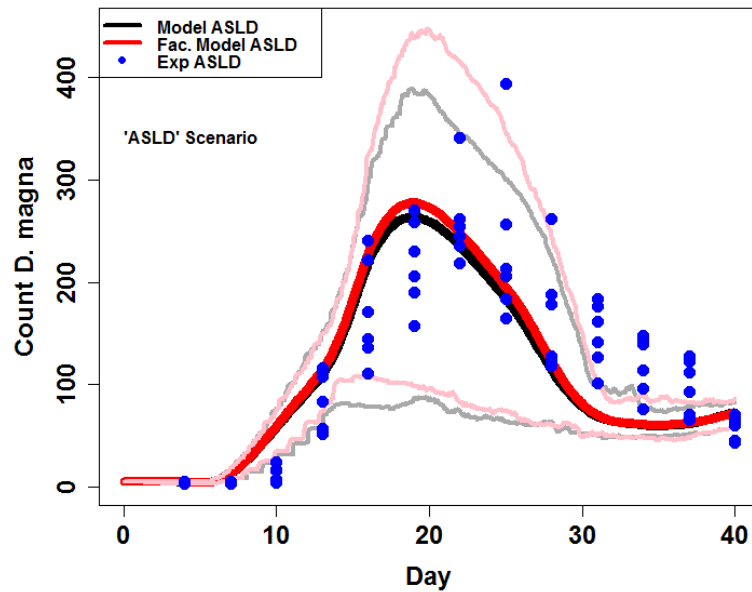


Figure 19. Model output (red and black lines) against experimental output (blue points) for ASLD scenario. Dark lines are means and light lines are maximum and minimum. Model data are of 50 simulations with algae levels set to normal and lettuce to minimum.

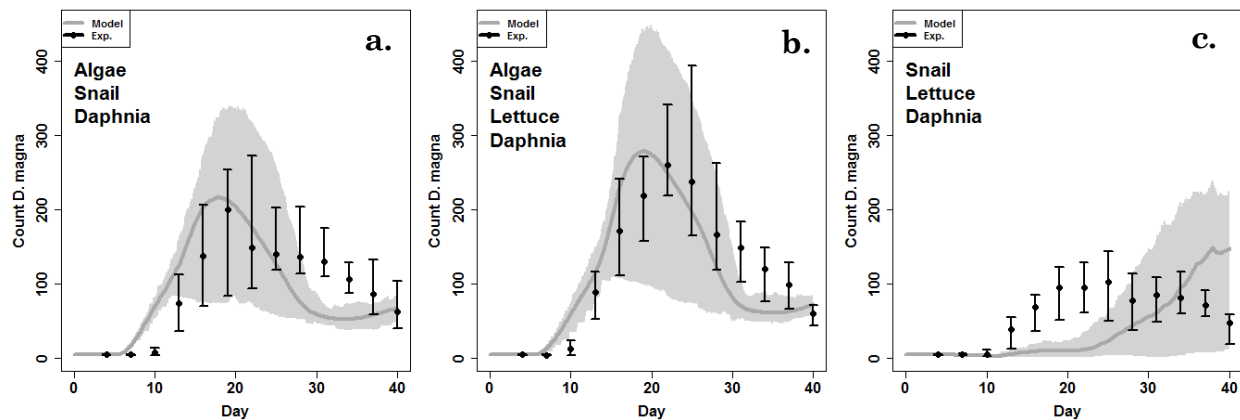


Figure 20a, 20b, 20c. Mean model (solid lines gray areas) and experimental (points with error bars) daphnid population sizes through 40 days. Shading limits and error bars represent maximum and minimum values for model output and data, respectively. Treatment conditions mimicked in simulations are 'ASD' in a., 'ASLD' in b., and 'SLD' in c.

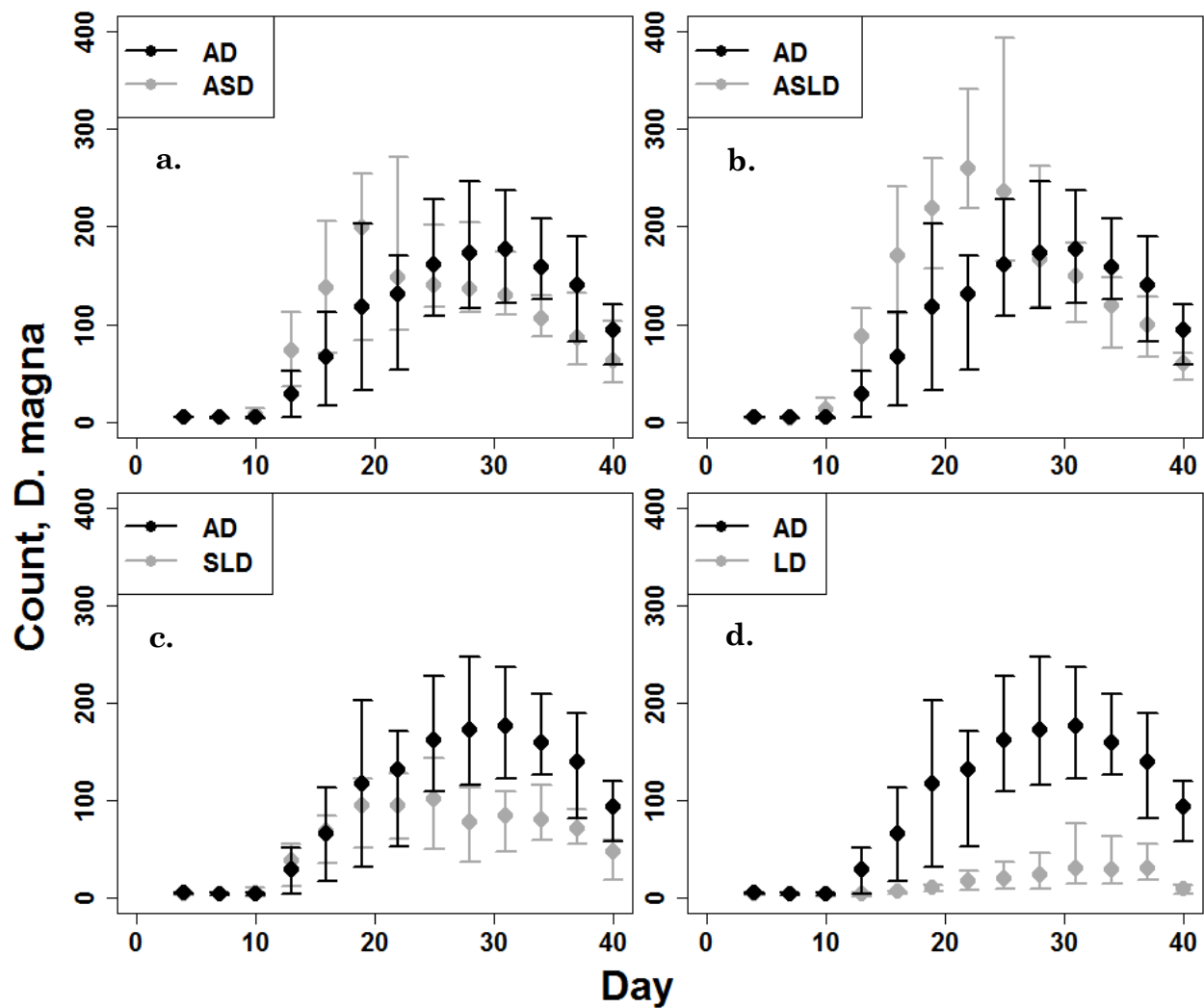


Figure 21a, 21b, 21c, and 21d. Experimental output of each treatment plotted against control ('AD') treatments. Points are mean of six replicates and error bars are maximum and minimum of six replicates.

In summary, indirect facilitation between *L. stagnalis* and *D. magna* appeared to be relevant in contributing to experimental observations of individual, organismal, and system level energetic dynamics. In particular, increased contribution of overall energy content (ASLD) caused the largest individuals (snails and daphnids), largest and earliest daphnid population peaks, and the greatest level of suspended total and chlorophyll-sourced carbon. The next highest treatment in system energetic concentration (carbon concentration), the SLD treatment, provided strong evidence that indirect facilitation played a major role in population persistence under experimental conditions. The ASD treatment represented the ‘intermediate’ energetic condition in that the energetic content (carbon concentration) was not largely greater than AD treatments, and this subsequently did not create a strong differential response in daphnid populations. Lastly, but surely not least, the LD treatment provided evidence that addition of an indirect source of carbon (lettuce alone) can support a small population of diminutive daphnids.

From the modelling perspective, the goal was to attempt a very simple but mechanistic approach for indirect energetic facilitation. As the model generally captured daphnid population dynamics, it appears that a rather simple snail waste to algal cell conversion sub-model may provide the core framework for the influence of indirect energetic facilitation between *L. stagnalis* and *D. magna*. This point is made particularly clear by the SLD mimic conditions (Figure 19), in which facilitation alone created enough energy to support a daphnid population.

Discussion:

Experimental Observations:

The key observation from the experiments was that daphnid populations had distinct responses to the experimental treatments that generally represent different energetic conditions. The addition of a gradient of snail-sourced energetic input produced a gradient of daphnid individual and population level responses. In the most complex and energy rich condition (ASLD), individual growth (snails and daphnids) was the largest and daphnid populations showed the highest and earliest peak. An intermediate condition (ASD) with limited facilitation showed a modest increase in daphnid size both individually and at the population level. While the SLD treatment was hypothesized to be of moderate energy content (no algae applied), it demonstrated the clear existence and value of facilitation on individual daphnia and their populations. The lowest energetic condition (LD) presented the interesting case of a daphnid population existing at low densities on what could be considered energy amendment from the applied, but largely unavailable, lettuce.

Each of these findings provided valuable insight on experimental conditions that affect study organisms and may be of value to ecological risk assessors. In particular, the goal of complex system, ‘top-down,’ experiments with relevant and common organisms under a wide suite of energetic states could be a strong connection between the commonly discordant organismal and “cosm”-based approaches to toxicity tests and ecological risk assessments (Rohr et al., 2016). The findings that I present are largely in sync with the intent of the work of Sanchez and Tarazona (2002). Improving the environmental relevance of experimental designs and outputs is hypothesized to be both more cost efficient (Rohr et al., 2016) but also an improvement in linking regulatory protection goals and system-level effects (Stampfli et al.,

2011). In essence, the experimental design demonstrated here fits between normal single-species/single individual toxicity tests and more complicated mesocosm studies (Landner et al., 1989; Culp et al., 2000; Kennedy et al., 2002, among others). While there is some information lost in the experimental simplification such as effects of temperature or sunlight (Stampfli et al., 2011), this loss is offset by more approachable individual energetic metrics. As the strength and value of individual-based mechanistic effect models increase (as suggested by Grimm and Martin, 2013), they may replace coarser energetic models (e.g., AQUATOX; Park, 2008) and this will likely require experimental validation. An experimental level that makes energetic metrics accessible (carbon content of all compartments—lettuce, algae, daphnids, snails, and water) also allows for increased insight into differentiating effects of chemical stressors and abiotic or biotic interactions (Fischer et al., 2013; Congdon et al., 2001; Vinebrooke et al., 2004).

By comparison, one current methodology used to extrapolate individual-level observed toxic effects to community-level effects is the AQUATOX model (among others, Park et al., 2008). Lombardo et al. (2015) demonstrated the use of AQUATOX in predicting seasonal biomass of many food-web members based on their direct and indirect predator/prey and competitive interactions. Toxicant data used were published LC_{50} (concentration killing 50% of organisms in single-species standard toxicity test) values. These were applied against all food-web compartments during the simulated time period and compartment biomass through time was a model output. One very important metric was the relation between LC_{50} concentration and % perturbation of biomass with the food-web approach. The non-linearity of these relations (Figure 5 of Lombardo et al. (2015)) demonstrated the importance of food-web level interactions (predation/competition) in predicting perturbation due to chemical exposure. While the conceptual underpinnings of organism-to-community stressor effect connections of the

AQUATOX model seem reasonable and are considered state-of-the-art (Chen et al., 2013), there remains several key uncertainties (Lombardo et al., 2015). Specifically, an incomplete understanding of individual chemical tolerance or effect (Grimm and Martin, 2013; Jager et al., 2011) leads to unknown levels of variability in organismal parameters in the AQUATOX framework (Lombardo et al., 2015). As highlighted by Suter et al. (2005), lack of clarity about model resolution can lead to uncertainty regarding key model components like stressor effect or interaction parameters.

As my experimental observations support the overall objective of describing a hypothesized indirect interaction between two relevant ecotoxicological model organisms, a secondary objective has emerged from the results. Attempting to apply experimental results to a multi-species DEB-IBM highlighted the importance of synchronizing model parameter and experimental metrics. This misalignment of parameter resolution presented by Lombardo et al. (2015) is akin to the misalignment presented by Rohr et al. (2016) in relation to ERA methods. I argue that linking different levels of organization required in ERA can be aided by a useful experimental design that fits between individual toxicity tests and large, complex mesocosms. In particular, individual level metrics (such as LC_{50}) are very useful to infer effects of acute exposures, but conservation goals are generally at higher levels of biological organization and environment exposures are often far below concentrations that are acutely toxic. As such, the experimental results of this chapter, alongside Sanchez and Tarazona (2002), demonstrated that a relatively simple system can be constructed that produces population level metrics of exposure, while simultaneously producing individual level output. Arguably, this method relies on mechanistic effects of exposure to produce emergent properties. This conceptual design is

presented by Grimm and Martin (2013) as a method to improve ERA model frameworks, but strong validating experimental evidence should follow the same overall framework.

Model Observations:

The model output suggested, firstly, that the overall conceptual model of using individual based bioenergetic models (DEB-IBM) to link levels of biological organization can be successfully applied. Supporting evidence was that mean daphnid population size showed a graded increase with increasing energetic facilitation by snails (Figures 17 and 20). This model output was validated in experimental observations against graded levels of snail-driven facilitation (Figure 22). Additionally, capturing the persistence of a daphnid population under solely facilitated energy sources is a key success of the model (Figure 19). This suggests that the very simplistic model mechanism for indirect energetic facilitation was aligned with what is a likely mechanism in experimental settings. That said, additional research and model development is warranted to further improve model fit and performance in regards to indirect energetic facilitation.

As the model is an individual-based model (IBM), population dynamics emerge from the processes and mechanisms modelled at the individual level (Grimm and Railsback, 2005). This principle is a key characteristic of model method improvements suggested by proponents of mechanistic effect models in ecological risk assessments (Grimm and Martin, 2013; Martin et al., 2014; Jager et al., 2006; Forbes et al., 2009). As described by Chen et al. (2013) many modelling methods in use in ERA and ecotoxicology analyses already make use of emergent properties or rely on a conceptual construct that effects at higher levels of organization emerge from interactions among relevant organisms plus the effects of the chemical stressor(s) at lower

levels. The AQUATOX example of Lombardo et al. (2015) above demonstrated this quality quite well. By plotting the modelled/predicted % perturbation against the LC_{50} values of each organism in the food-web, it was abundantly clear that percent population/community level effect was not a 1:1 relationship with % individual level effect. However, in the case of AQUATOX, this emergent property does not account for some processes observed at the individual level. Using the examples of Beauduoin et al (2015), Martin et al (2014), and Murphy et al. (2008), zebrafish, daphnid, and larval Atlantic croaker models performed best by explicitly accounting for impacts of size/age class structure-based diets and behaviors. These impacts at individual levels played a role in accounting for emergent effects of stressor exposure at higher levels (see trait-based and resource allocation-based approaches by Fischer et al. (2013) and Congdon et al. (2001)).

In the model presented here, daphnid population dynamics emerge from interactions between individual growth, the Neighborhood Effect (see Chapter 1), and resource density. Individual growth was a function of local resource density, internal starvation resistance functions, and stressor exposure. Size influences reproduction along with localized daphnid density (the Neighborhood Effect). Movement patterns were a function of local resource density and the Neighborhood Effect. Local resource densities were influenced by the size, condition, and density of local snails. Meanwhile, snail facilitative contribution was a function of its movement patterns, local resource density, and its size and condition. All of these interactions were influenced by the experimental design and feedback from snails and daphnids. Other system level dynamics that can influence daphnids (such as stressor effect levels or distributions or overall resource density) were controlled by the experimenter.

Both the snails and daphnid individual process-based models were designed separately (See Chapters 1 and 2) using the overall NetLogo (Wilensky, 1999) DEB-IBM approach of Martin et al. (2012), but amended along several fronts. These amendments for local density-dependent effects (the Neighborhood Effect), starvation sub-models, juvenile assimilation lag, and non-random walk patterns were key to improving the trait-based or resource allocation-based factors in these organisms and individuals (Fischer et al., 2013; Congdon et al., 2001). Linking these two previously unconnected models through a simple indirect energetic facilitation sub-model was used to address the major underlying hypothesis of this work—can the emergent daphnid population dynamics be predicted by facilitation from similarly emergent properties of snails?

Model output suggested that a.) Individual level parameterized snail size and a condition-dependent facilitation sub-model can produce observed daphnid survival under facilitation only conditions (SLD scenarios and treatments) and b.) Graded facilitation contribution produces graded daphnid population responses as observed in experiments (ASD and ASLD). The model results discussed above suggest that a multi-species framework can be successfully constructed and capture experimentally observed dynamics. The value of these results are that capturing a suite of potential interactions (Vinebrooke et al., 2004; Fischer et al., 2013; and Stampfil et al., 2011) through process based mechanism effect models (Jager et al., 2006; Grimm and Martin, 2013) is proposed as one potential methodological tool to improve ecological risk assessment (Rohr et al., 2016).

In summary, this chapter presents two main themes: 1.) An experimental design using two common toxicity test organisms that could provide enough complexity to infer stressor effects at system levels, but maintain knowledge of the effects at individual levels and 2.) A bioenergetic individual-based model framework that was able to largely capture the experimentally observed daphnid population dynamics under a range of snail-driven facilitative input. The overall motivation for exploration of these topics was to provide ecotoxicology researchers experimental and model frameworks that could improve ecological risk assessment outputs at higher levels of biological organization. Experimental results suggested that a.) Indirect energetic facilitation between *L. stagnalis* and *D. magna* occurs and b.) Indirect energetic facilitation can manifest at population and individual levels. Model results suggested that a.) Energetically linking two individual-based models in the NetLogo environment is possible and performs well and b.) Indirect facilitation from *L. stagnalis* to *D. magna* may be fairly simple quantitatively.

Future validation of this framework would likely necessitate a suite of chemical stressor exposures. Exposures at individual levels to parameterize DEB models and then exposures to experimental systems to observe effect of facilitation on exposed organisms. Successful model prediction of experimental observations of exposed system would more fully validate the individual to system ERA framework proposed here.

Literature Cited:

- Baas, J., Jager, T. and Kooijman, B., 2010. A review of DEB theory in assessing toxic effects of mixtures. *Science of the total environment*, 408(18), pp.3740-3745.
- Beaudoin, R., B. Goussen, B. Piccini, S. Augustine, J. Devillers, F. Brion, and A.R.R. Pery, 2015. An individual-based model of zebrafish population dynamics accounting for energy dynamics. *PLoS ONE* 10(5): e0125841. doi:10.1371/journal.pone.0125841
- Cardoso, J.F., van der Veer, H.W. and Kooijman, S.A., 2006. Body-size scaling relationships in bivalve species: A comparison of field data with predictions by the Dynamic Energy Budget (DEB) theory. *Journal of Sea Research*, 56(2), pp.125-139.
- Chen, S., Chen, B. and Fath, B.D., 2013. Ecological risk assessment on the system scale: A review of state-of-the-art models and future perspectives. *Ecological Modelling*, 250, pp.25-33.
- Clements, W.H., Hickey, C.W. and Kidd, K.A., 2012. How do aquatic communities respond to contaminants? It depends on the ecological context. *Environmental Toxicology and Chemistry*, 31(9), pp.1932-1940.
- Congdon, J.D., Dunham, A.E., Hopkins, W.A., Rowe, C.L. and Hinton, T.G., 2001. Resource allocation-based life histories: A conceptual basis for studies of ecological toxicology. *Environmental Toxicology and Chemistry*, 20(8), pp.1698-1703.
- Culp, J.M., Podemski, C.L., Cash, K.J. and Lowell, R.B., 2000. A research strategy for using stream microcosms in ecotoxicology: integrating experiments at different levels of biological organization with field data. *Journal of Aquatic Ecosystem Stress and Recovery*, 7(2), pp.167-176.
- Davidson, D.W., Inouye, R.S. and Brown, J.H., 1984. Granivory in a desert ecosystem: experimental evidence for indirect facilitation of ants by rodents. *Ecology*, 65(6), pp.1780-1786.
- EPA, 1998. Guidelines for Ecological Risk Assessment EPA/630/R-95/002F
- Fath, B., Jørgensen, S., Patten, B., Straškraba, M., 2004. Ecosystem growth and development. *Biosystems* 77, 213-228.
- Fischer, B.B., Pomati, F. and Eggen, R.I., 2013. The toxicity of chemical pollutants in dynamic natural systems: the challenge of integrating environmental factors and biological complexity. *Science of the Total Environment*, 449, pp.253-259.
- Forbes, V.E., Calow, P., Grimm, V., Hayashi, T.I., Jager, T., Katholm, A., Palmqvist, A., Pastorok, R., Salvito, D., Sibly, R. and Spromberg, J., 2011. Adding value to ecological risk assessment with population modeling. *Human and Ecological Risk Assessment*, 17(2), pp.287-299.
- Forbes, V.E., Hommen, U., Thorbek, P., Heimbach, F., Van den Brink, P.J., Wogram, J., Thulke, H.H. and Grimm, V., 2009. Ecological models in support of regulatory risk assessments of

- pesticides: developing a strategy for the future. *Integrated Environmental Assessment and Management*, 5(1), pp.167-172.
- Frost, P.C., Ebert, D. and Smith, V.H., 2008. Bacterial infection changes the elemental composition of *Daphnia magna*. *Journal of animal ecology*, 77(6), pp.1265-1272.
- Glazier, D.S. and Calow, P., 1992. Energy allocation rules in *Daphnia magna*: clonal and age differences in the effects of food limitation. *Oecologia*, 90(4), pp.540-549.
- Grimm, V. and B. Martin, 2013. Mechanistic effect modeling for ecological risk assessment: Where to go from here? *Integrated Environmental Assessment and Management* 9(3):e59-e63.
- Grimm, V., S.F. Railsback, 2005. Individual-based modeling and ecology. Princeton University Press.
- Gutiérrez, J.L., Jones, C.G., Strayer, D.L., Iribarne, O.O., 2003. Mollusks as ecosystem engineers: the role of shell production in aquatic habitats. *Oikos*. 101:79-90.
- Heugens, E.H.W., Hendriks, A.J., Dekker, T., van Straalen, N.M., Admiraal, W., 2001. A review of the effects of multiple stressors on aquatic organisms and analysis of uncertainty factors for use in risk assessment. *Critical Reviews in Toxicology* 31, 247–284.
- Jager, T., Albert, C., Preuss, T.G. and Ashauer, R., 2011. General unified threshold model of survival-a toxicokinetic-toxicodynamic framework for ecotoxicology. *Environmental Science & Technology*, 45(7), pp.2529-2540.
- Jager, T., Heugens, E.H. and Kooijman, S.A., 2006. Making sense of ecotoxicological test results: towards application of process-based models. *Ecotoxicology*, 15(3), pp.305-314.
- Jager, T., Zimmer, E., 2012. Simplified Dynamic Energy Budget model for analysing ecotoxicity data. *Ecological Modelling* 225, 74–81.
- Jusup, M., Sousa, T., Domingos, T., Labinac, V., Marn, N., Wang, Z., Klanjscek, T., 2016. Physics of Metabolic Organization. *Physics of Life Reviews*.
- Kennedy, J.H., La Point, T.W., Balci, P., Stanley, J. and Johnson, Z.B., 2002. Model aquatic ecosystems in ecotoxicological research: considerations of design, implementation, and analysis. *Handbook of ecotoxicology*, 2, pp.45-74.
- Knillmann, S., Stampfli, N.C., Beketov, M.A. and Liess, M., 2012. Intraspecific competition increases toxicant effects in outdoor pond microcosms. *Ecotoxicology*, 21(7), pp.1857-1866.
- Kooijman S. 2010. Dynamic energy budget theory for metabolic organization. 3rd ed. Cambridge, UK: Cambridge University Press.
- Kooijman, S.A.L.M., 2001. Quantitative aspects of metabolic organization: a discussion of concepts. *Philosophical Transactions of the Royal Society of London B: Biological Sciences*, 356(1407), pp.331-349.
- Landner, L., Blanck, H., Heyman, U., Lundgren, A., Notini, M., Rosemarin, A. and Sundelin, B., 1989. Community testing, microcosm and mesocosm experiments: ecotoxicological tools

- with high ecological realism. In *Chemicals in the Aquatic Environment* (pp. 216-254). Springer Berlin Heidelberg.
- Lika, K., Kearney, M.R. and Kooijman, S.A., 2011. The “covariation method” for estimating the parameters of the standard Dynamic Energy Budget model II: Properties and preliminary patterns. *Journal of Sea Research*, 66(4), pp.278-288.
- Lika, K., Kearney, M.R., Freitas, V., van der Veer, H.W., van der Meer, J., Wijsman, J.W., Pecquerie, L. and Kooijman, S.A., 2011. The “covariation method” for estimating the parameters of the standard Dynamic Energy Budget model I: philosophy and approach. *Journal of Sea Research*, 66(4), pp.270-277.
- Lombardo, A., Franco, A., Pivato, A. and Barausse, A., 2015. Food web modeling of a river ecosystem for risk assessment of down-the-drain chemicals: A case study with AQUATOX. *Science of the Total Environment*, 508, pp.214-227.
- Lukowiak, K., Martens, K., Rosenegger, D., Browning, K., Caigny, P., Orr, M., 2008. The perception of stress alters adaptive behaviours in *Lymnaea stagnalis*. *Journal of Experimental Biology* 211, 1747–56.
- Martin, B., Jager, T., Nisbet, R., Preuss, T., Grimm, V., 2014. Limitations of extrapolating toxic effects on reproduction to the population level. *Ecological Applications*.
- Martin, B., Jager, T., Nisbet, R., Preuss, T., Hammers-Wirtz, M., Grimm, V., 2013. Extrapolating ecotoxicological effects from individuals to populations: a generic approach based on Dynamic Energy Budget theory and individual-based modeling. *Ecotoxicology* (London, England) 22, 574–83.
- Martin, B., Zimmer, E., Grimm, V., Jager, T., 2012. Dynamic Energy Budget theory meets individual-based modelling: a generic and accessible implementation. *Methods in Ecology and Evolution* 3, 445–449.
- Murphy, C.A., Rose, K.A., del Carmen Alvarez, M. and Fuiman, L.A., 2008. Modeling larval fish behavior: Scaling the sublethal effects of methylmercury to population-relevant endpoints. *Aquatic toxicology*, 86(4), pp.470-484.
- Nisbet, R.M., Muller, E.B., Lika, K. and Kooijman, S.A.L.M., 2000. From molecules to ecosystems through dynamic energy budget models. *Journal of animal ecology*, 69(6), pp.913-926.
- OECD (2012), *Test No. 211: Daphnia magna Reproduction Test*, OECD Publishing, Paris. DOI: <http://dx.doi.org/10.1787/9789264185203-en>
- OECD (2016), *Test No. 243: Lymnaea stagnalis Reproduction Test*, OECD Publishing, Paris. DOI: <http://dx.doi.org/10.1787/9789264264335-en>
- Park RA, Clough JS, Coombs Wellman M. AQUATOX: modelling environmental fate and ecological effects in aquatic ecosystems. 2008. *Ecological Modelling*;213:1–15.
- R Core Team (2016). R: A language and environment for statistical computing. R Foundation for Statistical Computing, Vienna, Austria. URL <https://www.R-project.org/>.

- Rasband, W.S., ImageJ, U. S. National Institutes of Health, Bethesda, Maryland, USA, <http://imagej.nih.gov/ij/>, 1997-2016.
- Reátegui-Zirena, E.G., Fidler, B.N. and Salice, C.J., 2016. A cost or a benefit? Counterintuitive effects of diet quality and cadmium in *Lymnaea stagnalis*. *Ecotoxicology*, pp.1-11.
- Ren, J.S. and Schiel, D.R., 2008. A dynamic energy budget model: parameterisation and application to the Pacific oyster *Crassostrea gigas* in New Zealand waters. *Journal of Experimental Marine Biology and Ecology*, 361(1), pp.42-48.
- Rohr, J.R., Salice, C.J., Nisbet, R.M., 2016. The pros and cons of ecological risk assessment based on data from different levels of biological organization. *Critical Reviews in Toxicology* 46, 756–84
- Sánchez, P. and Tarazona, J.V., 2002. Development of a multispecies system for testing reproductive effects on aquatic invertebrates. Experience with *Daphnia magna*, *Chironomus prasinus* and *Lymnaea peregra*. *Aquatic toxicology*, 60(3), pp.249-256.
- Sibly, R., Grimm, V., Martin, B., Johnston, A., Kulakowska, K., Topping, C., Calow, P., Nabe-Nielsen, J., Thorbek, P., DeAngelis, D., 2013. Representing the acquisition and use of energy by individuals in agent-based models of animal populations. *Methods in Ecology and Evolution* 4, 151–161.
- Sokolova, I., 2013. Energy-Limited Tolerance to Stress as a Conceptual Framework to Integrate the Effects of Multiple Stressors. *Integrative and Comparative Biology*.
- Stampfli, N.C., Knillmann, S., Liess, M. and Beketov, M.A., 2011. Environmental context determines community sensitivity of freshwater zooplankton to a pesticide. *Aquatic toxicology*, 104(1), pp.116-124.
- Steiner, C.F., Darcy-Hall, T.L., Dorn, N.J., Garcia, E.A., Mittelbach, G.G. and Wojdak, J.M., 2005. The influence of consumer diversity and indirect facilitation on trophic level biomass and stability. *Oikos*, 110(3), pp.556-566.
- Suter, G.W., Norton, S.B. and Fairbrother, A., 2005. Individuals versus organisms versus populations in the definition of ecological assessment endpoints. *Integrated environmental assessment and management*, 1(4), pp.397-400.
- van der Meer, J., Klok, C., Kearney, M.R., Wijsman, J.W. and Kooijman, S.A.L.M., 2014. 35years of DEB research. *Journal of Sea Research*, 94, pp.1-4.
- Vinebrooke, R., L Cottingham, K., Norberg, M.S., I Dodson, S., C Maberly, S. and Sommer, U., 2004. Impacts of multiple stressors on biodiversity and ecosystem functioning: The role of species co-tolerance. *Oikos*, 104(3), pp.451-457.
- Wilensky, U. 1999. NetLogo. <http://ccl.northwestern.edu/netlogo/>. Center for Connected Learning and Computer-Based Modeling, Northwestern University. Evanston, IL.
- Zonneveld, C, Kooijman, S, 1989. Application of a dynamic energy budget model to *Lymnaea stagnalis* (L.). *Functional Ecology*.

Andrew East

Environmental Science and Studies Program
Towson University
8000 York Rd. Towson, MD, 21252

Education

Towson University

MS Environmental Science, 2016

Thesis Title: A modelling framework to explore bioenergetic effects of environmental stress and interspecific interactions.

Advisor: Dr. Chris J. Salice

Northland College

Ashland, WI

BS Natural Resource Management (Fish and Wildlife Ecology concentration), 2010

Magna Cum Laude

Professional Research Experience

Towson University; 2014—Present

Graduate Assistant and Lab Manager

Environmental Science and Studies Program

Applied Aquatic Ecology and Ecotoxicology Experimental and Modelling Projects

Texas Tech University; 2013—2014

Research Technician

Dept. of Environmental Toxicology and Dept. of Natural Resource Management

Molecular Toxicology of Hydrocarbons and Ungulate Translocation Projects

Wisconsin Dept. of Natural Resources; 2012

Research Technician

Green Bay Northern Pike Connectivity Project

Earthwatch Institute; 2012

Field Biologist

Wintering Ecology of Common Loons in the Gulf of Mexico Project

Oregon Dept. of Fish and Wildlife; 2010, 2011

Experimental Biological Aide

Coastal Chinook Research and Monitoring Project

Oregon State University / Real Time Research; 2011

Capture Technician

East Sand Island Avian Dissuasion Project

BioDiversity Research Institute ; 2011

Field Biologist

Winter Offshore Waterbirds and Oiling Rate Assessment Projects

Wisconsin Dept. of Natural Resources; 2009, 2010

Research Technician

Common Loon Demography and Lake Dependent Species and Climate Change Projects

Published and Technical Works

Paruk, J.D., Chickering, M.D., Long IV, D., Uher-Koch, H., **East, A.**, Poleschook, D., Gumm, V., Hanson, W., Adams, E.M., Kovach, K.A. and Evers, D.C., 2015. Winter site fidelity and winter movements in Common Loons (*Gavia immer*) across North America. *The Condor*, 117(4), pp.485-493.

Paruk, J.D., Long IV, D., Perkins, C., **East, A.**, Sigel, B.J. and Evers, D.C., 2014. Polycyclic aromatic hydrocarbons detected in Common Loons (*Gavia immer*) wintering off coastal Louisiana. *Waterbirds*, 37(sp1), pp.85-93.

Paruk, J.D., D. Long, IV and **A. East**. 2012. Common Loon (*Gavia immer*) Winter Ecology in the Gulf of Mexico. Report BRI 2012-30. BioDiversity Research Institute, Gorham, ME.

Presentations

East, A., T. Woo, and C.J. Salice, 2016. Predicting toxic effects of ion pulses from urban streams in Baltimore County, MD. Maryland Water Monitoring Council Annual Meeting.

Smith, M., **A. East**, and C.J. Salice, 2016. Bioenergetic Response to Stress: Lipid Content in Surface Water and Caddisfly Larvae across a Rural to Urban Gradient. Maryland Water Monitoring Council Annual Meeting. ***Won Best Student Poster Contest***

East, A. and C.J. Salice. 2016. Individual-based and system dynamic modeling frameworks to explore a complex energetic process in aquatic communities. North American Chapter of the Society of Environmental Toxicology and Chemistry Annual Meeting.

East, A. and C.J. Salice. 2016. Simulating system level effects of stress on aquatic systems through linked dynamic energy budget individual-based models (DEB-IBMs) in Netlogo. International Society of Ecological Modelling Annual Meeting. ***Platform***

East, A. and C.J. Salice. 2016. An individual-based model to link organismal energetic stress to population level effects. Young Environmental Scientists Annual Meeting. ***Platform***

Lockett, L, **A. East**, and C.J. Salice, 2016. An examination of the impacts of temperature on standard toxicological protocols using pyraclostrobin and *Daphnia magna*. Maryland Water Monitoring Council Annual Meeting.

Woo, T., **A. East**, and C.J. Salice, 2016. Timing is everything: assessing the effects of pulse exposure patterns on salt toxicity in *Daphnia magna*. North American Chapter of the Society of Environmental Toxicology and Chemistry Annual Meeting.

Lockett, L., **A. East**, and C.J. Salice, 2016. Exploring the impacts of multiple anthropogenic and environmental stressors: data needs for predicting ecological effects. North American Chapter of the Society of Environmental Toxicology and Chemistry Annual Meeting.

Pererira, V., T. Woo, **A. East**, and C.J. Salice. 2015. Effects of common anthropogenic pollutants on the surrogate freshwater invertebrate, *Daphnia magna*. Maryland Water Monitoring Council Annual Meeting.

East, A. and C.J. Salice. 2015. A mechanistic bioenergetic model to understand effects of anthropogenic stressors on multiple species aquatic systems. Chesapeake and Potomac Regional Chapter of the Society of Environmental Toxicology and Chemistry Annual Meeting.

Platform

East, A. and C.J. Salice. 2015. A bioenergetic modeling framework to understand effects of anthropogenic stressors on interacting aquatic species. North American Chapter of the Society of Environmental Toxicology and Chemistry Annual Meeting.

East, A. and C.J. Salice. 2014. Developing a bioenergetic framework for sentinel species and predicting effects of disturbance on Maryland streams. Maryland Water Monitoring Council Annual Meeting.

Salice, C.J., **A. East**, A. Olson, B. Perkins, and E. Reategui-Zirena. 2014. A Bioenergetic-Based Approach to Identify and Understand the Effects of Pesticides on Ground Nesting Birds. North American Chapter of the Society of Environmental Toxicology and Chemistry Annual Meeting.

Professional Societies

Society of Environmental Toxicology and Chemistry (SETAC)
Chesapeake and Potomac Regional Chapter of SETAC
International Society for Ecological Modelling (ISEM)
Maryland Water Monitoring Council (MWMC)

Teaching

Towson University, 2015
Conservation Biology Lab Section Teaching Assistant

Awards

Towson University Graduate Student Association Travel Award, 2016
SETAC MS Student Travel Award, 2015

Professional Service

Journal Reviewer for Ecological Modelling and PloS One.

Session Chair, International Society for Ecological Modelling Global Conference, 2016

Technical Skills

Proficient in several computational environments—R, NetLogo, STELLA, MS Office Suite, ESRI ARC Suite, and various open-source alternatives.

Proficient in standardized aquatic toxicity tests and analytical methods

Proficient in a variety of molecular toxicology assays

Proficient in a range of field sampling and organism capture techniques, both aquatic and terrestrial.

